CARRIER MEDIATED LIPID TRANSPORT

By

SCOTT D. COVEY, B.SC.

A Thesis

Submitted to the School of Graduate Studies

in Partial Fulfilment of the Requirements

for the Degree

Doctor of Philosophy

McMaster University

CARRIER MEDIATED LIPID TRANSPORT

DOCTOR OF PHILOSOPHY (2003) McMaster University
(Biochemistry) Hamilton, Ontario

TITLE: Carrier Mediated Lipid Transport

AUTHOR: Scott D. Covey, B.Sc. (McMaster University)

SUPERVISOR: Professor B.L. Trigatti

NUMBER OF PAGES: xviii, 178

Abstract

Lipids are essential molecules for cellular function; they are required for energy production, membrane structure, and can serve as signaling molecules. Normal metabolism requires cellular uptake and efflux as well as intercellular transport of lipids. Disruption of these events can lead to pathological processes like obesity and atherosclerosis.

Transport of lipids between tissues involves moving hydrophobic species through a polar environment. This is achieved by carrier mediated lipid transport. These carriers can have significant impact on cellular uptake and efflux of lipids. This thesis investigated carrier mediated lipid transport in two situations, 1) long chain fatty acids (LCFAs) and the carrier protein albumin, and 2) cholesterol (and other lipids) carried by high density lipoprotein particles.

Significant issues regarding cellular LCFA uptake from albumin remain unresolved. 1) How do LCFAs traverse the plasma membrane, and 2) is an albumin receptor involved in LCFA uptake? With respect to the first question, we hypothesized that the mechanism of LCFA uptake may be sensitive to cellular cholesterol. Our studies concluded that cholesterol-depleting agents inhibit LCFA uptake but not that of a non-carrier mediated substrate. In regard to the second question, we investigated if albumin binding proteins exist on the cell surface of adipocytes. We found that albumin binding

activity increased as cells undergo adipogenesis, and candidate proteins for this activity were found

We also investigated the role of the high density lipoprotein (HDL) receptor, scavenger receptor class B type I (SR-BI) in cholesterol metabolism and atherosclerosis. SR-BI has been found to be atheroprotective in mice, and this may involve cholesterol efflux from macrophage foam cells to HDL. We investigated the affect of bone marrow specific ablation of SR-BI on atherosclerosis in mice. We concluded that SR-BI expression in bone marrow-derived cells can protect against atherosclerosis in the absence of any changes in overall lipoprotein metabolism.

Publications

Covey, S. D., Krieger, M., Wang, W., Penman, M. and Trigatti, B. L. (2003) Scavenger Receptor Class B Type I-Mediated Protection Against Atherosclerosis in LDL Receptor-Negative Mice Involves Its Expression in Bone Marrow-Derived Cells. *Arterioscler Thromb Vasc Biol.* **23,** 1589-1594.

Trigatti, B., Covey, S., Rizvi, A. (2004) SR-BI in HDL metabolism, atherosclerosis and heart disease: Lessons from gene-targeted mice. Biochem Soc Trans. **32**, part I.

Acknowledgments

Many people were instrumental in completion of this thesis, and I would like to express my sincere gratitude to all of them. In particular, I would like to thank Dr Trigatti for his generosity in terms of his time, knowledge and ideas. In addition, I also thank Dr Gerber for his supervision, patience and encouragement. I would also like to thank the members of my supervisory committee, Dr Andrews, Dr Capone, and Dr Leber who have provided valuable guidance and input into the completion of this work. In addition I would also like to thank Dr Jae-Hoo Yoo who unselfishly provided his time and experience and for providing useful discussion.

Furthermore I wish to express my gratitude to the project students who I have worked with, in particularly Mike Hudson and Judy Lin. I also wish to thank all the current members of Dr Trigatti's lab and the former members of Dr Gerber's lab.

I would also like to thank Dr Christy Thomson who has accompanied me throughout my studies, provided support, served as a source of continual motivation and enhanced every part of this experience. I am also grateful to my entire family who has supported and encouraged this endeavor from the very beginning.

Table of Contents

List of Figures

List of Tables

Abbreviations

ACAT-2	acyl-CoA:cholesterol acyltransferase 2
ACS	aqueous counting scintillant
ADRP	adipose differentiation related protein
BSA	bovine serum albumin
BCA	bicinchoninic acid
CHAPS	3-[(3-cholamidopropyl)dimethyammonio]-1-1-propane-sulfonate
CETP	cholesterol ester transfer protein
cPBS	complete PBS
CHO	Chinese hamster ovary cells
CS	calf serum
cGY	centigray
dKO	double knockout (compound mutant)
DIC	differential interference contrast
DIDS	4,4′-diisothiocyanostilbene-2-2′-sulfonate
DMEM	Dulbecco's modified Eagle's media
DMSO	dimethyl sulfoxide
DNase	deoxyribonuclease
EDTA	ethylenediaminetetraacetic acid
EGTA	ethylene glycol bis(2-Aminoethyl ether) N,N,N′ N′ tetracetic acid
eNOS	endothelial nitric oxide synthetase

ER	endoplasmic reticulum
FABPpm	plasma membrane fatty acid binding protein
FACS	fluorescent activated cell sorting
FAT	fatty acid translocase
FATP	fatty acid transport protein
FBS	fetal bovine serum
GFP	green fluorescent protein
GFPtg	green fluorescent protein transgene
HEPES	4-(2-Hydroxyethyl)piperazine-1-ethanesulfonic acid
HDL	high density lipoprotein
IDL	intermediate density lipoprotein
KO	knockout
LCAT	lecithin:cholesterol acyl transferase
LCFA	long chain fatty acid
LDL	low density lipoprotein
LDLR	low density lipoprotein receptor
LDM	low density microsomes
Mito	mitochondria
MSA	murine serum albumin
NCLPDS	newborn calf lipoprotein deficient serum
oxLDL	oxidized LDL

PAGE	polyacrylamide gel electrophoresis
PM	plasma membrane
PMSF	phenylmethylsulfonylfluoride
PPAR	peroxisome proliferator activator receptor
PVDF	polyvinylidene fluoride
PBS	phosphate buffered saline
RCT	reverse cholesterol transport
rfu	Relative fluorescent unit
RNase	ribonuclease
TBS-T	200 mM tris-HCl pH 7.4, 137 mM NaCl, 0.1% tween 20
TEMED	N,N,N′, N′-tetramethylethylenediamine
Tris	2-Amino-2-(hydroxymethyl)-1,3-propanediol
SCAP	SREBP cleavage-activating protein
SDS	sodium dodecyl sulphate
SNP	single nucleotide polymorphism
SR-BI	scavenger receptor class B type I
SREBP	sterol regulatory element binding protein
VLDL	very low density lipoprotein

A Introduction

A.1 Fatty Acids and Triglycerides

Triglycerides (also known as triacylglycerols) are composed of a glycerol molecule with 3 fatty acids attached through an ester linkage. Triglycerides are highly abundant in the body as they are stored in large amounts in specialized cells known as adipocytes (Flier 1995). The adipocytes serve as a reserve of triglyceride, and hence fatty acids (Flier 1995). Fatty acids are vital molecules. Fatty acids are substrates for the synthesis of molecules such as phospholipids and sphingolipids that are required for cellular membranes (Kent 1995). Fatty acids can also serve as signaling molecules, either indirectly as substrates for the synthesis of eicosanoids (which are cellular regulator molecules)(Calder 2002) or directly as activators of peroxisome proliferator activated receptors (PPARs)(reviewed in (Kersten 2002)). Fatty acids are also an abundant energy source, providing energy via the beta-oxidation pathway. Fatty acid oxidation is a principal source of energy for many tissues, especially the heart (Zierler 1976).

A.2 Cholesterol

Cholesterol belongs to the sterol (steroid alcohol) class of molecules. Sterols are derivatives of tetracyclic compounds comprised of three six-carbon rings and one five-carbon ring (Mathews et al. 2000). Cholesterol is a key component of cellular membranes and its relative abundance can affect the structure and properties (such as

fluidity) of the membrane (Yeagle 1985). In addition cholesterol is also the principal substrate for the synthesis of steroid hormones (Simpson et al. 1967).

A.3 Lipid Metabolism

A.3.1 Absorption of Triglycerides and Cholesterol

Triglycerides and cholesterol are obtained from 2 primary sources, 1) de novo synthesis (Bloch 1965; Bell et al. 1980) and 2) dietary intake (Greenberger et al. 1966; Wilson et al. 1994). Lipids in the small intestine are emulsified by bile salts and hydrolyzed by pancreatic lipases and cholesterol esterases (Carey et al. 1983). Lipases liberate fatty acids and 2-monoacylglycerols that are taken up by the enterocytes of the intestine (Ho et al. 2001). The fatty acids and 2-monoacylglycerol are used to re-synthesize triglycerides in the intestinal mucosal cells (Ho et al. 2001). Cholesterol esterases in the bile hydrolyze the cholesterol esters and then the free cholesterol is taken up by the enterocytes (Turley et al. 2003). The mechanism of intestinal cholesterol absorption is not known (Turley et al. 2003). However, intestinal cholesterol absorption, and plasma cholesterol levels can be effectively decreased by treatment with the drug ezetimibe (Bays et al. 2001). Ezetimibe binds SR-BI (see Section A.4.2) but this binding does is not necessary for the inhibitory activity of ezetimibe as the drug is equally effective in wild type and SR-BI knockout mice (Altmann et al. 2002). The absorption of cholesterol into the intestine is a selective process as plant and shellfish sterols typically do not reach the circulation (Turley et al. 2003). This selectively is achieved through the

action of the half transporters ABCG5 and ABCG8, which can selectively pump certain sterols out of the enterocytes (Berge et al. 2000).

Within the enterocytes acyl-CoA:cholesterol acyltransferase 2 (ACAT-2) re-esterifies the cholesterol (Turley et al. 2003). Then triglycerides and cholesterol esters, as well as a small amount of free cholesterol are packaged into chylomicrons (Turley et al. 2003). The chylomicrons enter into the lymph and deliver the triglycerides to cells. In a similar manner, triglycerides synthesized in the liver are packaged into very low density lipoproteins (VLDL) for transport into the plasma (reviewed in (Shelness et al. 2001)) (see Figure 1).

A.3.2 Lipoproteins

Chylomicrons and VLDL are members of a group of molecular complexes called the lipoproteins. The lipoproteins are classified according to their relative density (Alaupovic 1996). Lipoproteins are used as a means of mobilizing hydrophobic lipids through the polar environment of the plasma. These molecular complexes are comprised of an outer polar shell comprised mainly of phospholipid, cholesterol and proteins (apolipoproteins) (reviewed in (Smith et al. 1978)). Within the core of the lipoprotein there are neutral lipids (e.g. triglycerides and cholesterol esters) (reviewed in (Smith et al. 1978)). Different classes of lipoproteins have distinct lipid and apolipoprotein compositions (see Table 1).

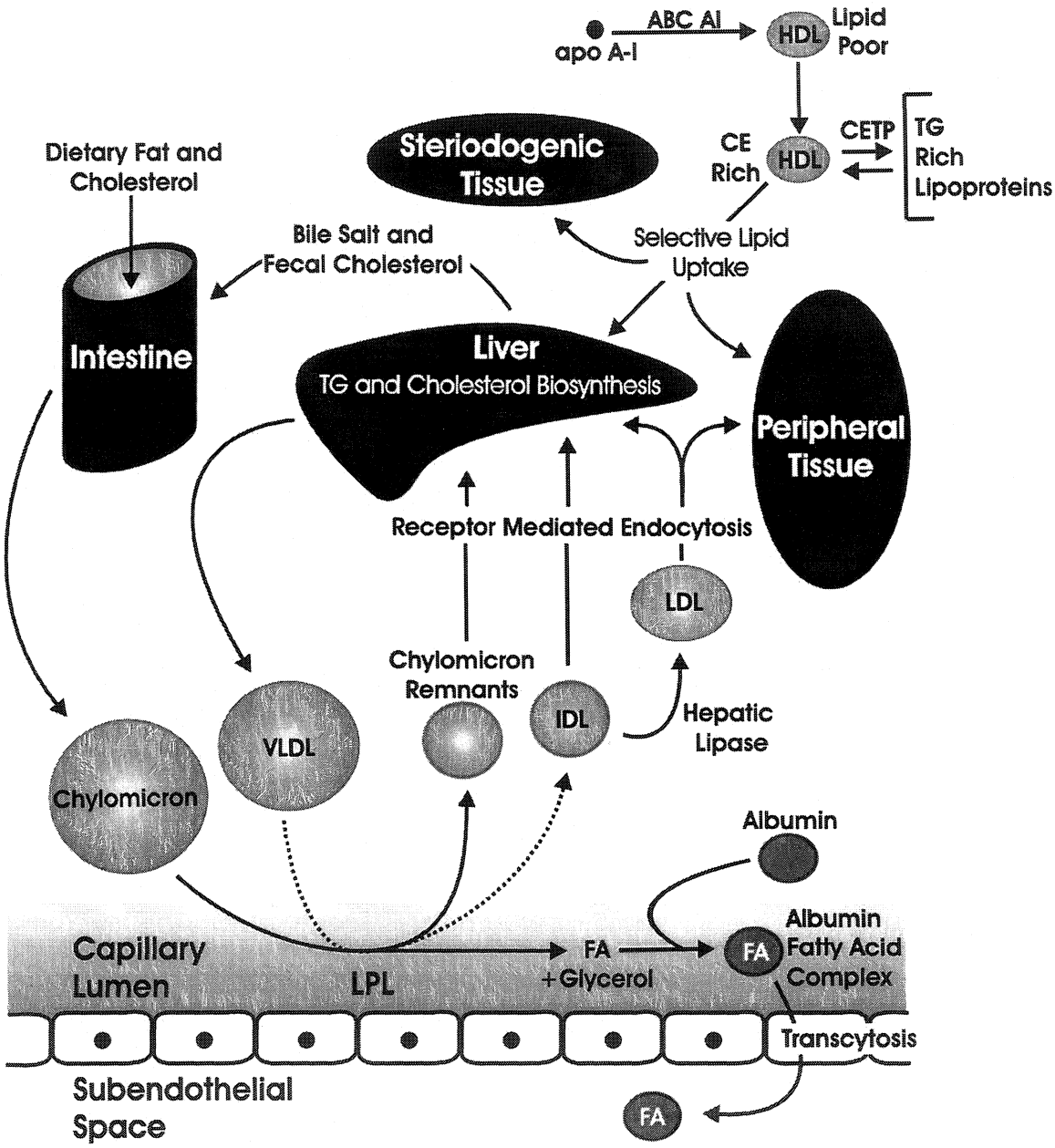

Figure 1. Overview of the Major Lipoprotein Pathways in Mice. The major pathways involved in lipid delivery and lipoprotein metabolism are outline and described in the text. Note that lipid poor HDL can also be produced by the intestinal mucosal, the liver and formed following remodeling of chylomicrons and VLDL by lipoprotein lipases. LPL (lipoprotein lipase), FA (fatty acid), TG (triglyceride), CE (cholesterol ester), CETP (cholesterol ester transfer protein). Figure adapted from (Mathews et al. 2000).

Table 1. Properties of the major plasma lipoprotein classes.

	Chylomicrons	VLDL	IDL	LDL	HDL
Density (g/ml)	<0.950	0.950-1.006	1.006-1.019	1.019-1.063	1.063-1.210
Components [a]					
Protein	2	8	15	22	40-55
Triglyceride	86	55	31	6	4
Free Cholesterol	2	7	7	8	4
Cholesterol Esters	3	12	23	42	12-20
Phospholipid	7	18	22	22	25-30
Apolipoprotein Composition	A-I, A-II, B-48, C-I, C-II, C-III	B-100, C-I, C-II, C-III, E	B-100, C-I, C-II, C-III, E	B-100	A-I, A-II, C-I, C-II, C-III, D, E

-adapted from (Mathews et al. 2000)

-[a] percentage of dry weight

A.3.3 Transport of Triglycerides to Tissues

The triglycerides in chylomicrons and VLDL are hydrolyzed back into fatty acids and glycerol in the lumen of capillaries. The hydrolysis of triglycerides is performed by lipoprotein lipase (see Figure 1) (Pedersen et al. 1983). Lipoprotein lipase is synthesized in the parenchymal cells and is transported to the luminal face of the endothelial cells where it is attached to cell surface heparan sulfate proteoglycans (Preiss-Landl et al. 2002). The liberated fatty acids can then either be taken up by the endothelial cells or bound to serum albumin, which has capacity to bind several molecules of fatty acid (Spector et al. 1969). The albumin fatty acid complexes are transported through the endothelial cell via transcytosis to the underlying cells for delivery of the fatty acids for cellular uptake (Schnitzer 1992)(see Figure 1).

A.3.4 The Mechanism of Cellular Long Chain Fatty Acid Uptake

Long chain fatty acid (LCFA)(fatty acids with 12 to 20 carbons) uptake into cells can be considered as a series of 3 steps: 1) dissociation of LCFA from albumin at the extracellular surface, 2) LCFA transmembrane movement, and 3) binding or metabolism of the LCFA on the cytosolic side of the plasma membrane. None of these individual steps are well understood. There are several models of LCFA uptake, which propose very different mechanisms for the aforementioned 3 steps. The two key issues that distinguish most models are: 1) Is the dissociation of LCFAs from albumin spontaneous or is it assisted at the cell surface? 2) Do LCFAs traverse the plasma membrane passively or do

proteins facilitate the process? Despite a great deal of experimental data these questions remain unresolved.

A.3.4.1 Dissociation of LCFAs from Albumin

A.3.4.1.1 Albumin Receptor Kinetics

Traditional views of LCFA uptake had assumed that prior to cellular uptake, fatty acids must first spontaneously dissociate from albumin. This concept of LCFA uptake was brought into question by an important set of experiments performed by Weisiger and colleagues (Weisiger et al. 1981). In these experiments it was demonstrated that LCFA uptake increased up to saturation when the concentration of an oleate:albumin complex (at a constant fatty acid to albumin molar ratio) was increased. Under these conditions the free fatty acid concentration was essentially constant. When LCFA uptake was measured under conditions where the total fatty acid concentration was increased and the albumin concentration was held constant (thereby increasing the free fatty acid concentration) LCFA uptake increased. The increase was linear with respect to the total fatty acid concentration (but not the free fatty acid concentration). From these experiments (Weisiger et al. 1981) developed a model of uptake where LCFA:albumin complexes bind to a receptor on the cell surface facilitating the release of the LCFA for cellular uptake.

Since then similar observations have been made in several other cell types including, T-lymphocytes (Uriel et al. 1994), cardiomyocytes (Hutter et al. 1984), and adipocytes (Trigatti et al. 1995). Since the initial proposal that an albumin receptor facilitates LCFA uptake from albumin, others have suggested mechanisms by which the cell surface may facilitate uptake, see Section A.3.4.1.1.3. In addition two other models, dissociation limited uptake (Section A.3.4.1.1.1) and codiffusion (Section A.3.4.1.1.2) have been proposed in an attempt to account for the observations.

A.3.4.1.1.1 Dissociation Limiting Uptake

The dissociation limiting uptake model suggests that albumin receptor kinetics arise as a result of limited dissociation of LCFAs from albumin (Weisiger 1985; Sorrentino et al. 1989). According to this model, at low albumin concentration (in which many experiments finding albumin receptor kinetics are performed) the rate-limiting step of LCFA uptake is the rate of dissociation of LCFAs from albumin. However at higher albumin concentrations (those closer to physiological levels), dissociation of LCFAs from albumin no longer limits the rate of LCFA. Thus as the concentration of albumin increases the rate of LCFA uptake increases and begins to saturate as cellular uptake becomes the rate limiting step of uptake. Experiments by (Trigatti et al. 1995) provided evidence that uptake is not limited by the pool of free fatty acid even at low albumin concentrations. Therefore at least for adipocytes, LCFA uptake is not limited by dissociation of fatty acids from albumin.

A.3.4.1.1.2 The Unstirred Layer Effect/Codiffusion

Another model of LCFA uptake from albumin accounts for albumin receptor kinetics as an effect of the unstirred layer that surrounds cells. This unstirred layer acts as a barrier that limits the diffusion of fatty acids from the bulk solution to the cell surface. LCFAs can diffuse through this layer as either free fatty acids or complexed to albumin. Since the amount of complexed fatty acid is much greater than free fatty acid, the amount of albumin present dictates the capacity for diffusion through this layer (Weisiger et al. 1989). At low albumin concentrations, LCFA uptake is limited by diffusion through the unstirred layer. As the albumin concentration increases, uptake becomes limited by cellular uptake rates. However Burczynski and Cai have reported that this theoretical analysis of LCFA uptake cannot fully account for albumin receptor kinetics (Burczynski et al. 1989; Burczynski et al. 1994).

A.3.4.1.1.3 Facilitation

The facilitation hypothesis of LCFA uptake from albumin is based on the concept that albumin interacts with the cell surface and this interaction facilitates the dissociation of LCFAs from albumin for cellular uptake. The original proposal of facilitation focused on the presence of an albumin receptor (Weisiger et al. 1981). Subsequently others have suggested that albumin interacts with the cell surface either nonspecifically (Horie et al. 1988), due to ionic interactions (Burczynski et al. 1997), or as a result of a subpopulation of albumin with an increased affinity for the cell surface (Reed et al. 1989).

A.3.4.1.2 Albumin Binding Proteins

Consistent with the facilitation hypothesis, albumin has been found to bind several cell types including rat hepatocytes (Horie et al. 1988; Reed et al. 1989), rat cardiomyocytes (Popov et al. 1992), human B-lymphoma cells, human blood mononuclear cells (Torres et al. 1992), rat endothelial cells (Schnitzer et al. 1988), 3T3-L1 adipocytes (a murine cell line that can be induced to differentiate to an adipocyte phenotype)(Trigatti et al. 1995), and rat primary adipocytes (Brandes et al. 1982). Furthermore cell surface albumin binding proteins have been discovered. Several groups have identified, 31 kDa and 18 kDa glycoproteins with albumin binding activity (Ghinea et al. 1988; Popov et al. 1992; Torres et al. 1992). However these proteins have subsequently been found to preferentially bind chemically modified albumin (e.g. gold conjugated, maleylated and formaldehyde treated albumin)(Schnitzer et al. 1992). In addition, binding of albumin to these proteins results in their internalization and degradation (Schnitzer et al. 1993). Thus these proteins are not likely to be involved in LCFA uptake, as albumin is not internalized during the process (Samuel et al. 1976; Brandes et al. 1982; Ockner et al. 1983). In addition to identifying the 18 and 31 kDa albumin binding proteins, Ghinea et al. also detected novel albumin binding proteins of 56 kDa and a 73 kDa in endothelial cells (Ghinea et al. 1989). The relevance of these proteins is not known, as the albumin binding activity was weak (accounting for less than 30% of the total albumin binding activity) and the binding specificity has not been determined.

A 60 kDa endothelial protein has been found to bind albumin and was named albondin (Schnitzer 1992). In contrast to the 18 and 31 kDa proteins discussed above, this protein has preferential affinity for native albumin and does not lead to albumin degradation (Schnitzer et al. 1993). This protein is involved in transcytosis of albumin from the capillary lumen across endothelial cells (Schnitzer et al. 1994). To date there has been no evidence that this protein is involved in facilitating LCFA release for cellular uptake. Despite numerous studies and the identification of several albumin binding proteins, none of them have been shown to act as albumin receptors mediating cellular LCFA uptake.

A.3.4.2 Translocation of LCFAs Across the Plasma Membrane

A.3.4.2.1 Passive Diffusion

Some models of LCFA uptake contend that cells take up LCFAs by a passive process driven by a chemical gradient (reviewed in (Hamilton 1998)). The 3 steps of LCFA uptake outlined in Section A.3.4 can be considered in physio-chemical terms as adsorption to the plasma membrane extracellular leaflet, transmembrane movement (commonly referred to as flip-flop) and desorption from the cytosolic leaflet of the plasma membrane. Proponents of a passive diffusion model suggest that the 3 steps can all occur spontaneously (i.e. in the absence of protein facilitation) at a rate fast enough to account for cellular uptake (as reviewed in (Hamilton 1998)). LCFAs can spontaneously dissociate from albumin and partition into phosphatidylcholine vesicles (Hamilton et al.

1986), although it is not certain if this can occur at physiological fatty acid to albumin ratios (Abumrad et al. 1998). The issue of membrane flip-flop has been a more controversial matter. Some experimental data suggests that flip-flop can occur on the millisecond time scale (Thomas et al. 2002), while other data suggests flip-flop may take upwards of 3 seconds, which would be rate limiting (Kleinfeld et al. 1997). The rates obtained from such studies may depend largely on the methodology employed (Hamilton 1998). For example, many studies make use of synthetic fluorescent derivatives of fatty acids, which may behave differently than natural fatty acids (Hamilton 1998). Furthermore the use of small versus large unilamellar phospholipid vesicles may affect the flip-flop rate (Hamilton 1998). In addition, the conclusions drawn from some of the experimental approaches may depend on assumptions made regarding the adsorption and desorption rates (Hamilton 1998). Studies by Zhang et al., have found that desorption of fatty acids from small unilamellar vesicles can be rapid (on the time scale of seconds) and the rate is chain length dependent. These authors suggest that the measured rates of desorption are sufficiently fast to account for cellular uptake (Zhang et al. 1996).

Although LCFA absorption, flip-flop, and desorption may occur passively in model systems, its contribution to cellular uptake is not certain. Uptake experiments performed over a range of free fatty acid concentrations (generated by increasing the fatty acid to albumin molar ratio) are often modeled to consist of a saturable component and a non-saturable or low affinity process (Abumrad et al. 1981; Trigatti et al. 1991; Berk et

al. 1999). A common interpretation is that the latter process is due to passive diffusion (Abumrad et al. 1981; Berk et al. 1999). Attempts have been made to determine the contribution of passive diffusion at physiological conditions (Trigatti et al. 1996; Kamp et al. 2003), however the issue remains unresolved.

A.3.4.2.2 Facilitated Diffusion

Several lines of evidence have supported the hypothesis that LCFA uptake is protein mediated: 1) Uptake is saturable, 2) uptake can be competed by other LCFAs but not short chain fatty acids, and 3) uptake is sensitive to numerous protein modifying agents (reviewed in (Abumrad et al. 1998)). In addition to evidence of protein involvement, several proteins have been identified with clear evidence supporting their role in LCFA uptake. These proteins include, CD36 (also known as fatty acid translocase (FAT)), fatty acid transport protein (FATP), and the plasma membrane fatty acid binding protein (FABPpm) (reviewed in (Hui et al. 1997; Abumrad et al. 1998; Luiken et al. 1999)). Furthermore, caveolin and the adipose differentiation related protein (ADRP) have also been implicated in LCFA uptake (Gao et al. 1999; Trigatti et al. 1999), although there is less experimental support for their role. How these proteins may function with respect to each other is not known.

A.3.4.2.2.1 CD36/FAT

Abumrad et al. initially suggested that a protein of approximately 85 kDa in adipocyte plasma membranes might be a LCFA transporter (Abumrad et al. 1984). Consistent with this prediction, treatment of cells with sulfo-N-succinimidyl derivatives of oleic acid (Harmon et al. 1991) and 4,4′-diisothiocyanostilbene-2-2′-sulfonate (DIDS) (Abumrad et al. 1984) resulted in both the inhibition of LCFA uptake and the labeling of a protein of approximately 85 kDa. Further studies resulted in the cloning of the cDNA for the protein, which was named FAT. The cDNA coded for a protein with a predicted molecular weight of 53 kDa, and also contained 10 potential glycosylation sites (N-X-S/T) thereby accounting for the discrepancy with the observed molecular weight of 88 kDa (Abumrad et al. 1993). The cloning of the cDNA revealed that the protein was in fact CD36, a plasma membrane protein that has been localized to caveolae (Lisanti et al. 1994). CD36 binds to a wide array of substrates including modified LDL, thrombospondin, anionic phospholipids, rod outer segments, collagen and *Plasmodium falciparum* infected erythrocytes (reviewed in (Krieger 1999)). Furthermore CD36/FAT is expressed in numerous tissues including, adipose, heart, testis, spleen, intestine, skeletal muscle (Abumrad et al. 1993), macrophages, monocytes, platelets, epithelial cells and endothelial cells (reviewed in (Krieger 1999))

Numerous studies have demonstrated a role for CD36/FAT in LCFA uptake. Expression of exogenous CD36/FAT in a fibroblast cell line (that did not express

CD36/FAT) increased LCFA uptake approximately 3.5 fold (Ibrahimi et al. 1996). Furthermore CD36 antisense expression, which reduced CD36 protein levels by 3 fold, also reduced LCFA uptake from 3 to 6 fold in 3T3-F442A adipocytes (Sfeir et al. 1999). In addition, a null mutation in the CD36 gene in mice resulted in a significant 2 fold increase in fasting levels of free fatty acids (a finding consistent with decreased tissue extraction of fatty acids) and a 1.5 fold decrease in oleate uptake by adipocytes from CD36 null mice versus wild-type mice (Febbraio et al. 1999). In humans, CD36 deficiency is associated with increased plasma triglyceride levels relative to control groups, consistent with a role for CD36 in LCFA uptake (Furuhashi et al. 2003). Furthermore, human CD36 deficiency (Yoshizumi et al. 2000; Kintaka et al. 2002) and the spontaneous hypertensive rat (SHR) that has a defective CD36 gene (Aitman et al. 1999), have impaired LCFA uptake. Although CD36/FAT is clearly involved in LCFA uptake, the mechanism remains elusive.

A.3.4.2.2.2 FATP

FATP is a 63 kDa integral plasma membrane protein that has been implicated in mediating LCFA uptake. The FATP cDNA was identified from a 3T3-L1 adipocyte cDNA library, based on its ability to increase the uptake of LCFA when expressed in cultured mammalian cells (Schaffer et al. 1994). Subsequently other FATP genes have been identified. The FATP family currently consists of 6 members, FATP 1 through 6 (reviewed in (Stahl 2003)). *Mus musculus* FATP1 (mmFATP1) shows a wide tissue

distribution including heart, brain, lung, skeletal muscle, kidney, testis (Hirsch et al. 1998) and adipose tissue (Schaffer et al. 1994). Of the mFATP family, mmFATP2 is expressed predominately in the liver and kidney, mmFATP3 is expressed in lung, liver and testis, and mmFATP4 is highly expressed in brain, liver, kidney (Hirsch et al. 1998), skin and small intestine (Herrmann et al. 2001). mmFATP5 expression appears liver specific (Hirsch et al. 1998). Human FATP6 has recently been cloned and it is principally expressed in the heart (Gimeno et al. 2003).

There has been some uncertainty regarding the activity of the FATP proteins. Several of the FATP family members have been demonstrated to have acyl-CoA synthetase activity (with high activity on very long chain fatty acids), including FATP1 (Coe et al. 1999) and FATP4 (Herrmann et al. 2001). Interestingly the screen that was used to identify the mmFATP1 cDNA also identified one other protein that increased lipid uptake, FACS, a fatty acyl-CoA synthetase (Schaffer et al. 1994). Further experiments will need to be performed to determine if FATP has intrinsic acyl-CoA synthetase activity or if it interacts tightly with another protein with acyl-CoA synthetase activity, and if this activity is related to its LCFA uptake activity.

Recently mice have been generated with a targeted disruption of the FATP4 gene (Herrmann et al. 2003). Heterozygous mice appeared normal while homozygous FATP4 mutant pups died within hours of birth apparently as a result of altered formation of the

epidermal barrier (Herrmann et al. 2003). This is likely attributable to decreased very long chain fatty acids in epidermal ceramides (Herrmann et al. 2003). The lipid composition of the intestine, liver, lung, and brain from homozygous mutant FATP4 mice were similar to wild-type mice (Herrmann et al. 2003). Furthermore differentiation of embryonic fibroblasts from the FATP4 homozygous mutant mice to adipocytes in culture appeared normal (Herrmann et al. 2003). Further analysis of these mice should provide insight into the physiological activity of FATP4.

A.3.4.2.2.3 FABPpm

FABPpm was first identified as a membrane fatty acid binding protein from oleate affinity chromatography experiments (Stremmel et al. 1985). The 43 kDa FABPpm has been purified from detergent solubilized (Stremmel et al. 1985) or salt extracted (Potter et al. 1987) plasma membranes. In chromatography experiments purified FABPpm was found to co-migrate with a variety of LCFAs but not other lipid species such as cholesterol esters of oleate or phosphatidylcholine (with oleate in position 2) (Stremmel et al. 1985). Surprisingly FABPpm was found to be identical to another protein, mitochondrial aspartate aminotransferase (mAspAT) (Stump et al. 1993). Immunofluorescence and immunogold electron microscopy studies with an antibody to mAspAT have provided evidence that the protein is indeed located at both the plasma membrane and mitochondria (Isola et al. 1995; Cechetto et al. 2002).

The participation of FABPpm in LCFA uptake was suggested by the ability of antibodies directed against FABPpm to inhibit LCFA uptake in several cell types including hepatocytes (Stremmel et al. 1986), adipocytes (Schwieterman et al. 1988), cardiomyocytes (Sorrentino et al. 1988) and jejunal enterocytes (Stremmel 1988). In addition, expression of the FABPpm cDNA in 3T3 fibroblasts resulted in a 3-fold increase in LCFA uptake and this increase could be partially blocked by an antibody to FABPpm (Isola et al. 1995). It is not known how FABPpm mediates LCFA uptake, but it is unlikely that it does so by intrinsic translocase activity, as FABPpm is a peripheral membrane protein (Stump et al. 1993).

A.3.4.2.2.4 ADRP

The 53 kDa adipose differentiation related protein (ADRP) was identified using a differential hybridization screen of 1246 cells (a mouse cell line that can differentiate to the adipocyte phenotype) to identify genes whose expression was turned on early in differentiation (Jiang et al. 1992; Jiang et al. 1992). Subsequently ADRP has been found to be expressed in numerous cell types including brain, lung liver and testes (Gao et al. 1999). Expression of the ADRP cDNA in COS cells resulted in a 3-fold increase in LCFA uptake over empty vector transfected cells (Gao et al. 1999). Expression of ADRP did not alter the metabolic fate of LCFA (e.g. free, phospholipids, and neutral lipids) and thus did not drive uptake in this manner (Gao et al. 1999). However the role of ADRP in LCFA is not clear, as it appears to be localized predominately at the lipid droplet

(Brasaemle et al. 1997). Gao et al. suggest that ADRP may act as a shuttle for LCFA from the plasma membrane to the lipid droplet, although this remains speculative (Gao et al. 1999).

A.3.4.2.2.5 Caveolin

The caveolins are a class of proteins comprised of caveolin 1, 2 and 3, encoded by 3 distinct genes. Caveolin-1 and 2 are expressed in many tissues but are highly abundant in lung and adipose tissue (Scherer et al. 1997). Caveolin-3 is expressed predominately in skeletal muscle (Tang et al. 1996). There are two isoforms (α and β) of caveolin-1, which differ in their amino terminus as a result of an alternate translation start site (Scherer et al. 1995).

Caveolin-1 has been found in several different cellular locations including the Golgi, vesicular structures (Kurzchalia et al. 1992), lipid droplets (Pol et al. 2003), mitochondria and the cytoplasm (Li et al. 2001). However the preferred location for caveolin is at the cell surface in a specialized domain called caveolae (Liu et al. 2002). Caveolae were first identified in 1953 as small flask shaped structures in the plasma membrane (Palade 1953). Caveolae are a particular form of a membrane domain known as lipid rafts (Brown et al. 2000). In fact it is the presence of caveolin in a lipid raft that is often used as an operational definition of caveolae (Rothberg et al. 1992; Lai 2003).

Lipid rafts are rich in sphingolipids and cholesterol (Brown et al. 2000). The enrichment of these lipids in lipid rafts results in their resistance to solubilization with non-ionic detergents at low temperature (Brown et al. 2000). This property is commonly exploited to biochemically fractionate lipid rafts (Brown et al. 1992; Lai 2003). Other methods to biochemically fractionate lipid rafts employ the low density of rafts, their adsorption to cationized silica, or immunoabsorption by anti-caveolin antibodies (in the case of caveolae)(reviewed in (Anderson 1998)). However the lipid rafts generated by these techniques may not be equivalent (Anderson 1998) and may lead to misinterpretations (Lai 2003).

Caveolae have been implicated in numerous processes including; transport processes, signaling events, and vesicular trafficking events (Maxfield 2002). Examples include; transcytosis, potocytosis, viral entry, processing of Alzheimer disease–related protein APP, signal transduction by receptor tyrosine kinases and G proteins (reviewed in (Engelman et al. 1998)) and bi-directional transport of cholesterol between the endoplasmic reticulum (ER) and plasma membrane (Uittenbogaard et al. 1998; Uittenbogaard et al. 2002). Previous work from the Gerber lab has found that caveolin is also a fatty acid binding protein. Caveolin-1 was specifically labeled in plasma membranes from 3T3-L1 adipocytes by a photoreactive fatty acid analogue (Trigatti et al. 1999). The relevance of this binding though is not clear.

A.3.5 Cholesterol Transport to Tissues via LDL

Hydrolysis of VLDL and chylomicrons by lipoprotein lipases leads to particles called intermediate density lipoprotein (IDL) and chylomicron remnants respectively (reviewed in (Mead et al. 2002)). IDL and chylomicron remnant particles are returned to the liver and undergo receptor-mediated endocytosis leading to degradation (reviewed in (Chappell et al. 1998; Mead et al. 2002))(see Figure 1). In the plasma IDL can be converted into LDL through the action of lipoprotein lipase and hepatic lipase (reviewed in (Kwiterovich 2000; Zambon et al. 2003))(see Figure 1). Triglycerides and cholesterol esters can be transferred between the lipoproteins through the action of cholesterol ester transfer protein (CETP) (reviewed in (Barter et al. 2003)). However CETP is not expressed in all species (Ha et al. 1982) and the mouse is among those that lack CETP (Hogarth et al. 2003).

Cellular uptake of cholesterol from LDL occurs primarily by binding to the LDL receptor, which leads to receptor-mediated endocytosis (Brown et al. 1986)(see Figure 1). LDL receptors are localized in coated pits on the cell surface and following binding of LDL to the receptor the complex is internalized (Anderson et al. 1977). Internalization occurs by the coated pit forming a coated vesicle that eventually becomes an endosome (Anderson et al. 1977). In the endosomes the receptor and lipoprotein dissociate and the receptor is recycled back to the plasma membrane (reviewed in (Brown et al. 1986)). The lipoprotein is delivered to lysosomes where the particle is degraded releasing cholesterol

for cellular metabolism (Goldstein et al. 1975). Cellular uptake of cholesterol via the LDL receptor pathway is under negative feed back control (reviewed in (Brown et al. 1986)). This is accomplished by membrane bound transcription factors called sterol regulatory element binding proteins (SREBP-1 and SREBP-2) that bind to sterol regulatory elements in the promoters of genes involved in cholesterol metabolism including the LDL receptor (reviewed in (Brown et al. 1999)). In conditions of low membrane sterol SREBP forms a complex with sterol cleavage-activating protein (SCAP) (Sakai et al. 1997) that allows for transport of SREBP from the ER to the Golgi (Nohturfft et al. 1999). In the Golgi SREBPs are converted to a soluble form by two proteolytic events performed by site-1 protease (Sakai et al. 1998) and then site-2 protease (Rawson et al. 1997). The soluble form of SREBP then enters to the nucleus binding to sterol regulatory elements of several genes including the LDL receptor (Sakai et al. 1996). In the presence of sterols these are events are blocked by the association of SCAP with the insulin induced genes 1 and 2 (INSIG-1 and INSIG-2), which prevents the transport of SCAP from the ER to the Golgi (Yabe et al. 2002; Yang et al. 2002).

A.3.6 Reverse Cholesterol Transport

Glomset was the first to propose reverse cholesterol transport (RCT) as a pathway for cholesterol transfer from non-hepatic (peripheral tissues) back to the liver for excretion in the bile or re-secretion in nascent lipoproteins (Glomset 1968). HDL is a key component of this pathway (Glomset 1968). Lipid rich HDL arises from lipid poor or

lipid free apolipoproteins (reviewed in (von Eckardstein et al. 2001))(see Figure 1). Nascent lipid poor HDL is produced by the liver and intestinal mucosal, alternatively it can also be formed following remodeling of chylomicrons and VLDL by lipoprotein lipases (reviewed in (von Eckardstein et al. 2001)). Lipid poor HDL acquires free cholesterol from cells in a process that is mediated by ABCA1 (Lawn et al. 1999; Wang et al. 2000)(see Figure 1). A mutation in ABCA1 was found to be the cause of a rare genetic disorder, Tangier disease (Bodzioch et al. 1999; Brooks-Wilson et al. 1999; Rust et al. 1999). This disease is a condition associated with a lack of HDL cholesterol and decreased cellular efflux of cholesterol and phospholipid (Francis et al. 1995). Free cholesterol in HDL is esterified by LCAT (lecithin: cholesterol acyl transferase)(reviewed in (von Eckardstein et al. 2001)). Cholesterol esters in lipid rich HDL can either be 1) transferred to VLDL, IDL, or LDL by cholesterol ester transfer protein (CETP), 2) under go selective lipid uptake (transfer of HDL's lipid but not protein components, see Section A.4.3) at peripheral tissues such as steroidogenic tissue, or 3) taken up by the liver and re-secreted in VLDL or excreted in the bile (reviewed in (Fielding et al. 1995; Angelin et al. 2002; Sviridov et al. 2002)).

A.4 Scavenger Receptor Class B Type I

A.4.1 Lipoproteins and The Scavenger Receptors

Scavenger receptors can be defined as cell surface proteins that bind chemically modified lipoproteins (Krieger 2001). Numerous scavenger receptors have been

identified (reviewed in (Itabe 2003)). Several of these scavenger receptors have been shown to play critical roles in lipoprotein metabolism and atherosclerosis (see Section A.5.3)(Krieger 1999).

A.4.2 The HDL Receptor, Scavenger Receptor Class Type I

Scavenger receptor class B type I (SR-BI) originally cloned from a CHO variant (this variant Var-261 expressed a scavenger receptor activity distinct from that of SR-AI or SR-AII (Krieger 1999)) cDNA library and was found to have significant homology with CD36 (a scavenger receptor class B protein) (Acton et al. 1994). The predicted molecular weight of murine SR-BI (mSR-BI) is 57 kDa (Acton et al. 1996) but the protein migrates on SDS-PAGE with an apparent molecular weight of 82 kDa largely due to *N*-linked glycosylation (Babitt et al. 1997). SR-BI is an integral membrane protein that is palmitoylated and preferentially localizes to caveolae (Babitt et al. 1997). A splice variant of SR-BI with a different carboxy-terminal cytoplasmic domain has been identified, SR-BII (Webb et al. 1998). SR-BII also is preferentially localized in caveolae and has activities similar to those of SR-BI (see Section A.4.3 and A.4.4)(Webb et al. 1998).

SR-BI protein is most abundant in the liver, ovaries, and adrenal glands (Acton et al. 1996). These same tissues are also very active in a particular form of cholesterol uptake, selective lipid uptake (described in Section A.4.3) (Acton et al. 1996)(see Figure

1). SR-BI is also expressed (at lower levels) in many other tissues including testis Sertoli cells, heart, mammary gland (Acton et al. 1996), astrocytes (Husemann et al. 2001), smooth muscle cells (Husemann et al. 2001), endothelial cells (Uittenbogaard et al. 2000) and macrophages (Ji et al. 1997; Hirano et al. 1999; Chinetti et al. 2000).

SR-BI binds a wide array of ligands, including HDL (Acton et al. 1996), oxidized HDL (Marsche et al. 2002), native and acetylated LDL (Acton et al. 1994; Murao et al. 1997), oxidized LDL (Calvo et al. 1997; Murao et al. 1997; Gillotte-Taylor et al. 2001), maleylated BSA (Acton et al. 1994), anionic phospholipids (Rigotti et al. 1995), VLDL (Calvo et al. 1997), and advanced glycation end products (AGE) (Ohgami et al. 2001). SR-BI can also bind to several apolipoproteins present on HDL (see Table 1) apoA-I, apoA-II, apoC-III (Xu et al. 1997; Liadaki et al. 2000) and apoE (Bultel-Brienne et al. 2002). However SR-BI does not have affinity for several polyanions (fucoidin, carrageenan, and polyguanosinic acid) that are established ligands of class A scavenger receptors (Acton et al. 1994). Although SR-BI binds a number of ligands, the HDL binding activity was considered likely to be significant in vivo as LDL was found to compete poorly for HDL binding (Acton et al. 1996).

A.4.3 SR-BI and Selective Lipid Uptake

The mechanism of cellular cholesterol uptake from HDL occurs by a distinctly different pathway than the classical LDL receptor mediated endocytosis pathway (see

Section A.3.5)(Glass et al. 1983; Leitersdorf et al. 1984; Glass et al. 1985). Selective lipid uptake refers to the preferential uptake of neutral lipids (e.g. cholesterol ester and triglyceride) over protein components of the lipoprotein particle (Glass et al. 1983; Leitersdorf et al. 1984; Glass et al. 1985). SR-BI mediates selective lipid uptake from HDL (Acton et al. 1996) and LDL (Stangl et al. 1999; Swarnakar et al. 1999; Rhainds et al. 2003). One model of selective lipid uptake proposes that HDL can be internalized and resecreted in the absence of degradation, and that this transient internalization of HDL may be important for the selective uptake process (Silver et al. 2001)(reviewed in (Silver et al. 2001)). However in experiments with multilamellar vesicles consisting of phosphatidylcholine, cholesterol and purified SR-BI, selective lipid uptake still occurred, suggesting internalization is not required (Liu et al. 2002).

The molecular details of SR-BI mediated selective lipid uptake are not known. Mechanisms have been proposed whereby transfer of cholesterol esters from HDL occurs spontaneously, and one possible model is that SR-BI tethers HDL in close proximity to the cell surface and thereby facilitates uptake (Gu et al. 1998). However, HDL being in close proximity to the cell surface alone is not sufficient for uptake. Several experiments including domain-swapping experiments with CD36 (which also binds HDL but does not mediate lipid transfer) (Gu et al. 1998; Connelly et al. 2001), insertion mutants of SR-BI (Connelly et al. 2003), and studies with small molecule inhibitors (Nieland et al. 2002), have shown that lipid uptake can be inhibited while HDL binding is maintained.

A.4.4 SR-BI and Cellular Cholesterol Efflux

In addition to mediating selective lipid uptake SR-BI can also mediate cholesterol efflux from cultured cells. Several studies have shown that overexpression of SR-BI can increase cellular cholesterol efflux (Ji et al. 1997; Stangl et al. 1998; Gu et al. 2000; Ohgami et al. 2001; Huang et al. 2002). Furthermore the rate of cholesterol efflux from a number of cell lines correlated with the level of SR-BI expression (Ji et al. 1997). SR-BI can mediate cholesterol efflux to several cholesterol acceptors including HDL, LDL (Gu et al. 2000), phospholipid vesicles (Jian et al. 1998) and phospholipid-rich but not lipid-free apolipoprotein A-I (Ji et al. 1997). Despite the potential importance to RCT, the physiological significance of cholesterol efflux via SR-BI has not been determined.

A.4.5 Physiological Significance of SR-BI

The physiological significance of SR-BI in lipoprotein metabolism has been clearly demonstrated by studies of mice with a targeted mutation in the SR-BI gene. Mice were generated by homologous recombination that replaced the first coding exon of the SR-BI gene with a neomycin resistance expression cassette (Rigotti et al. 1997). The resulting mice did not express any detectable SR-BI in the liver (Rigotti et al. 1997). Complete ablation of SR-BI in mice resulted in disruption of HDL cholesterol metabolism (Rigotti et al. 1997). Relative to wild-type mice, mice that were heterozygous for the SR-BI mutant allele had a 1.3 fold increase in plasma cholesterol and a near 50% reduction in adrenal gland cholesterol (Rigotti et al. 1997). In

comparison mice that were homozygous for the mutant allele (referred to as SR-BI KO) had a 2.2-fold increase in plasma cholesterol, and a greater than 70% decrease in adrenal gland cholesterol (Rigotti et al. 1997). In all mice apoA-I levels were normal (Rigotti et al. 1997). The changes in plasma cholesterol correlated with an increase in HDL associated cholesterol as well as an increase in the apparent size of HDL particles (as determined by size exclusion chromatography) (Rigotti et al. 1997). These changes in plasma cholesterol are consistent with SR-BI playing a key role in selective lipid uptake in the liver and adrenal gland (Rigotti et al. 1997).

These findings were confirmed and extended by studies of a mouse with attenuated SR-BI expression (SR-BI att). SR-BI att mice, which were generated by introduction of a neomycin resistance gene into the promoter region of the SR-BI gene, had approximately 50% less hepatic expression of SR-BI than wild-type mice (Varban et al. 1998). Relative to wild-type mice, the SR-BI att mice had a 1.5-fold increase in plasma cholesterol, which was attributable to increased HDL cholesterol (Varban et al. 1998). Furthermore selective lipid uptake in the livers from SR-BI att mice was reduced by approximately 50% relative to wild-type mice (Varban et al. 1998).

In addition to the above studies with global attenuation or ablation of SR-BI, studies of mice with liver specific alterations in SR-BI expression have provided evidence that hepatic SR-BI mediates HDL selective lipid uptake. Acute adenovirus-mediated

overexpression of SR-BI in the liver resulted in a near complete elimination of HDL cholesterol, a substantial increase in biliary cholesterol, and an increase in HDL clearance (Kozarsky et al. 1997). Likewise in experiments with chronic hepatic SR-BI overexpression in transgenic mice there was a decrease in plasma cholesterol relative to wild-type mice (Wang et al. 1998; Ueda et al. 1999) and an increase in biliary cholesterol (Sehayek et al. 1998). Furthermore there was also an increase in the clearance of HDL as well as of VLDL and LDL (Wang et al. 1998; Ueda et al. 1999). Thus these studies provide evidence that hepatic SR-BI promotes overall reverse cholesterol transport by increasing selective uptake and or increased biliary cholesterol excretion.

A.4.6 SR-BI Polymorphisms and HDL Metabolism

Studies with mice have clearly demonstrated that SR-BI has an important role in lipoprotein metabolism in these animals, however the impact of SR-BI on human lipoprotein metabolism is not certain. Studies assessing the correlation between SR-BI genetic variation and lipid metabolism have begun to address this. In a study of the human SR-BI gene, Acton et al., identified 3 common single nucleotide polymorphisms (SNP) (Acton et al. 1999). A SNP in exon 1 (resulting in a glycine to serine substitution at the second amino acid) was found to be associated with a statistically significant increase in HDL cholesterol and decrease in LDL cholesterol in men, but not women (Acton et al. 1999). This SNP may have particular consequence in type 2 diabetics (Osgood et al. 2003). Expression of SR-BI with a mutation at this glycine (to an alanine)

in cultured cells did not affect SR-BI expression levels, activity or localization (Gu et al. 1998). Another SNP in exon 8 (which did not result in any amino acid changes) was associated with lower LDL cholesterol in women but not men while a SNP in exon 5 (which did not result in any amino acid changes) was associated with an increased body mass index in women (Acton et al. 1999). Furthermore Hsu et al. have found a SR-BI promoter deletion in a Taiwanese population (Hsu et al. 2003). The mutation occurs between bases -140 to –150 from the transcription start site and corresponds to an Sp1 binding sequence, which may be required for optimal transcription of the gene (Hsu et al. 2003). This promoter deletion was associated with a statistically significant increase in plasma HDL cholesterol levels (Hsu et al. 2003). Thus the data emerging from these studies is consistent with SR-BI having an impact on lipid metabolism in humans.

A.5 Atherosclerosis

A.5.1 Development and Progression of Atherosclerosis

Atherosclerosis is a progression of vascular events that can ultimately culminate in the occlusion of blood vessels leading to the pathogenesis of myocardial and cerebral infarction (reviewed in (Lusis 2000)). The earliest distinctive feature of atherosclerosis is the appearance of fatty streak lesions (Ross 1993). The fatty streak lesion is characterized by the accumulation of lipid-rich macrophages (also known as foam cells) in the subendothelial space (the intima) of the blood vessel (see Figure 2). As a fatty streak lesion advances an extracellular lipid-rich necrotic core forms and smooth muscle cells

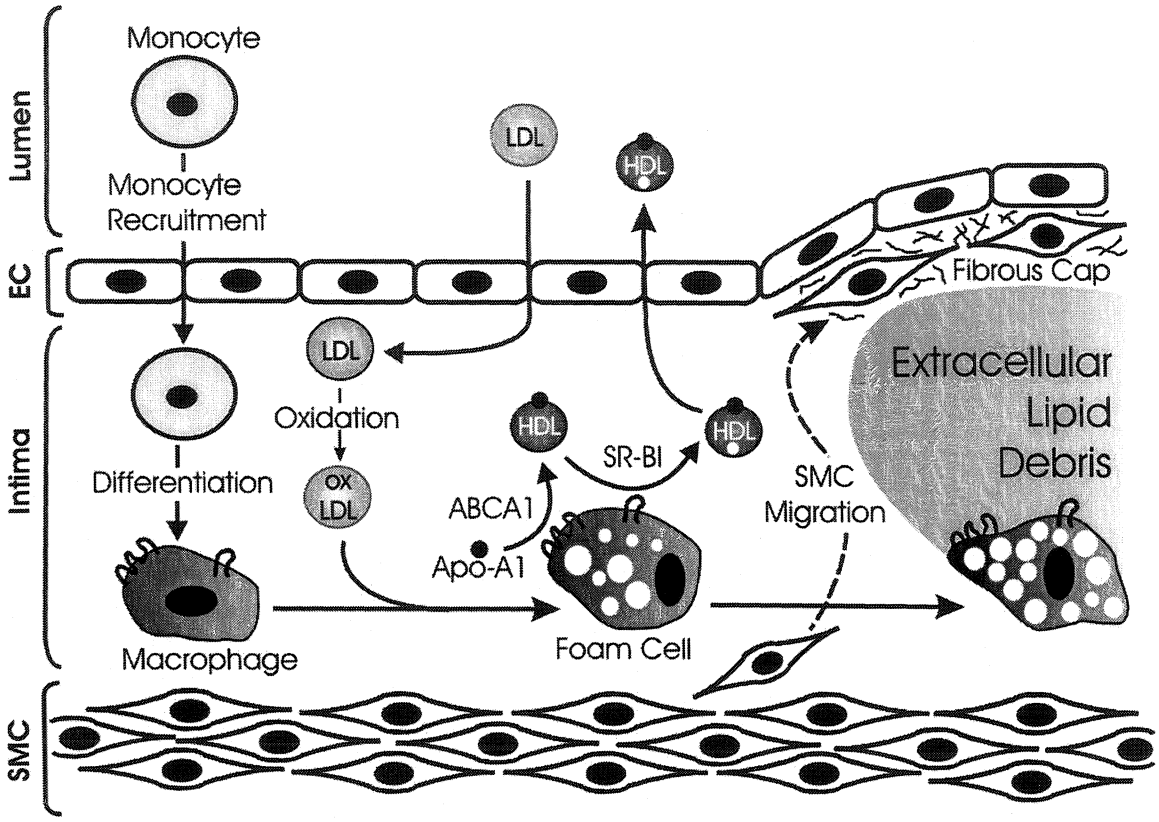

Figure 2. Formation of an Atherosclerotic Fibrous Plaque. LDL that enters into the intima can become oxidized (oxLDL). OxLDL can recruit monocytes in the lumen to cross the endothelial cell (EC) layer. Monocytes differentiate into macrophages in the intima. OxLDL is taken up by macrophages leading to formation of macrophage foam cells. Foam cells can become engorged with lipid and die producing a necrotic core of extracellular lipid debris. Smooth muscle cells (SMC) migrate to cover the extracellular debris and secrete extracellular matrix and produce a fibrous cap. Cholesterol efflux from foam cells to either apo-AI (by ABCA1) or HDL (possibly by SR-BI) may limit accumulation of lipid, and hinder progression of the lesion. Figure adapted from (Lusis 2000).

migrate in from the underlying media layer of the vessel. The smooth muscle cells deposit extracellular matrix and form a fibrous cap over the lipid-rich necrotic core (Lusis 2000). Lesions with these features are called fibrous lesions. The size of a fibrous lesion can increase and partially restrict blood flow through the vessel lumen. However vessel occlusion from thrombus formation as a result plaque rupture into the vessel lumen is a more clinically significant event (Lusis 2000).

Fatty streaks are initiated by the accumulation of LDL in the subendothelial space (the intima) see Figure 2. Fatty streaks preferentially form in regions of the vessel where blood flow is disturbed (e.g. branching points and areas of curvature)(Gimbrone 1999). LDL in the intima becomes converted to a proatherogenic form by oxidation, by mechanisms that are not entirely clear (Li et al. 2002). Minimally oxidized LDL in the intima can stimulate the overlying endothelial cells to produce pro-inflammatory molecules leading the recruitment of monocytes and lymphocytes from the lumen to the intima (Lusis 2000). Within the intima monocytes undergo proliferation and differentiation. Differentiation to macrophages results in up regulation of scavenger receptors (Li et al. 2002). Scavenger receptors (class A-I/II and CD36) mediate the uptake of chemically modified lipoproteins such as oxidized LDL (Kunjathoor et al. 2002). A key difference in cholesterol uptake via the LDL receptor pathway and the scavenger receptor pathway is that the latter is not under negative feedback control (Krieger 1999). Thus macrophages can continue to take up oxidized LDL leading the

macrophage to convert to a lipid loaded foam cell and thus initiate or progress the fatty streak (Pentikainen et al. 2000).

A.5.2 Lipoproteins and Atherosclerosis

It is well established that the risk of developing atherosclerosis is correlated with the level LDL cholesterol and inversely correlated with the level of HDL cholesterol. A key factor in the relationship between LDL and atherosclerosis is the accumulation of LDL-derived cholesterol in macrophages and their subsequent conversion to foam cells (Pentikainen et al. 2000). The correlation between HDL and atherosclerosis appears to be complex as HDL mediated protection may be attributable to several mechanisms. 1) HDL can impede the oxidation of LDL and thus hinder foam cell formation and therefore slow the development and progression of fatty streaks. The antioxidant properties of HDL are largely a result of association with the enzyme paraoxonase (Mackness et al. 2002). The antioxidant property of paraoxonase appears to be physiologically relevant, as mice with a targeted null mutation in the gene for paraoxonase have increased susceptibility to atherosclerosis (Shih et al. 1998). In addition HDL also carries lipid soluble antioxidant vitamins (e.g. vitamin E) (Behrens et al. 1982), which may play a role in preventing lipoprotein oxidation or cellular oxidative stress (reviewed in (Brigelius-Flohe et al. 1999)). 2) HDL can regulate vascular endothelial function. HDL binding can stimulate the production of nitric oxide via endothelial nitric oxide synthetase (eNOS) (Yuhanna et al. 2001). Nitric oxide production causes vasodilation, decreases adherence of circulating

blood cells to the vascular endothelium and inhibits the proliferation and migration of smooth muscle cells (Cooke et al. 1997). Thus stimulation of eNOS via HDL binding can inhibit processes central to the development of fatty streak lesions. 3) The atheroprotection provided by HDL may be due to facilitation of reverse cholesterol transport (RCT, see Section A.3.6). RCT can promote the flux of cholesterol from peripheral tissues (e.g. macrophage foam cell) to the liver for excretion, thereby limiting or even reversing foam cell formation (Tall et al. 2001).

A.5.3 SR-BI and Atherosclerosis

As discussed above SR-BI can influence plasma cholesterol levels, HDL structure and levels, biliary cholesterol secretion, cellular cholesterol uptake (in the liver and other tissues) (Rigotti et al. 1997), and possibly cholesterol efflux (Ji et al. 1997). This suggested that SR-BI might have a profound influence on the development of atherosclerosis. To test if ablation of SR-BI altered the progression of atherosclerosis, Trigatti et al. generated SR-BI/apolipoprotein E (apoE) compound mutant mice. The apoE knockout (apoE KO) mouse is a well-characterized model of atherosclerosis (Trigatti et al. 1999). ApoE KO mice have elevated plasma cholesterol levels and spontaneously develop atherosclerotic lesions by 3 months of age (Zhang et al. 1992). Indeed SR-BI/apoE double knockout mice (SR-BI/apoE dKO) had a substantial increase in atherosclerotic lesion sizes in the aortic root through the proximal aorta (40 and 100-fold increase relative to apoE and SR-BI KO mice respectively) (Trigatti et al. 1999).

The increased atherosclerotic plaque size was accompanied by an increase in plasma cholesterol (mainly associated with the HDL sized lipoproteins) and a decrease in biliary cholesterol, relative to mice with either individual mutation (Trigatti et al. 1999). This suggested that decreased RCT might account for the increased atherosclerosis. However other factors such as SR-BI mediated cholesterol efflux from peripheral tissues (including macrophage derived foam cells) might have contributed. It is noteworthy that the SR-BI/apoE dKO mice spontaneously develop severe occlusive coronary artery disease and myocardial infarctions, exhibit reduced heart function and die at a young age (approximately 6 weeks of age) (Braun et al. 2002).

The effect of SR-BI on atherosclerosis has also been examined in the LDL receptor (LDLR) knockout background. The fat fed LDLR knockout mouse is another well-established model of aortic atherosclerosis (Ishibashi et al. 1994). Huzar et al. investigated the effect of attenuated expression of SR-BI on atherosclerosis in the fat fed LDLR KO mouse (Huszar et al. 2000). Attenuation of SR-BI expression in fat fed LDLR KO mice resulted in a 170% increase in aortic atherosclerosis (Huszar et al. 2000). The SR-BI att/LDLR KO mice had increased plasma cholesterol relative to LDLR KO mice (40% and 70% for females and males respectively) (Huszar et al. 2000). Thus similar results for the effect of SR-BI on atherosclerosis development were found in 2 distinct models of atherosclerosis.

Recently Van Eck et al., have demonstrated that SR-BI mutant mice (not on an atherogenic background) can develop atherosclerosis. After 20 weeks on a high fat diet there was a 72-fold increase in aortic atherosclerosis in SR-BI KO mice relative to wild-type controls. Furthermore these authors found that mice heterozygous for the SR-BI mutant allele were similar to wild-type mice in that they did not develop any detectable arterial atherosclerotic lesions (Van Eck et al. 2003).

The effect of hepatic overexpression of SR-BI on atherosclerosis development has also been examined. Acute adenovirus-mediated overexpression of SR-BI in the liver of LDLR KO mice fed a high fat diet resulted in a 3.4-fold reduction in aortic atherosclerosis (Kozarsky et al. 2000). The atherosclerotic lesion size in the mice correlated well with the amount of HDL associated cholesterol (Kozarsky et al. 2000). In another study, chronic hepatic overexpression of SR-BI in mice heterozygous for the LDLR mutant allele (which results in moderate hypercholesterolemia) also resulted in decreased atherosclerosis (Arai et al. 1999). However in these mice the effect was only present when mice were fed a high fat diet that included bile salts (Arai et al. 1999). In theses mice atherosclerosis did not correlate with HDL cholesterol levels but rather VLDL and LDL cholesterol levels (Arai et al. 1999). The reasons for the differences between the two studies is not clear but may be related to differences in chronic versus acute overexpression and the effect of mice heterozygous versus homozygous for the mutant LDLR allele. The relationship between SR-BI hepatic expression levels and

atherosclerosis has also been studied (Ueda et al. 2000). In that study, transgenic mice with either moderate (2-fold) or high-level (10-fold) hepatic overexpression of SR-BI were crossed with human apo B transgenic mice (which are susceptible to high fat diet-induced aortic atherosclerosis (Purcell-Huynh et al. 1995)). After 18 weeks on a high fat diet, mice with moderate hepatic overexpression of SR-BI had 2.3-fold less atherosclerosis than the apo B transgenic control mice. Interestingly, high-level (10-fold) hepatic overexpression of SR-BI in apo B transgenic mice resulted in a 3-fold increase in atherosclerosis relative to the apo B transgenic mice with moderate hepatic SR-BI overexpression (Ueda et al. 2000). The reasons for this complex relationship between hepatic SR-BI expression and atherosclerosis remain to be determined.

Taken together these experiments demonstrate that normal expression of SR-BI protects against atherosclerosis. Furthermore, hepatic SR-BI appears to play an important role in such protection, likely owing to an increased hepatic cholesterol uptake and efflux into the bile, thus promoting RCT. The role of macrophage SR-BI in atherosclerosis, however, remains to be determined.

A.6 Rationale and Objectives

Lipids are vital molecules and as such their proper metabolism is critical for normal physiological function. Furthermore aberrant lipid metabolism (e.g. diabetes, obesity, and atherosclerosis) can have dire pathological consequences. Atherosclerosis is a leading cause of mortality in Western society (Hackam et al. 2003) and obesity and diabetes are becoming increasingly prevalent (Campbell 2003). As such, an understanding of lipid metabolism is of considerable interest.

The hydrophobic nature of lipids necessitates that carrier molecules transport them. The involvement of carrier molecules in the intercellular transport of lipids is a distinctive characteristic of lipid metabolism. The interaction of these carriers with cells is likely to impact the cellular uptake and efflux of the lipids they carry. Despite the potential impact on metabolism, many aspects of the interactions of carrier molecules with cells and the mechanism of cellular lipid transfer remain unresolved. The studies in this thesis were aimed at addressing some of these unresolved issues.

First, we sought to investigate the mechanism of LCFA uptake in the adipocyte cell line 3T3-F442A. We hypothesized that LCFA uptake would be sensitive to plasma membrane cholesterol content. To test this we examined the effect of cholesterol depleting agents on LCFA uptake. We found that two well established cholesterol

depleting reagents (cyclodextrin and filipin) inhibited LCFA uptake. This inhibition was not the result of a general disruption of cellular uptake processes, as filipin treatment did not affect the uptake of another substrate (2-deoxy-D-glucose).

Next, we attempted to further the understanding of the role of albumin in LCFA uptake. Since 3T3 adipocytes have previously been reported to display albumin receptor kinetics (see Section A.3.4.1.1) and to bind albumin, we sought to determine if albumin binding proteins are present in the plasma membrane of 3T3 adipocytes. Our results discovered that albumin binding to 3T3 adipocytes is sensitive to proteolysis and that albumin binding increases as 3T3 cells undergo differentiation to adipocytes. We found several proteins in 3T3 adipocyte plasma membranes with albumin binding activity.

The final studies were directed towards expanding our knowledge of the role of the HDL receptor, SR-BI, in the development of atherosclerosis. Based on the hypothesis that SR-BI in macrophages may mediate cholesterol efflux, we sought to determine if ablation of SR-BI in bone marrow-derived cells (which includes macrophages) promoted atherosclerosis. We determined that expression of SR-BI in bone marrow-derived cells is atheroprotective. Furthermore this protection occurs in the absence of changes in the level or distribution plasma cholesterol.

B Materials and Methods

B.1 Materials

3T3-F442A cells were kindly provided by Dr. K.S. Cook (Dana-Farber Cancer Institute, Boston, MA). ldlA7 and ldlA[mSR-BI] cells were provided by Dr. M. Krieger (Massachusetts Institute of Technology, Cambridge, MA). Dr. M. Okabe (Osaka University, Japan) provided green fluorescent protein transgenic (GFPtg) founders and C57BL/6 LDLR KO founders were purchased from The Jackson Laboratories (Bar Harbor, ME). SR-BI KO (both mixed background and C57BL/6) and SR-BI/LDLR dKO founders were provided by Dr. M. Krieger.

Biotinylated anti-CD11b, anti-mouse CD16/CD32 (Fc Block), and anti-caveolin antibodies were purchased from BD Biosciences (Mississauga, ON), as were streptavidin-Cy-Chrome conjugates. The 495 anti-SR-BI and the anti-εCOP antibodies were provided by Dr. M. Krieger (Massachusetts Institute of Technology, Cambridge, MA). Dr Karen Kozarsky (SmithKline Beecham Pharmaceuticals, King of Prussia, PA) provided the KK anti-SR-BI antibody. The alexa 488 conjugated goat anti-rabbit antibodies were purchased from Molecular Probes Inc. (Eugene, OR). Goat anti-rabbit antibodies conjugated to horseradish peroxidase and enhanced chemiluminescence reagent were purchased from PerkinElmer Life Sciences (Boston, MA).

Deoxynucleotide triphosphates (dNTPs) were purchased from MBI Fermentas (Burlington, ON). Taq polymerase was purchased from Promega (Madison, WI). Bovine serum albumin for PCR was purchased from Invitrogen (Carlsbad, CA) and PCR primers were synthesized at the McMaster Institute for Molecular Biology and Biotechnology (MOBIX central facility).

Free and total cholesterol assay kits were purchased from Wako Diagnostics (Richmond, VA). Blood Quick Pure Mini kits were purchased from BD Biosciences (Burlington, ON). The BCA protein assay kit was purchased from Pierce (Rockford, IL), as were the Iodobeads.

Unless noted otherwise all cell culture reagents were purchased from Invitrogen (Carlsbad, CA). Newborn calf lipoprotein deficient serum (NCLPDS), LDL, VLDLD and HDL were prepared by Danny Wang.

The low fat diet, high fat diet (see Table 2 for compositions) and low fat diet containing 0.5% probucol were purchased from Harlan Teklad (Madison, WI). Apo-sulfatrim (sulfamethoxazole timethoprim) was purchased from Apotex (Toronto, ON), and Nutrical was purchased from Evsco Pharmaceuticals (Buena, NJ). Isoflurane was from Abbott Laboratories (Montreal, PQ).

Table 2. Composition of mouse diets.

Component	Composition (%)	
	Low Fat Diet [a]	High Fat Diet [b]
Protein	17.0	22.2
Carbohydrate	53.7	48.6
Fat	11.0 [c]	21.0
Cholesterol	trace	0.15
Fiber	3.5	5.6
Ethoxyquin		0.01

[a] Harlan Teklad (product code # 7904)
[b] Harlan Teklad (basal mix #TD 88122 plus 20% butter fat, 1% safflower oil and 0.15% cholesterol)
[c] animal fat

[1,2-^{3}H] Cholesterol was purchased from American Radiolabeled Chemicals Inc. (St. Louis, USA). [^{3}H] Oleic acid, [^{3}H] 2-deoxy-D-glucose, and Na[^{125}I] were all purchased from DuPont, NEN (Boston, MA).

Acetone, glacial acetic acid, formaldehyde, glycerol, Triton X-100, ammonium chloride, and ammonium sulfate were all purchased from BDH Inc (Toronto, ON). 95% ethanol, and methanol were purchased from McMaster University Scientific stores. Nonidet P40 was from United States Biochemical Corporation (Cleveland, OH). Oleic acid was purchased from Fisher Scientific (Fairlawn, NJ). All of the following were purchased from Sigma Chemical Corp. (St Louis, MO); aprotinin, bovine serum albumin fraction V essentially fatty acid free (BSA), 3-[(3-cholamidopropyl)dimethyammonio]-1-1-propane-sulfonate (CHAPS), hexadecyltrimethylammonium bromide (CTAB), ethylenediaminetetraacetic acid (EDTA), deoxyribonuclease (Dnase), dimethyl sulfoxide (DMSO), deoxy-D-glucose, filipin, formalin, glycerol-gelatin, gelatin, heparin sodium salt, hepes, hematoxylin, isopropanol, leupeptin, lubrol, insulin (Sigma catalogue number I-6634), methyl-β-cyclodextrin (Sigma catalogue number C-4555), 2-mercaptoethanol, paraformaldehyde, pepstatin, phenylmethylsulfonylfluoride (PMSF), poly-D-lysine, ribonuclease A (RNase), oil red-O, phloretin, sarkosyl, sodium cholate, sodium deoxycholate, sodium dodecyl sulfate (SDS), sudan IV, tertiary amyl alcohol, N,N,N′, N′-tetramethylethylenediamine (TEMED), tetrahydrofuran, thioglycollate medium, triton X-114, 2,2,2 tribromoethyl alcohol, tween 80, tween 40, tween 20 and trypan blue.

Isopentane and magnesium chloride hexahydrate were purchased from EM Science (Darmsstadt, Germany). Acrylamide, ethylene glycol bis(2-aminoethyl ether) N,N,N′ N′ tetracetic acid (EGTA), ammonium persulfate, glycine, potassium hydroxide, sodium chloride, sodium hydroxide, sodium phosphate, 2-amino-2-(hydroxymethyl)-1,3-propanediol (Tris base) were purchased from Bioshop Inc. (Burlington, ON). Sucrose was purchased from ACP (Montreal, Quebec).

Tissue embedding molds were purchased from Polysciences Inc (Warrington, PA), and cryomatrix was purchased Thermo Shandon (Pittsburgh, PA). Aqueous counting scintillant, PD10 desalting columns were purchased from Amersham Pharmacia (Uppsala, Sweden). X-Omat AR autoradiography film was purchased from Kodak (Rochester, NY). PVDF and nitrocellulose membranes were purchased from Millipore (Bedford, PA). GF/C filters were from Whatman (Maidstone, England). Glass microscope slides (colorfrost yellow) were from Fischer Scientific (Toronto, ON).

Karnovsky's fixative (1% paraformaldehyde, 12.5% glutaraldehyde (v/v), 0.1 M sodium cacodylate pH 7.4) and 2% glutaraldehyde were kindly provided by the McMaster University Medical Centre Electron Microscopy Facility.

B.2 Methods

B.2.1 Mouse and Tissue Procedures

B.2.1.1 Mice

All experiments with mice were done in accordance with guidelines of the Canadian Council on Animal Care. A colony of LDLR KO mice on a C57BL/6 background was established from founders purchased from The Jackson Laboratories (Bar Harbor, ME) and subsequently bred in house. The SR-BI KO mice were either on a 50:50 C57BL/6:129 background (Rigotti et al. 1997) or were backcrossed 9 times onto a pure C57BL/6 background (Miettinen et al. 2001). SR-BI/LDLR dKO mice were generated by crossing LDLR KO mice to SR-BI KO mice (50:50 C57BL/6:129 background). A colony of wild type C57BL/6 mice was derived from the SR-BI KO breeding colony by breeding SR-BI heterozygotes.

Mice were housed in micro isolator cages in the Barrier Unit or the bio-containment room (for mice that had received bone marrow transplants) of the Central Animal Facility at McMaster University. Mice had free access to food and water. Mice were fed either a normal low-fat diet or an atherogenic high fat Western type diet containing 0.15 % cholesterol and 21% fat as indicated (for details of composition see Table 2). The C57BL/6 wild-type and C57BL/6 SR-BI KO mouse colonies used to generate bone marrow donors were maintained on Prolab 3000 with 0.5% probucol (Harlan Teklad, Madison WI) because it rescues 1) fertility of the SR-BI KO females

(Miettinen et al. 2001) and 2) recovery of SR-BI KO pups on a C57BL/6 background (Trigatti unpublished data).

The offspring from breeding pairs were weaned when pups were 3 weeks old. The pups were segregated into males and females and housed in micro isolator cages. When heterozygotes were bred, the genotype of the offspring was determined from DNA prepared from tail biopsies obtained 2-days post weaning. Biopsies were performed on mice anesthetized with isoflurane. Tail biopsies of 0.5 to 1 cm were taken and the tails were cauterized. DNA preparation and PCR analysis were performed (as described in Section B.2.1.3).

B.2.1.2 Bone Marrow Transplantation

Female mice (2 months of age) were used as bone marrow transplant recipients. Recipients in a 14 x 27 cm sterile shipping crate were subjected to 1000 cGy total body irradiation from a ^{60}Co source delivered as two single doses of 600 and 400 cGy, spaced by 3 hours (performed by Robert Pasuta McMaster University Hot Cell Nuclear Facility).

Bone marrow was obtained from male mice (less than 3 months old). Mice were euthanized by asphyxiation with CO_2. The tibias and fibulas were removed from the mice, adherent tissue was trimmed away and bones were kept on ice in complete Iscove's media (Iscove's media, 2% heat inactivated (55°C for 30 minutes) fetal bovine serum (FBS), streptomycin 50 units/ml, penicillin 50 μg/ml, 2 mM L-glutamine). When all

bones were trimmed the ends of the bones were cut off with sterile forceps and the marrow was flushed from the bones by injecting 0.5 ml of complete Iscove's media through a 26G needle into one end of the bone and then the other. Cells were dispersed by passage twice through a 21 G needle and then twice through a 26 G needle. Cells were counted and diluted to approximately $1.5x10^7$ cells/ml of the large bright cells. Immediately after the second irradiation, recipient mice were transferred to the Central Animal Facility bio-containment room and were anesthetized with 2.5% avertin (0.25% tribromoethyl alcohol, 0.25% (v/v) tertiary amyl alcohol, in phosphate buffered saline (PBS, 0.14 M NaCl, 2.7 mM KCl, 15 mM Na_2HPO_4 and 1.5 mM KH_2PO_4 at pH 7.4)) and 3-5 x 10^6 bone marrow cells (in a total volume of 150 to 250 μl) were injected into the retro-orbital venous plexus of each recipient mouse.

After transplantation, recipients were given antibiotics (sulfamethoxazole at 1.25 mg/ml and trimethoprim at 0.25 mg/ml in drinking water), as well as wet powdered food containing Nutrical. In addition mice were injected subcutaneously with 0.5 ml lactated ringers solution daily for two weeks post irradiation. Two weeks post irradiation mice were switched to antibiotic free water and wet powdered food was no longer provided. At one month post transplantation, mice were anesthetized with 2.5% avertin and blood was collected from the tail vein into heparinized tubes for PCR analysis (see Section B.2.1.3), flow cytometric analysis (see Section B.2.1.4), or for preparation of plasma (see Section B.2.1.8).

B.2.1.3 PCR Analysis

DNA was either prepared from blood samples using the BD Blood Quick Pure kit or was prepared from tail biopsies as described in (Laird et al. 1991). For PCR reactions from blood DNA, 10 µl of DNA was diluted in both 90 µl and 990 µl of water. For PCR reactions from tail derived DNA, 5 µl of DNA was diluted in 495 µl of water. Following dilution, DNA samples were warmed to 37° C for several hours prior to the PCR reaction. For all PCR reactions 5 µl of the diluted template DNA was added to a mixture consisting of 10 µg/ml BSA, 1.25 mM of each dNTP, 12.5% DMSO, 0.0375 U/µl Taq polymerase, 1 µg/ml of each a forward and reverse primer in a 1X PCR buffer (67 mM Tris-HCl pH 8.8, 16.6 mM $(NH_4)SO_4$, 6.7mM $MgCl_2$, 0.035% (v/v) 2-mercaptoethanol, 6.7 µM EDTA). For a list of PCR primer sequences and amplicon sizes see Table 3. Reactions were carried out with 1 cycle of 94°C for 2 minutes, 57°C for 2 minutes and 65°C for 5 minutes, then 41 cycles of 94°C for 30 seconds, 57°C for 30 seconds and 65°C for 90 seconds followed by 10 minutes at 65°C in an Eppendorf Mastercycler (note that the ramping speed was set at 1°C per second for all temperature transitions). Amplified DNA fragments were separated by electrophoresis through 1% agarose in the presence of 0.5 µg/ml ethidium bromide. 0.5X TAE (4 mM tris, 5.7% (v/v) acetic acid 0.1 mM EDTA) was used as the electrophoresis running buffer (Sambrook et al. 2001).

Table 3. PCR primers and amplicon sizes.

Allele	Primer Name	PCR Primers (5′ to 3′)	Amplicon (bp)
SR-BI	oAB2	GAT GGG ACA TGG GAC ACG AAG CCA TTC T [c]	1500[a],1000[b]
	oAB3	TCT GTC TCC GTC TCC TTC AGG TCC TGA [c]	
LDLR wt	OIMR46	ACC CCA AGA CGT GCT CCC AGG ATG A [e]	383
	OIMR59	CGC AGT GCT CCT CAT CTG ACT TGT [e]	
LDLR mut	LDLR1	GGC AAG ATG GCT CAG CAA GCA AAG GC [d]	2000
	oSI75	GAT TGG GAA GAC AAT AGC AGG CAT GC [d]	

[a] mutant SR-BI
[b] wild-type SR-BI
[c] (Rigotti et al. 1997)
[d] (Ishibashi et al. 1993)
[e] http://jaxmice.jax.org/pub-cgi/protocols/protocols.sh?objtype=protocol&protocol_id=297

B.2.1.4 Flow Cytometry

Mice were anesthetized with 2.5% avertin, and blood was collected into heparinized tubes from the tail vein. 30 µl of the blood sample was added to a single well of a round bottom 96 well plate. To lyse red blood cells, 100 µl of Tris-NH_4Cl (17 mM Tris-HCl, 0.747% NH_4Cl) was added and samples were incubated at 37°C for 10 minutes. Cells were pelleted by centrifugation at 1000xg for 3 minutes at 4°C. The supernatant was removed and the cells were treated a second time with Tris-NH_4Cl, as described above. Cells were then pelleted as above and washed once in ice-cold PBS with 0.1% BSA (fraction V essentially fatty acid free). Cells were incubated with a biotinylated anti-CD11b antibody (0.5 µl of antibody with 0.1 µl of Fc blocker) in 50 µl of PBS with 0.1% BSA for 30 minutes at 4°C. Cells were washed as above and incubated with 0.3 µl of a streptavidin-Cy-Chrome conjugate in 50 µl of PBS with 0.1% BSA at 4°C in the dark for 30 minutes. Cells were then washed twice as described above and resuspended in 50 µl of PBS with 0.1% BSA at 4°C. Flow cytometry was performed on a BD FACSVantage by Hong Liang (McMaster University Flow Cytometry Facility). Typically 50 000 to 100 000 cells were analyzed.

B.2.1.5 Tissue Harvest from Mice

At the time of harvest mice were anesthetized with 0.4ml of 2.5% avertin. Blood samples were obtained by cardiac puncture into the left ventricle of the heart with a 25G 5/8 needle pre-rinsed with heparin (10 000 U/ml). The vasculature was then perfused

with 10 ml of ice cold PBS containing 5 mM EDTA injected into the left ventricle and allowed to flow out via a nick in the right atria. Aortas (still attached to the heart) were removed from the iliac bifurcation up to the heart, rinsed in ice cold PBS, the heart and aorta were separated mid way between the top of the heart and the innominate artery under a dissecting microscope (Leica GZ6E). The aorta was then fixed for at least 1 week at room temperature in 5-10 ml of neutral buffered 3.8% formaldehyde. Hearts were bisected open between the ventricles and atria perpendicular to the plane at which the aorta exits the left ventricle and were placed cut face down in an embedding mold. Tissues were embedded in Cryomatrix in an isopentane-dry ice bath for 10 minutes and then stored at –80 °C.

B.2.1.6 Sudan IV Staining of Aortas

Stained aortas were prepared by the method of (Tangirala et al. 1995). Formalin fixed aortas (see Section B.2.1.5) were dissected free of adventitial fat and branching arteries. Aortas were then rinsed in water followed by 70% ethanol with gentle mixing for 30 seconds. Aortas were stained in 2 ml of a sudan IV solution (0.5% sudan IV in 36.8% acetone and 50% ethanol filtered and stored in the dark) for 15 minutes with gentle mixing. Excess stain was removed by a 1-minute wash in 80% ethanol followed by a brief rinse in water. Any pieces of lipid rich tissue still remaining on the outside of the aorta were then removed. A longitudinal incision along the inner curvature of the aortic arch and down the ventral surface of the descending aorta was made, followed by a

second longitudinal incision along the outer curvature of the aortic arch. The aorta was then mounted onto a glass slide with a glycerol-gelatin solution (59% (w/v) glycerol, 0.9% gelatin and 1% (w/v) phenol) warmed to 55°C.

Images of the aortas were captured on slide film and then digitized (Audio Visual Services McMaster University or by Tom Baumgartner). The surface area covered by lipid rich sudan IV stained lesions was then determined using Scion Image software and expressed as the percentage of the total lumen surface area (Tangirala et al. 1995).

B.2.1.7 Lesion Area in the Aortic Sinus

Hearts that had been embedded in cryomatrix were sectioned on a Thermo Shandon Cryostat, perpendicular to the aortic sinus. 10 μm thick sections were obtained, fixed in formaldehyde (37%) for 1 minute at room temperature and washed several times with tap water. The excess water was removed and sections were incubated with an oil red-O solution for 15 minutes (0.5% oil red-O in isopropanol diluted 1.6 fold in water and filtered) and washed several times with tap water. Sections were counter stained with Mayer's Hematoxylin solution. Sections were imaged using a Zeiss Axiovert 200M microscope and plaque area was measured with Scion Image software.

B.2.1.8 Plasma Preparation

Mice were fasted overnight (12 to 14 hours) and blood was collected either from the tail vein or by cardiac puncture (on avertin overdosed mice). Plasma was prepared from heparinized blood by centrifugation at 16000xg for 3 minutes at 4°C.

B.2.1.9 Fractionation of Plasma Lipoproteins by FPLC

Plasma lipoproteins were separated by gel filtration FPLC as described in (Rigotti et al. 1997). Lipoproteins were fractionated from 0.1 ml of plasma (prepared as described in Section B.2.1.8) with an AKTA FPLC with 2 Superose 6 HR 10/30 columns (Amersham Biosciences, Buckinghamshire England) connected in series. Columns were developed with 154 mM NaCl, 1 mM EDTA pH 8.0 column buffer. Columns were run at 0.5 ml/min and 47 0.5 ml fractions were collected after the first 14 ml (0.3 column volumes) of buffer had eluted from the column. Plasma fractions were then stored at –20°C. The fractions in which VLDL, LDL and HDL eluted in was determined by performing gel filtration using lipoproteins prepared by density gradient centrifugation from human plasma (prepared by Danny Wang)(Figure 3).

B.2.1.10 Cholesterol Analysis

Both free cholesterol and total cholesterol levels were assayed using kits from Wako Diagnostic. The cholesterol ester levels were calculated as the difference between

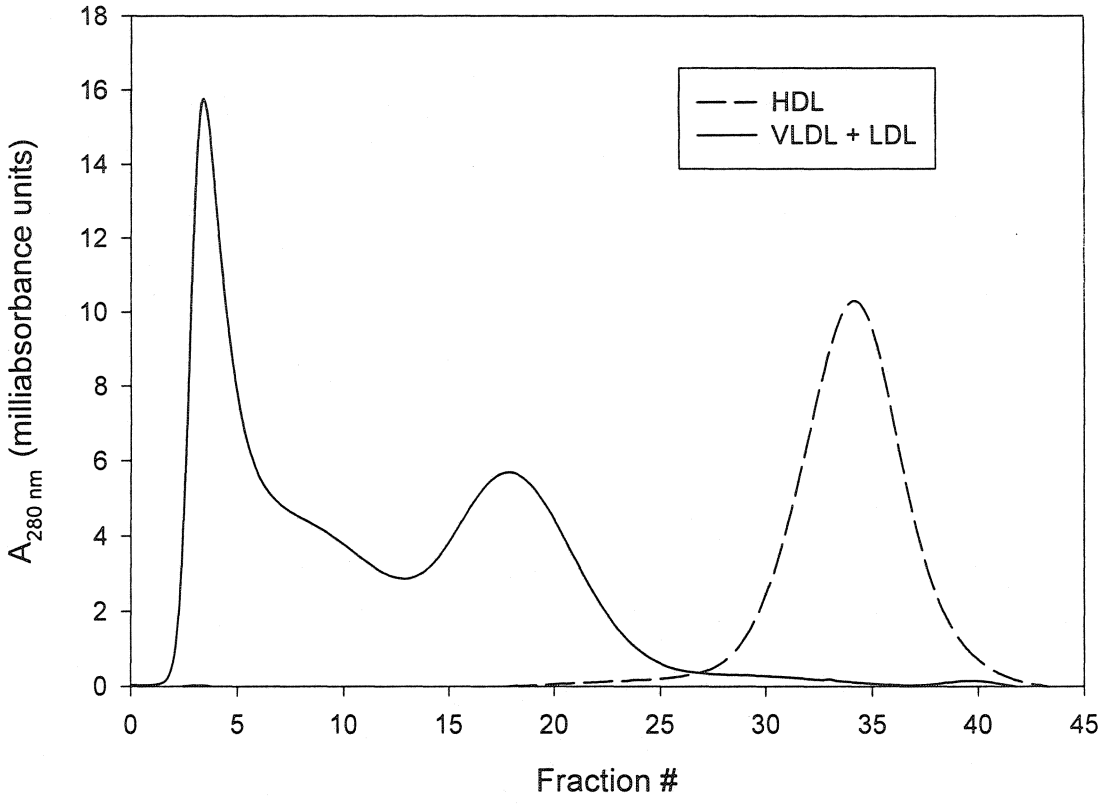

Figure 3. Fractionation of Purified Lipoproteins by Gel Filtration FPLC. HDL, and VLDL + LDL were prepared by density gradient centrifugation from human plasma (performed by Danny Wang). 800 μg of protein of either HDL (dashed line) or VLDL + LDL (solid line) were loaded onto a AKTA FPLC with 2 Superose 6 HR 10/30 columns (Amersham Biosciences, Buckinghamshire England) connected in series. Lipoproteins were eluted at 4°C with 154 mM NaCl and 1mM EDTA pH 8.0 (as described in Section B.2.1.9). Protein was detected in line by absorbance. Absorbance is plotted versus the fraction number (0.5 ml per fraction) for comparison with mouse plasma. The first fraction was collected after 14 ml (void volume) had eluted.

the total and free cholesterol levels. Plasma was assayed following the Wako Diagnostic kit protocol for a 96 well assay; using a 1:10 dilution of plasma.

B.2.2 Cell Culture

B.2.2.1 Growth and Propagation of Cells

For growth and propagation of 3T3-F442A preadipocytes, $3x10^5$ to $6x10^5$ cells were seeded in a 100mm cell culture plate in Dulbecco's Modified Eagle Medium supplemented with 10% calf serum (CS), 50 units/ml penicillin, 50 μg/ml streptomycin and 2 mM L-glutamine. For the purpose of propagation cells were not allowed to reach confluence.

ldlA7 (a cell line of LDL receptor-deficient Chinese hamster ovary cell mutants (Krieger et al. 1981)) and ldlA[mSR-BI] (ldlA cells overexpressing murine SR-BI (Acton et al. 1996)) were seeded at $2x10^6$ cells per 100mm culture plates and cultured in Ham's F12 medium supplemented with 5% FBS, 50 units/ml penicillin, 50 μg/ml streptomycin, and 2mM L-glutamine.

To propagate 3T3-F442A, ldlA7 and ldlA[mSR-BI] cells, monolayers were washed twice with 5 ml of PBS pre-warmed to 37°C and incubated at 37°C for 3 minutes with 1 ml of trypsin-EDTA (0.05% trypsin, 0.53mM EDTA, 14 mM NaCl in PBS) pre-warmed to 37°C. Following the 3-minute incubation plates were gently knocked to

dislodge cells from the plate. Culture media was then added to the plate (4 or 9 ml depending on the cell concentration required) and the plate surface was washed several times. Cells were then counted with a hemacytometer and seeded onto new cell culture plates.

B.2.2.2 Long Term Storage of Cells

For long-term storage of 3T3-F442A cells, pre-confluent cells were released from the culture plate by trypsinization (as described in Section B.2.2.1) and resuspended in 9 ml of Dulbecco's Modified Eagle Medium supplemented with 10% calf serum, 50 units/ml penicillin, 50 μg/ml streptomycin and 2 mM L-glutamine and 10% DMSO. For ldlA7 and ldlA[mSR-BI] cells, pre-confluent cells were released from the culture plate by trypsinization (as described in Section B.2.2.1) and resuspended in 1 ml of FBS with 10% DMSO. For all cell types 1 ml of the cell suspension was added to a cryovial and chilled on ice for 15 minutes, transferred to –80°C for 24 hours and then stored in a $N_2(l)$ storage tank. When frozen stocks of cells were needed, they were thawed rapidly at 37°C, added to a culture plate containing growth media. The cells were allowed to attach for 12 to 16 hours and then the media was replaced with fresh growth media.

B.2.2.3 Differentiation of 3T3-F442A Cells

Cells were seeded at $6x10^4$ cells per 100mm culture dish and cultured in Dulbecco's Modified Eagle Medium supplemented with 10% FBS, 50 units/ml penicillin,

50 μg/ml streptomycin, 2 mM L-glutamine and 5 μg/ml insulin (Sigma catalogue number I-6634) until 2 days post confluence at which time cells were cultured in the above media without added insulin and the media was replaced every second day (see schematic diagram in Figures 5).

For the sake of simplicity we refer to the differentiating 3T3-F442A cells as adipocytes, although they are not fully mature adipocytes. We define the length of differentiation from the day that the culture becomes confluent, e.g. under differentiation stimulating conditions, cells that are four days post confluence, we refer to as day 4 adipocytes. 3T3-F442A cells that are not stimulated to differentiate (i.e. cultured in Dulbecco's Modified Eagle Medium supplemented with 10% CS, 50 units/ml penicillin, 50 μg/ml streptomycin and 2 mM L-glutamine) are referred to as preadipocytes are were typically cultured for 1 day post confluence.

B.2.2.4 Harvesting Cells

Monolayers of cells were washed twice with PBS at 37°C and were incubated with 1 mM EDTA in PBS for 3 minutes at 37°C (1 ml per 100 mm culture plate). The 1mM EDTA in PBS was removed by aspiration. Cells were dislodged by agitation and suspended in 3 ml of PBS. Cells were pelleted by centrifugation at 500xg for 3 minutes at room temperature, washed twice with PBS, counted with a hemacytometer and resuspended to the required density.

B.2.3 Cellular Assays

B.2.3.1 Trypan Blue Exclusion Assays

Cells were harvested (as described in Section B.2.2.4) and resuspended in 1 ml PBS. 200 µl of cells were mixed with 500 µl of 0.4% trypan blue and 300 µl PBS and incubated for 5 minutes at room temperature. An aliquot of the cells was then counted in hemacytometer, keeping separate counts of cells that excluded trypan blue (viable cells) and those stained with trypan blue (non-viable cells).

B.2.3.2 Oleate and Glucose Uptake Assays

Cellular uptake of [9,10-^{3}H]-oleate was assayed using the method described by (Abumrad et al. 1981) and modified by (Trigatti et al. 1991). 2-[^{3}H]-deoxy-D-glucose uptake was assayed using a modified protocol described in (Ibrahimi et al. 1996).

[9,10-^{3}H]-oleate:BSA was prepared as follows: The appropriate amount of [9,10-^{3}H]-oleic acid (5 mCi/ml) in ethanol was mixed with non-radiolabeled oleic acid in ethanol to generate the final specific radioactivity of 200 µCi/µmol. The oleic acid was neutralized by the addition of 1.1 equivalents of KOH. The solvent was removed using a Savant Speed-Vac concentrator. The residue was dissolved at 37°C in PBS containing the appropriate amount of BSA (Sigma, Fraction V essentially fatty acid free) so that the final concentration of oleate and BSA were each 300 µM.

2-[^{3}H]-deoxy-D-glucose was prepared as follows: The appropriate amount of 2-[^{3}H]-deoxy-D-glucose in ethanol was prepared by removing the solvent using a Savant Speed-Vac concentrator, and mixing it with non-radioactive 2-deoxy-D-glucose in PBS to generate a 4 mM solution with a specific radioactivity of 10 μCi/μmol.

To reduce binding of [^{3}H]-oleate:BSA or 2-[^{3}H]-deoxy-D-glucose to the filters, the filters were pre-filtered with 0.1% BSA in PBS and kept at 4°C. Non-specific retention of radioactivity by the filters was measured. These values (typically less than 10% of the ^{3}H signal in the presence of cells (data not shown)) were subtracted from values obtained in the presence of cells.

Cells were harvested (as described in Section B.2.2.4) and resuspended to $1.5x10^6$ cells/ml in PBS. Assays were initiated by addition of equal volumes (from 200-700 μl) of cells and either [9,10-^{3}H]-oleate:BSA (1:1, 300 μM) or 4 mM 2-[^{3}H]-deoxy-D-glucose. The mixtures were incubated at 37°C with constant gentle agitation. 300 μl aliquots were removed at different times, diluted into ice-cold stop solution (PBS containing 0.1% BSA, and 200 μM phloretin) and immediately filtered through a Whatman GF/C filter under negative pressure using a vacuum filter manifold. Filters where immediately washed 3 times with ice-cold stop solution, and placed in 5 ml aqueous scintillation fluid. The filters were allowed to sit for 24 hours in the scintillation fluid prior to scintillation counting.

B.2.3.3 Cholesterol Efflux Assay

Cultured cells were loaded with [^{3}H]-cholesterol as follows: ldlA7 and ldlA[mSR-BI] cells ($5x10^6$ cells) were seeded onto 35 mm cell culture plates and cultured (as described in Section B.2.2.1). Two days after being seeded, cells were loaded with [1,2-^{3}H] cholesterol by incubating cells with 2 ml of DMEM containing 5 μCi/ml [1,2-^{3}H] cholesterol, 10 mM HEPES pH 7.4, 2 mM L-glutamine, 50 units/ml streptomycin, 50 μg/ml penicillin, and 10% heat inactivated FBS that had been incubated with the [1,2-^{3}H] cholesterol for 12 hours at 37°C. After 2 days of incubation with the [^{3}H] cholesterol labeling media cells were washed and incubated overnight with an equilibration media (DMEM containing 10 mM HEPES pH 7.4, 2% fatty acid free BSA, 2 mM L-glutamine, 50 μg/ml streptomycin, and 50 units/ml penicillin).

Mouse peritoneal macrophages were loaded in situ with [^{3}H]-cholesterol as follows: Mouse peritoneal macrophages were elicited by intraperitoneal injection of 10% thioglycollate (Fortier 1994). Five days post-thioglycollate injection, peritoneal cells were loaded in situ with [1,2-^{3}H] cholesterol by injection of 0.5 ml of 50 μCi of [1,2-^{3}H] cholesterol incubated overnight in heat inactivated FBS. 3-hours later mice were euthanized by asphyxiation with CO_2 and peritoneal macrophages were recovered by intraperitoneal injection of 10 ml of 5 mM EDTA in PBS warmed to 37°C followed by vigorous agitation for 3 minutes. The lavage fluid was aspirated from the peritoneal cavity and cells were collected by centrifugation at 500xg for 5 minutes. The cells were

washed twice with equilibration media (as described above) and $2x10^6$ cells were plated per 35 mm cell culture plate. One hour later plates were washed vigorously with equilibration to remove weakly adherent, non-macrophage cells.

Net efflux assays were initiated by the addition of 2 ml of efflux media (DMEM, 2 mM L-glutamine, 50 U/ml streptomycin, 50 μg/ml penicillin, 10 mM HEPES pH 7.4, and either 50 μg/ml HDL or 10% FBS) and this was referred to as time 0. At the appropriate time 100 μl aliquots of the efflux media were centrifuged at 16 000xg for 10 minutes at 4°C, and 90 μl was diluted into scintillation fluid and the radioactivity was determined by scintillation counting. Following the final time point the efflux media was removed and the cells were washed twice with cPBS. 500 μl of 0.1N NaOH was added and the plates were incubated with rocking at room temperature for 15 minutes. Lysates were collected and the amount of cellular [^{3}H] cholesterol was determined by scintillation counting. Net efflux was expressed as the percentage of radioactivity in the media at each time point divided by the total radioactivity in the cells (Ji et al. 1997).

B.2.3.4 Filipin Staining of Cells

35mm culture plates with glass cover slip bottoms were prepared as described in (Howell et al. 2002). Plates were coated by incubation with 0.1 mg/ml poly-D-lysine (in ddH_20) for 5 minutes at room temperature. Excess poly-D-lysine was removed by rinsing the plates 3 times with PBS. $3x10^3$ 3T3-F442A cells were seeded and cultured to

differentiate (as described in Section B.2.2.3). On day 4 of differentiation cells were washed twice with complete PBS (cPBS)(PBS with 0.68 mM $CaCl_2$ and 0.5 mM $MgCl_2$) at 37°C and incubated at room temperature for 1 hour with Karnovsky's fixative. After fixation cells were washed twice with cPBS and incubated at room temperature in the dark with filipin (50 μg/ml) in cPBS for 2 hours. Filipin fluorescence was imaged with a Zeiss Axiovert 200M with an Fs01 Zeiss filter set (excitation: 365 nm, 12 nm band pass; emission: 397 nm long pass filter).

B.2.3.5 Immunofluorescence

3T3-F442A adipocytes were cultured on 35mm glass bottom plates (as described in Section B.2.3.4). On day 4 of differentiation cells were washed twice with cPBS and were fixed by incubating the cells at room temperature for 30 minutes with freshly prepared 2.5% paraformaldehyde in PBS. Following fixation, cells were washed 3 times with cPBS, incubated for 5-minutes at room temperature with 100 mM NH_4Cl and then washed 3 times with cPBS. Cells were permeabilized with 0.1% triton X-100 (w/v) at 4°C for 5 minutes, and washed 3 times with cPBS. Non-specific binding of the antibody was blocked by incubating cells at room temperature for 30 minutes with 10% FBS in cPBS. Afterwards cells were incubated at room temperature for 1 hour with 0.83 μg/ml anti-caveolin antibody in cPBS. Cells were washed 3 times with cPBS and incubated at room temperature in the dark for 30 minutes with 2 μg/ml goat anti-rabbit antibody conjugated to alexa 488 (in cPBS). Cells were then washed 3 times with cPBS, 0.5 ml of

cPBS was added to the plate and fluorescence was visualized with a Zeiss Axiovert 200M with an Fs10 Zeiss filter set (excitation: 450 nm, 40 nm band pass; emission: 515 nm, 50 nm band pass). 75 "Z-stack" images were collected at focal planes separated by 0.75 μm intervals and the image was deconvolved using a constrained iterative algorithm (Zeiss Axiovision software).

B.2.3.6 Electron Microscopy of Blood Cells

Heparinized blood was prepared from the mouse-tail vein. Blood samples (200 μl) were fixed at 4°C with 800 μl of 2% glutaraldehyde in 0.1 M sodium cacodylate buffer for a minimum of 12 hours. Cells were stained with Reynolds lead citrate and uranyl acetate and 750 to 1000 nm thick sections were prepared. The McMaster University Medical Centre Electron Microscopy Facility processed all samples for electron microscopy and Ernie Spitzer collected images.

B.2.3.7 Oil Red O Staining of Cells

3T3-F442A preadipocytes and adipocytes were cultured (as described in Section B.2.2.3) on poly-D-lysine coated glass bottom plates (as described in Section B.2.3.4). Cells were then washed twice with cPBS at 37°C and incubated for 30 minutes at room temperature with 3.8% neutral buffered formaldehyde. Cells were washed twice with cPBS and stained with 0.5 ml of (3.33% oil red O in 33% isopropanol (aq)) for 30

minutes at room temperature. Cells were washed twice with cPBS and 500 µl of cPBS was added to the plate and cells were visualized with a Zeiss Axiovert 200M microscope.

B.2.3.8 Cellular Albumin Binding Assays

Cells were harvested (as described in Section B.2.2.4) in PBS and were added to ^{125}I-BSA (see Section B.2.6.1) such that there was a final concentration of $1.8x10^6$ cells/ml and 0.83 µM ^{125}I-BSA. This mixture was incubated for 45 minutes at 37°C with gentle agitation. Cells were pelleted by centrifugation at 500xg for 3 minutes at room temperature, washed 3 times with PBS, and resuspended in PBS. The amount of cell-associated radioactivity was determined by scintillation counting.

B.2.4 Cellular Fractionation

B.2.4.1 Preparation of Total Cellular Homogenates

Cells were harvested from culture plates (as described in Section B.2.2.4) and resuspended (1 ml per 100 mm culture plate harvested) in ice-cold 10 mM sodium phosphate pH7.4 containing 1mM PMSF, 20 µg/ml aprotinin, 10 µg/ml leupeptin, and 10 µg/ml pepstatin. Cells were homogenized on ice using an Ultra Turrax T-8 homogenizer (with a minimum volume of 3 ml in a 5 ml culture tube), with 15-second bursts spaced by 15 seconds for a total of 4 rounds. Homogenates were either used immediately or were frozen in $N_2(l)$ and stored at -80°C.

B.2.4.2 Preparation of Total Membranes

Total membranes were prepared from homogenates by centrifugation at 100000xg for 60 minutes at 4°C in a MLA 130 rotor. Pellets were resuspended in 100 µl of ice-cold 10 mM sodium phosphate pH 7.4 containing 1mM PMSF, 20 µg/ml aprotinin, 10 µg/ml leupeptin, and 10 µg/ml pepstatin. Membranes were either used immediately or were frozen in $N_2(l)$ and stored at -80°C.

B.2.4.3 Preparation of Subcellular Fractions

Membrane enriched fractions were prepared by the method of Cushman and Wardzala (Cushman et al. 1980) as modified in (Trigatti et al. 1991). Cells from 10-30, 100 mm cell culture plates were harvested (as described in Sections B.2.2.4) and resuspended in ice-cold homogenization buffer (0.25 M sucrose, 1mM EDTA, 1mM HEPES pH 7.4). Cells were pelleted by centrifugation at 500xg for 10 minutes at 4°C and resuspended in 10 ml of ice-cold homogenization buffer containing 0.1 mM PMSF. Cells were homogenized on ice with 10 strokes of a motorized Teflon pestle at a moderate speed in a glass homogenization vessel.

RNase and DNase (at 50 µg/ml each) were added to the homogenate and it was incubated at 37°C for 10 minutes. An equal volume of ice-cold homogenization buffer containing 0.2 mM PMSF was added and the homogenate was chilled on ice for 5 minutes. A pellet was obtained from the total homogenate by centrifugation at 11000xg

for 20 minutes at 4°C. The supernatant (S_{11} fraction) was saved and the pellet was washed with 10 ml of homogenization buffer containing 0.1 mM PMSF and was collected by centrifugation at 11000xg for 20 minutes at 4°C. The supernatant was pooled with the previous S_{11} fraction and the pellet was resuspended in 5 ml of ice-cold homogenization buffer with 0.1 mM PMSF. The resuspended pellet was homogenized on ice with 5 strokes of a teflon pestle in a glass homogenization vessel (as above) and layered onto a discontinuous sucrose gradient consisting of 1.5, 1.12, or 0.87 M sucrose in 10 mM HEPES pH 7.4 containing 1 mM EDTA. Gradients were subjected to centrifugation in a SW28 rotor at 13000 rpm (corresponding to a minimum, average and maximum g force of 14000, 22000 and 30000xg respectively) for 90 minutes at 4°C. Plasma membranes were collected from the 0.25/0.87 M sucrose interface and mitochondria were recovered from the 1.12/1.5 M sucrose interface (Cushman et al. 1980; Trigatti et al. 1991).

Low density microsomes were prepared from the S_{11} fraction by centrifugation at 436000xg for 20 minutes. Mitochondria were prepared by diluting the band at the 1.12/1.5 M sucrose interface 5-fold with homogenization buffer containing 0.1 mM PMSF then the membranes were pelleted by centrifugation at 110004xg for 20 minutes at 4°C. Plasma membranes were prepared by diluting the band at the 0.25/0.87 M sucrose interface 5-fold in ddH_2O with 0.1 mM PMSF and then pelleting the membranes by centrifugation at 150000xg for 1 hour at 4°C. Membranes were typically resuspended to

2-5 mg/ml in 10 mM sodium phosphate pH 7.4 containing 0.1 mM PMSF, frozen in $N_2(l)$ and stored at –80°C.

B.2.5 SDS-PAGE, Electrophoretic Transfer, Immunoblotting and Ligand Blots

B.2.5.1 SDS-PAGE

SDS-PAGE was performed according to the method of Laemmli (Laemmli 1970). Protein samples were solubilized at 95°C for 3 minutes in 5% SDS, 0.125 M tris-HCl pH 6.8, 9% (v/v) glycerol, 8.9 % (v/v) 2-mercaptoethanol and 0.0005% bromophenol blue. Polyacrylamide gels consisted of a stacking gel (125 mM tris-HCl pH 6.8, 0.1% SDS, 4% acrylamide, 0.1% *N,N'*-methylene bisacrylamide) and a separating gel (375 mM tris-HCl pH 8.8, 0.1% SDS, and a final concentration of 7.5, 10, 12.5 or 15% acrylamide (37.5:1 acrylamide to *N,N'*-methylene bisacrylamide)). Electrophoresis was then performed using 25 mM tris pH 8.3, 192 mM glycine 1% SDS as the running buffer at 200 V.

B.2.5.2 Electrophoretic Transfer

Polyacrylamide gels (see Section B.2.5.1) were electrophoretically transferred as described in (Towbin et al. 1979). Gels were equilibrated for 15 minutes at room temperature with transfer buffer (25 mM tris pH 8.3, 192 mM glycine, and 20% methanol). During this time PVDF membranes were submerged in methanol for 20 seconds, ddH_2O for 2 minutes, and transfer buffer for 15 minutes. Proteins were electrophoretically transferred from the gel to the PVDF membrane at 4°C using either a

Bio-Rad Mini Trans-Blot apparatus at 100 V for 1 hour or an Idea Scientific transfer apparatus at 24 V for 1 hour.

B.2.5.3 Immunoblotting

Following SDS-PAGE (as described in Section B.2.5.1) and electrophoretic transfer (see Section B.2.5.2) PVDF membranes were incubated with 5% skim milk powder in tris buffered saline with 0.1% tween-20 (TBS-T, 200 mM tris-HCl pH 7.4, 137 mM NaCl, 0.1% tween 20) at 37° C for 1 hour with constant rocking. Blots were washed twice briefly and then 3 times for 10 minutes with 50 ml of TBS-T with constant agitation. Blots were incubated with primary antibody diluted in TBS-T (as indicated) for 60 minutes at room temperature with constant rocking. Blots were washed as described above, and incubated with secondary antibody (goat anti-rabbit antibody conjugated to horseradish peroxidase) diluted 1:5000 in TBS-T for 60 minutes with constant rocking at room temperature. Blots were then washed as described above.

Horseradish peroxidase was detected using a Western Lightning Enhanced Chemiluminescence Reagent Plus kit (PerkinElmer Life Sciences). Images were captured with either autoradiography film (Kodak X-omat XAR5) or with a Kodak Image Station 440CF. For quantitative immunoblotting, luminescence of both the samples to be quantified and a dilution series of a sample containing the antigen of interest was detected

with the Kodak Image Station 440CF. The luminescence from the dilution series was used to generate a standard curve of luminescence versus the relative amount of antigen.

B.2.5.4 Dot Blot Assay

Cellular membrane proteins (10 μg at 3.3 mg/ml) were solubilized at 37°C for 30 minutes in a solution containing 1% (w/v) detergent (unless specified otherwise) in 0.1M sodium phosphate pH 7.4 containing 0.25 M NaCl, 1 mM EDTA, 1 mM EGTA, 1 mM PMSF, and 10 μg/ml leupeptin. Proteins were spotted onto nitrocellulose and the spots were allowed to dry. Non-specific protein binding sites were blocked by incubating the nitrocellulose with 1.5% gelatin in TBS-T for 30 minutes at room temperature with constant agitation. The nitrocellulose was washed 3 times with TBS-T and probed with 50 μg/ml ^{125}I-BSA (prepared as described in Section B.2.6.1) for 60 minutes at room temperature with constant agitation. Blots were washed 3 times for 5 minutes with TBS-T, dried and exposed to autoradiography film (Kodak X-omat XAR5). Following an overnight exposure the film was developed and used to outline spotted regions on the nitrocellulose. The outlined regions were cut out using a hole punch. The punched spots were dissolved in 1 ml of tetrahydrofuran for 45 minutes at room temperature. Aqueous counting scintillant (ACS)(5 ml) was added and scintillation counting was performed.

B.2.5.5 Ligand Blotting

Membrane protein (20 μg) was separated by SDS-PAGE (as described in Section B.2.5.1) and electrophoretically transferred to a PVDF membrane (as described in Section B.2.5.2). Non-specific protein binding to the PVDF was blocked by incubating the blot with 1.5% gelatin in TBS-T for 30 minutes at room temperature with constant agitation. PVDF membranes were washed with TBS-T twice briefly, 3 times for 5 minutes at room temperature and were then probed with 50 μg/ml ^{125}I-BSA (prepared as in Section B.2.6.1) for 60 minutes at room temperature. Blots were washed as above, allowed to dry, wrapped in plastic, and exposed to autoradiography film (Kodak-xomat XAR5) for 3 days.

B.2.6 Other Assays and Methodologies

B.2.6.1 Iodination of BSA

Six Iodobeads (Pierce) were rinsed with 0.5 ml PBS, added to 0.5 ml PBS with 0.25 mCi Na^{125}I, and incubated for 5 minutes at room temperature. BSA (0.5 ml at 2 mg/ml in PBS) was added and incubated at room temperature for 15 minutes with gentle mixing every 30 seconds. BSA was then separated from free NaI on a PD10 desalting column (Pharmacia) equilibrated in TBS-T. Fractions of 1 ml were collected and scintillation counting was performed on 10 μl aliquots. The protein concentration of the first radiolabeled peak that eluted was determined by the BCA assay (as described in Section B.2.6.2).

B.2.6.2 Protein Concentration Assays

Protein concentrations were determined using the bicinchoninic acid (BCA) assay kit according to manufacture's instructions (Pierce (Rockford, IL)). Assays were performed in a 96 well plate, using 200 µl of BCA reagent and 25µl of protein solution incubated at 37° C for 30 minutes. Absorbance at 595 nm was measured using a spectrophotometric plate reader. BSA was used as a standard protein.

C Results and Discussion

C.1 Cholesterol Depleting Agents Inhibit LCFA Uptake in 3T3-F442A Adipocytes

The mechanism of LCFA movement across the plasma membrane is a controversial matter. Theories range from passive diffusion and transbilayer flip-flop of fatty acids (Hamilton 1998) to fatty acid uptake mediated by protein facilitated diffusion (Abumrad et al. 1984; Hui et al. 1997). To date the precise mechanism of LCFA uptake has not been elucidated, however in support of the protein mediated model several proteins have been proposed to act in facilitating LCFA transport across the plasma membrane. There is a large body of evidence supporting the contention that CD36/FAT, FATP and FABPpm mediate LCFA uptake (reviewed in (Hui et al. 1997; Abumrad et al. 1998; Luiken et al. 1999)).

Previous work from the Gerber lab demonstrated that caveolin-1 (a structural component of caveolae (Rothberg et al. 1992)) is a high affinity fatty acid binding protein in 3T3-L1 adipocytes (Trigatti et al. 1999). Interestingly, the putative fatty acid transporter CD36/FAT is also localized to caveolae in adipocytes (Souto et al. 2003) and in other cell types as well (Lisanti et al. 1994). The structure and function of caveolae are sensitive to plasma membrane cholesterol (Rothberg et al. 1992; Schnitzer et al. 1994). This led us to the hypothesis that LCFA uptake in 3T3-F442A adipocytes may be sensitive to plasma membrane cholesterol levels. To test this we investigated the effect of cholesterol depleting agents on LCFA uptake in 3T3-F442A adipocytes.

C.1.1 Adipocyte Differentiation of 3T3-F442A Cells

Previous work in the Gerber lab (Trigatti Ph.D. thesis, 1995) characterized LCFA uptake in the 3T3-L1 cell line. For this thesis, LCFA uptake was studied in the related cell line, 3T3-F442A. These cells, like the 3T3-L1 cells can be induced to differentiate into an adipocyte phenotype (Green et al. 1976). The differentiation of 3T3-F442A cells is stimulated by culturing them in media containing 10% fetal bovine serum (FBS) and 5 μg/ml insulin until 2 days post confluence at which point the media is no longer supplemented with insulin (see Section B.2.2.3). To observe the morphological changes in 3T3-F442A cells as they differentiate, preadipocytes (1 day post confluence, cultured in media with 10% calf serum, see Section B.2.2.3) and day 8 adipocytes (see Section B.2.2.3) were observed with differential interference contrast (DIC) imaging, unstained or stained with oil red O (a dye for neutral lipids)(as described in Section B.2.3.7)(Figure 4). Differentiation of the cells to adipocytes was marked by a change the shape of the cells from an elongated fibroblast like shape to a more rounded morphology, (Figure 4, compare panels A and B). In addition, the cells accumulated intracellular lipid droplets as they differentiated (Green et al. 1976) (Figure 4, note the red intracellular staining in panel D versus panel C). When cells were stimulated to differentiate these changes were typically first noted by day 2 of differentiation (e.g. 2 days post confluence), and by day 8 of differentiation the majority of cells demonstrated the adipocyte morphology.

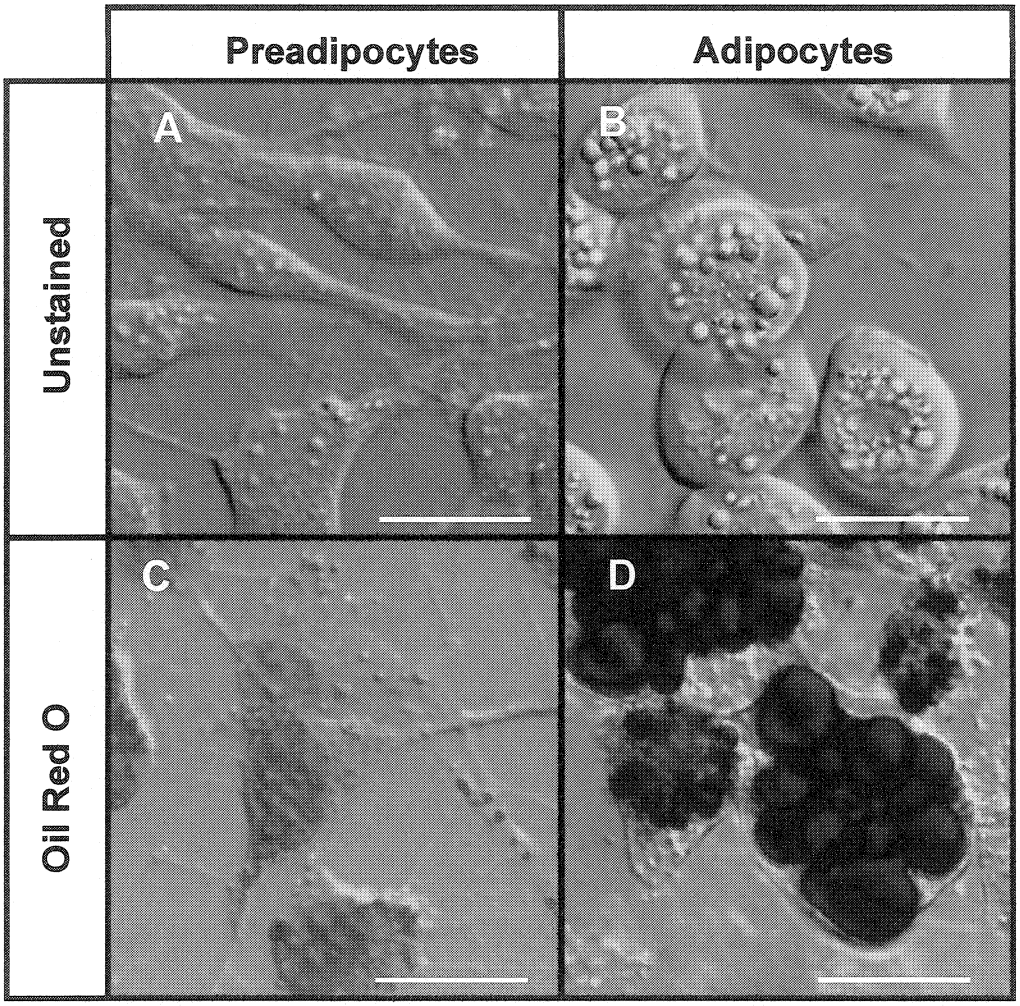

Figure 4. DIC Images of Unstained and Oil Red O Stained 3T3-F442A Preadipocytes and Adipocytes. 3T3-F442A preadipocytes (panels A and C) were cultured for 1 day post confluence (as described in Section B.2.2.1) or day 8 adipocytes (panels B and D)(cultured as described in Section B.2.2.3) were either unstained (panels A and B) or stained with oil red O (panels C and D) as described in Section B.2.3.7. Cells were imaged by differential image contrast (DIC). Scale bar represents 20 μm.

C.1.2 Long Chain Fatty Acid Uptake in 3T3-F442A Cells

As 3T3-L1 cells differentiate towards the adipocyte phenotype, the rate of LCFA uptake increases (Carnicero 1984; Trigatti et al. 1991). To investigate changes in LCFA uptake in 3T3-F442A cells as they differentiate, oleate uptake was measured using an assay originally described in (Abumrad et al. 1981) and modified by (Trigatti et al. 1991). Oleate uptake was assayed (as described in Section B.2.3.2) in 3T3-F442A preadipocytes and in 3T3-F442A day 4 adipocytes (Figure 5). Oleate uptake by both undifferentiated and differentiating cells increased with time from 30 seconds to 120 seconds. The rate of uptake by adipocytes (1.54 ± 0.06 nmols/min/10^6 cells) was 15-fold greater than that by preadipocytes (0.10 ± 0.04 nmols/min/10^6 cells).

To more precisely investigate how the rate of LCFA uptake changes over differentiation, oleate uptake was monitored daily from day 1 of differentiation through day 7 (Figure 6). Oleate uptake increased 10-fold from day 1 (0.2 nmols/min/10^6 cells) through day 4 (2.3 nmols/min/10^6 cells) of differentiation. After day 4 of differentiation the rate of uptake had reached a plateau, and then the rate of oleate uptake decreased beyond day 5 of differentiation. A similar decrease in oleate uptake was noted in 3T3-L1 adipocytes (Trigatti et al. 1991). Whether this decrease was truly a decrease in uptake or an artifact of the assay, such as cell lysis during filtration of lipid-laden cells (Trigatti et al. 1991), was not investigated further. Since the maximum rate of oleate uptake was achieved by day 4 of differentiation, day 4 adipocytes were used in all subsequent

A.

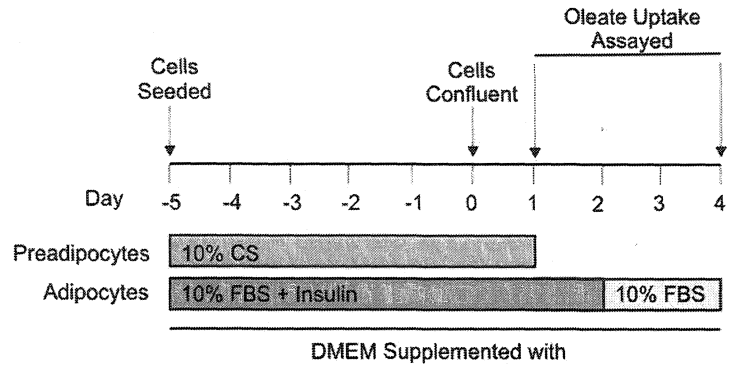

B.

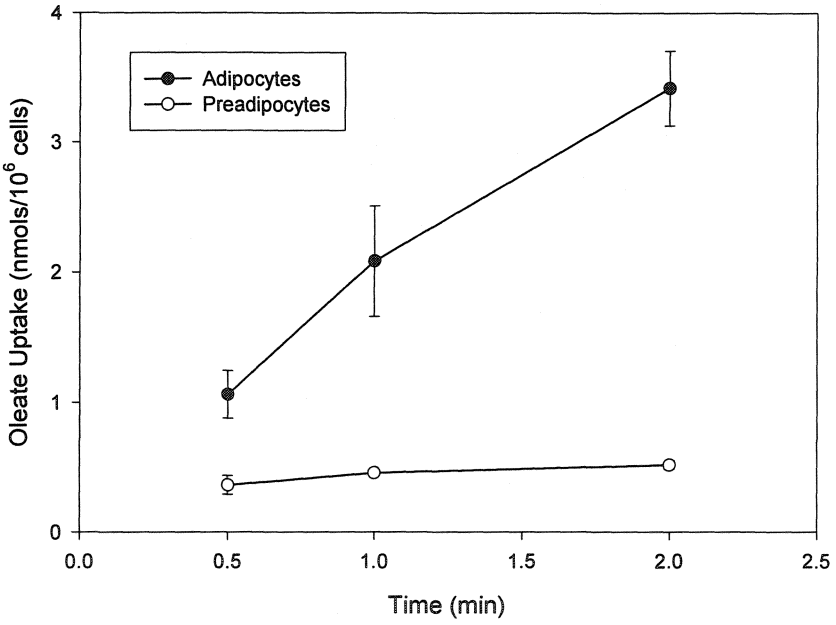

Figure 5. Oleate Uptake in 3T3-F442A Preadipocytes and Adipocytes. A. Schematic outline of the culture conditions and time line for the experiment. B. Oleate uptake was measured in 3T3-F442A preadipocytes (cultured 1 day post confluence)(open circle) or 3T3-F442A adipocytes (day 4 differentiating adipocytes)(closed circles). Cells were incubated in suspension with a 150 μM oleate:BSA complex (1:1 molar ratio with 200 μCi/μmol [^{3}H]-oleate) at 37°C. At the indicated time cells were filtered, washed 3 times with a stop solution (ice cold 0.1% BSA with 200 μM phloretin in PBS) and then the filter-associated ^{3}H was determined by scintillation counting (as described in Methods Section B.2.3.2). The rate of oleate uptake was 0.10 ± 0.04 nmol/min/10^6cells versus 1.54±0.06 nmol/min/10^6cells for preadipocytes and adipocytes respectively.

A.

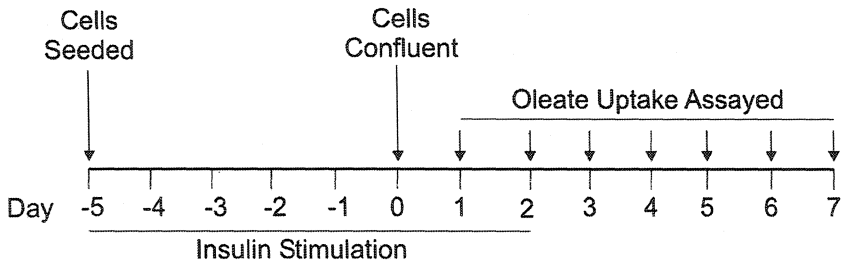

B.

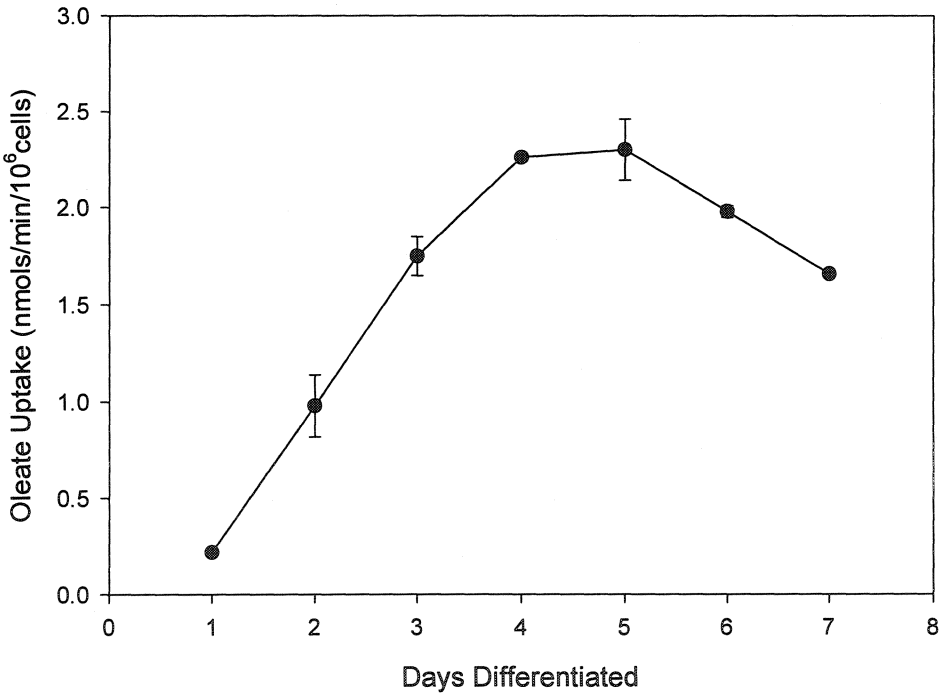

Figure 6. Oleate Uptake Activity During Adipocyte Differentiation of 3T3-F442A Cells. A. Schematic diagram of the timeline for the differentiation of the cells and assay time points. B. 3T3-F442A cells were seeded at $6x10^4$ cells per 100mm culture dish in Dulbecco's Modified Eagle Medium supplemented with 10% FBS, 50 units/ml penicillin, 50 µg/ml streptomycin, 2mM L-glutamine and 5 µg/ml insulin until 2 days post confluence at which time cells were cultured in the above media without insulin supplementation and the media was replaced every second day (see Section B.2.2.3). Each day beginning at day 1 of differentiation cells were harvested and assayed for oleate uptake was assayed (as described in the legend to Figure 5 and Section B.2.2.3). Data points are the mean ± standard deviation of single time points (n=3).

experiments.

It is noteworthy that the rate of oleate uptake in day 4 adipocytes was different between the experiments for Figure 5 and 6. Through further experiments we found the rate of LCFA uptake to be variable between experiments, with an average oleate uptake rate of 1.45 ± 0.53 nmols/min/10^6 cells for day 4 adipocytes (n=6). This variability may have been a result of differences in the degree of differentiation achieved (the ratio of cells which have undergone adipocyte differentiation, as judged by the presence of intracellular lipid droplets, versus those that had not) between distinct experiments. Although there was variability in the extent of adipose conversion, cells differentiated together (plates seeded and cultured at the same time), were found to reproducibly differentiate to similar levels and had very similar levels of oleate uptake.

C.1.3 Cholesterol Depletion in 3T3-F442A Adipocytes

As stated above, we had developed the hypothesis that LCFA uptake in 3T3-F442A adipocytes may be sensitive to the plasma membrane cholesterol content. To test this hypothesis, the effect of cholesterol depletion on oleate uptake was investigated. Cyclodextrin has been used in a variety of cultured cells including 3T3-L1 adipocytes (Parpal et al. 2001) to deplete cellular cholesterol and disrupt caveolae. We treated differentiating 3T3-F442A adipocytes with methyl-β-cyclodextrin and visualized cellular cholesterol in treated and untreated cells using filipin staining and fluorescent

microscopy. 3T3-F442A cells were stimulated to differentiate as described in Section B.2.2.3, except that at day 2 of differentiation the media was replaced with media containing 10 % newborn calf lipoprotein deficient serum (NCLPDS) for 2 days. On day 4 of differentiation cells were incubated with or without methyl-β-cyclodextrin (5 mM) for 2 hrs. Cells were fixed, stained with filipin and visualized by fluorescence microscopy (see Section B.2.3.4)(Figure 7). In untreated adipocytes the fluorescence was diffuse across the cell with intense fluorescence at the cell periphery (Figure 7 lower left panel). Note that an identical staining pattern was observed when cells were differentiated under standard conditions (data not shown). Adipocytes that had been treated with methyl-β-cyclodextrin had a distinctly different pattern of cholesterol distribution (Figure 7 lower middle panel). In these cells fluorescence was no longer predominately at the cell periphery nor was there a uniform staining throughout the cell, instead there was a punctate staining pattern across the cell. A similar punctate pattern has been observed in bovine aortic endothelial cells following cyclodextrin treatment (Park et al. 1998). The altered pattern of filipin staining suggested that methyl-β-cyclodextrin treatment either resulted in cholesterol depletion or in redistribution from the plasma membrane.

C.1.4 Methyl-β-Cyclodextrin Treatment Inhibits LCFA Uptake

To determine if methyl-β-cyclodextrin treatment affects LCFA uptake, day 4 3T3-F442A adipocytes were treated either with or without methyl-β-cyclodextrin (as

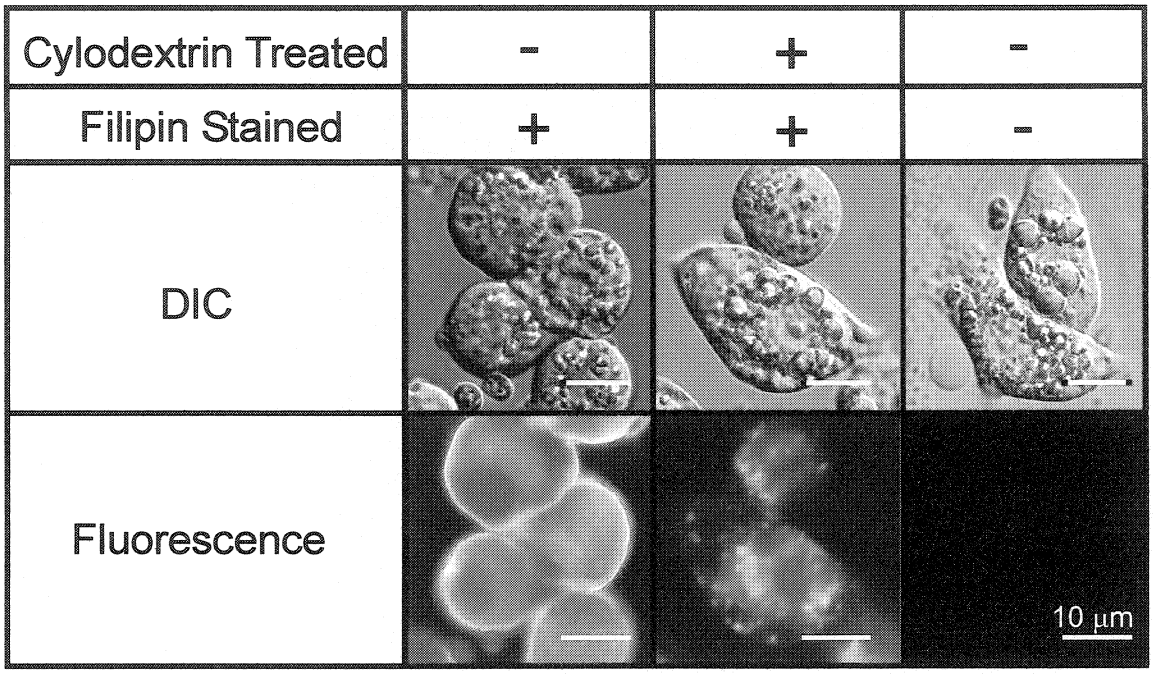

Figure 7. Effect of Cyclodextrin Treatment on Cholesterol Distribution in 3T3-F442A Adipocytes. $3x10^3$ cells per 35 mm glass bottom culture plate were stimulated to differentiate as described in Section B.2.2.3 until 2 days post confluence at which time the media was replaced with cultured in media (Dulbecco's Modified Eagle Medium supplemented with 50 units/ml penicillin, 50 µg/ml streptomycin and 2mM L-glutamine) containing 10 % newborn calf lipoprotein deficient serum (NCLPDS) for another 2 days. On day 4 of differentiation cells were incubated with or without methyl-β-cyclodextrin (5 mM) for 2 hrs at 37°C. Afterwards cells were washed with cPBS and then incubated at room temperature for 1 hour with Karnovsky's fixative. After fixation, cells were washed twice with cPBS and incubated at room temperature in the dark with filipin (50 µg/ml) in cPBS (see Section B.2.3.4). Cells were washed 3 times with cPBS at 37°C and visualized by either DIC microscopy (top panels) or fluorescence microscopy (bottom panels)(Zeiss filter set 01, excitation at 365nm (band pass 12nm) and emission above 397nm). Scale bar corresponds to 10 µm.

described in the legend to Figure 7) and then oleate uptake was measured (see Section B.2.3.2)(Figure 8). Treatment of cells with methyl-β-cyclodextrin resulted in a substantial 72% (p=0.0006) decrease in oleate uptake (Figure 8, 0.57 versus 0.16 nmols/min/10^6cells for treatment without and with methyl-β-cyclodextrin, respectively). Note that the rate of uptake was reduced in cells cultured the last 2 days in 10% NCLPDS relative to cells maintained in 10% FBS (0.57 nmols/min/10^6 versus 1.04 nmols/min/10^6 cells respectively).

C.1.5 Filipin Treatment Decreases LCFA Uptake

Filipin, chemically unrelated to cyclodextrin, has also been used to sequester cellular cholesterol and disrupt caveolar structure and function (Orlandi et al. 1998; John et al. 2001; Huo et al. 2003). Day 4 3T3-F442A adipocytes were treated with 5 μg/ml filipin (added as a stock in methanol where the final methanol concentration was 0.5%) or vehicle alone for 30 minutes, washed, harvested and then oleate uptake was assayed (as described in Section B.2.3.2)(Figure 9). Pretreatment of adipocytes with filipin resulted in a 58% decrease in oleate uptake (Figure 9, 1.92 nmols/min/10^6 and 0.80 nmols/min/10^6 cells for vehicle and filipin treated, p=0.0007). When cells were treated with filipin and then cultured for 1 hour in media containing 10% FBS, oleate uptake was partially restored (Figure 9, 1.21 nmols/min/10^6 cells, p=0.01 compared to filipin treated cells without a recovery period), suggesting that inhibition of oleate uptake by filipin was reversible. In five independent experiments filipin treatment resulted in a 25% decrease

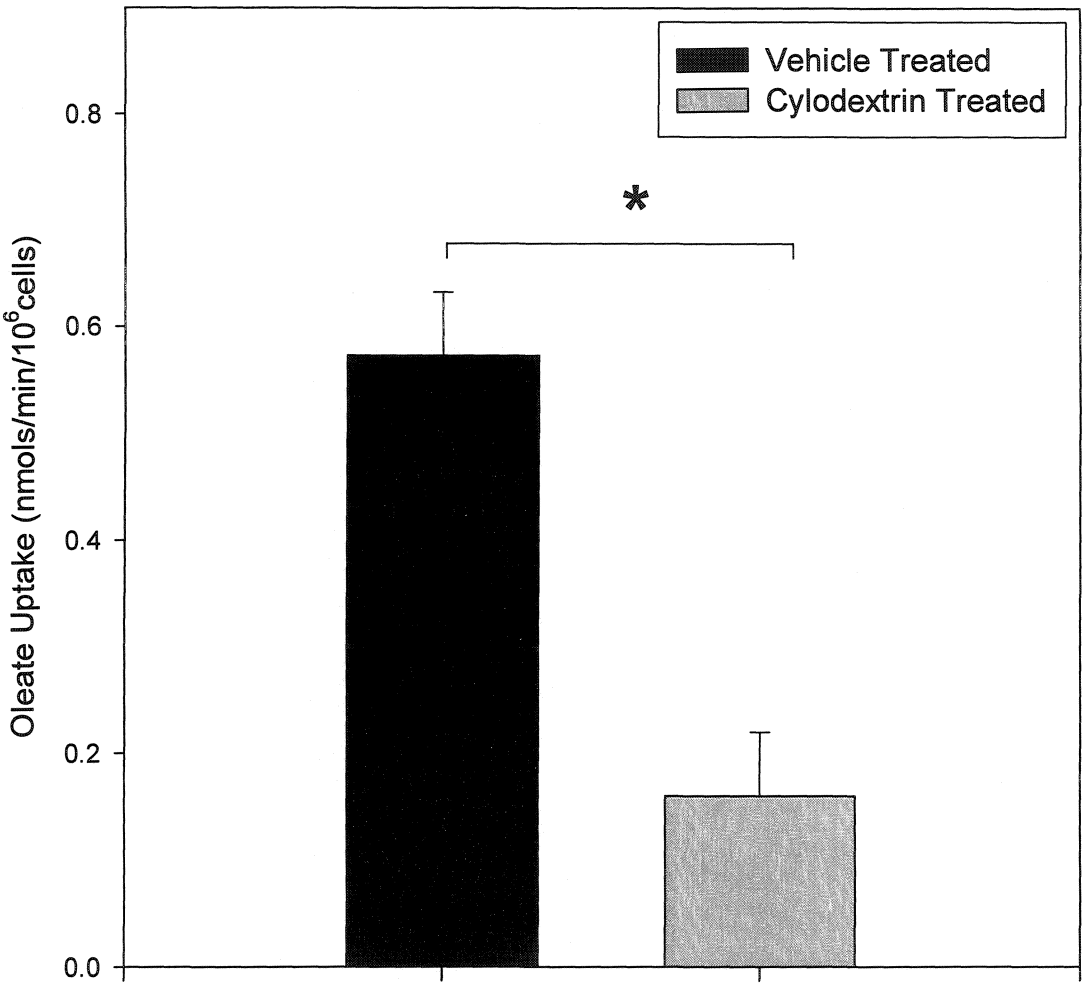

Figure 8. Effect of Methyl-β-Cyclodextrin Treatment of 3T3-F442A Adipocytes on Oleate Uptake Activity. $6x10^4$ cells per 10 cm culture plate were stimulated to differentiate as described in Section B.2.2.3 with the exception that cells were cultured from day 2 to 4 of differentiation in media containing 10% NCLPDS (as described in the legend to Figure 7). On day 4 of differentiation cells were either treated with vehicle or with 5 mM methyl-β-cyclodextrin for 2 hours at 37°C. Cells were washed, harvested and oleate uptake was assayed as described in Section B.2.3.2. Data represents the mean ± standard deviation, n=3, * p=0.0006.

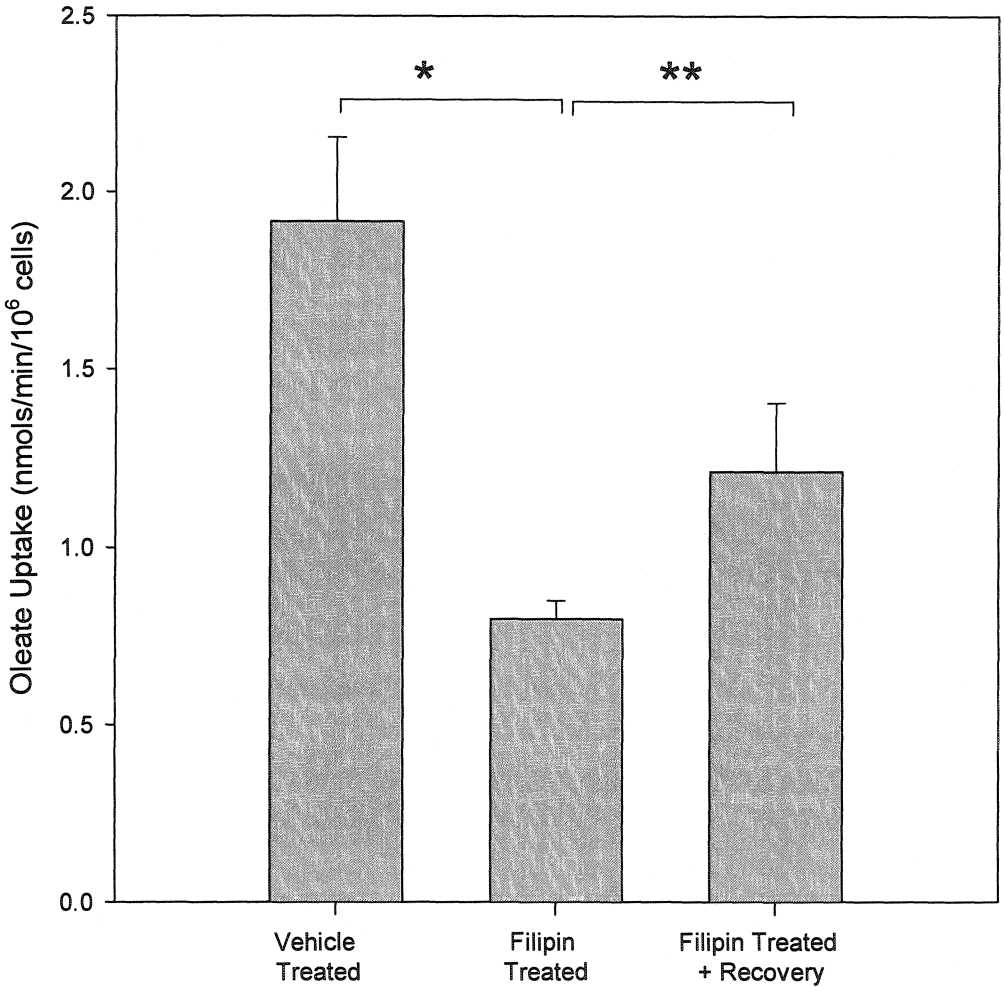

Figure 9. Effect of Filipin Treatment of 3T3-F442A Adipocytes on Oleate Uptake Activity. $6x10^4$ cells per 10 cm culture plate were stimulated to differentiate as described in Section B.2.2.3. On day 4 of differentiation cells were either treated with vehicle (methanol 0.5%) for 30 minutes at 37°C, 5 μg/ml filipin for 30 minutes at 37°C, or 5 μg/ml filipin for 30 minutes at 37°C followed by washing and a 1 hour recovery period in culture media (Dulbecco's Modified Eagle Medium supplemented with 10% FBS, 50 units/ml penicillin, 50 μg/ml streptomycin and 2 mM L-glutamine). Cells were washed, harvested and oleate uptake was assayed as described in Section B.2.3.2. Data represents the mean ± standard deviation, n=3, ** p=0.01 and * p=0.0007.

in oleate uptake (1.67 ± 0.40 nmols/min/10^6 cells versus 1.22 ± 0.43 nmols/min/10^6 cells for vehicle and filipin treated cells respectively, p=0.042).

At high concentrations, filipin can be toxic to cells, and different cell types have varying sensitivities to filipin (reviewed in (Bolard 1986)). To determine the effect of filipin on cell viability, cells were either treated with vehicle, filipin (5 μg/ml) or filipin (5 μg/ml) then a 60-minute recovery period (as described in the legend to Figure 9), and then stained with trypan blue (as described in Section B.2.3.1). Cells were counted in a hemacytometer to determine the number of cells stained with trypan blue (Table 4). Approximately 90% of the cells excluded trypan blue regardless of the treatment. Thus treatment of the cells with filipin did not appear to affect cell viability.

C.1.6 Filipin Treatment Does Not Affect 2-Deoxy-D-Glucose Uptake

To investigate if filipin specifically inhibited LCFA uptake or uptake processes in general, we measured 2-deoxy-D-glucose uptake in vehicle and filipin treated cells. Uptake of [^{3}H]-2-deoxy-D-glucose was measured using a modified filtration assay (Ibrahimi et al. 1996), see Section B.2.3.2. [^{3}H]-2-deoxy-D-glucose uptake increased with time over a 15-minute timecourse (Figure 10). To investigate if filipin treatment affected glucose uptake, adipocytes were pretreated with either vehicle or filipin (as described in the legend to Figure 9) and then oleate and glucose uptake were assayed (as described in Section B.2.3.2)(Figure 11). While filipin treatment

Table 4. Effect of Filipin Treatment of 3T3-F442A Adipocytes on Cell Viability as Assessed by Trypan Blue Staining.

	Trypan Blue		
Treatment [a]	Exclude ($x10^4$ cells/ml)	Stained ($x10^4$ cells/ml)	Viable Cells (%)
Vehicle	67±10	8±3	89±18
Filipin	86±10	13±2	87±13
Filipin + recovery [b]	77±9	8±2	91±14

[a] *treatments were performed as described in the legend to Figure 9*

[b] *filipin treated, washed and then cultured for 60 minutes in media containing 10% FBS*

- values are the mean ± standard deviation (n=3)

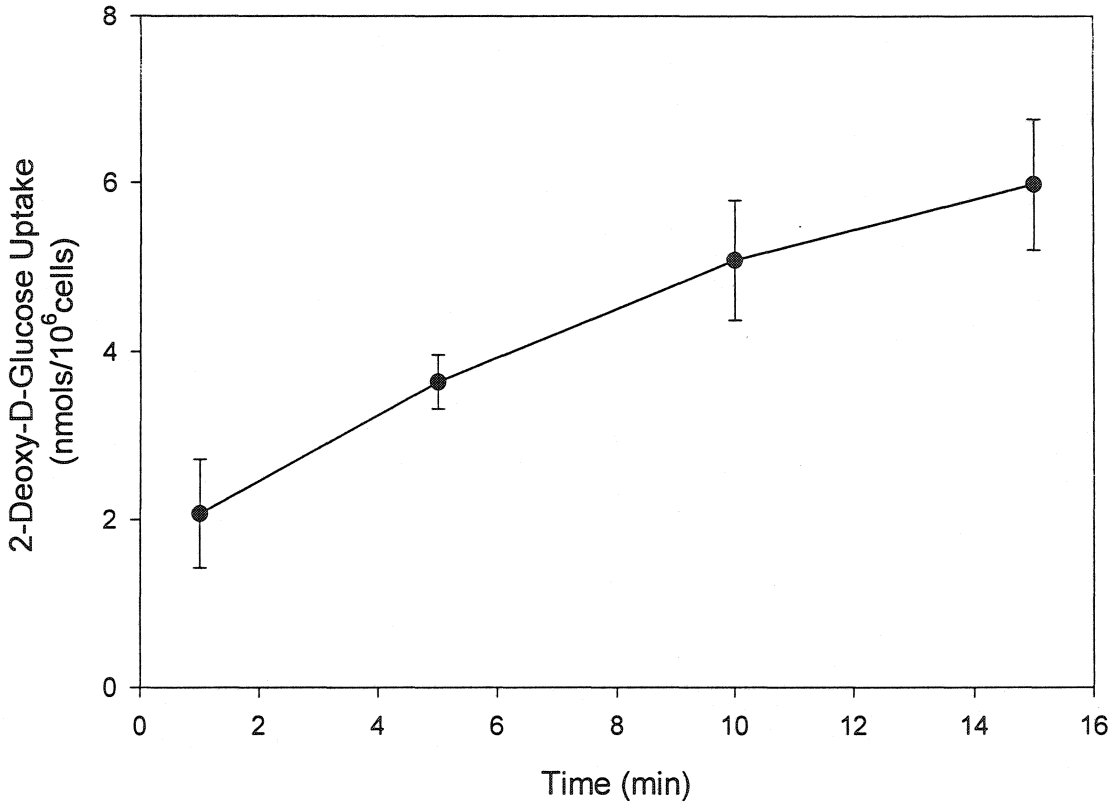

Figure 10. Timecourse of 2-Deoxy-D-Glucose Uptake in 3T3-F442A Adipocytes. $6x10^4$ cells per 10 cm culture plate were stimulated to differentiate as described in Section B.2.2.3. On day 4 of differentiation cells were washed, harvested in PBS and incubated at 37°C in suspension with 2 mM 2-deoxy-D-glucose (at 10 μCi/μmol). At the indicated time cells were filtered, washed 3 times with a stop solution (ice cold 0.1% BSA with 200 μM phloretin in PBS) and then the filter-associated ^3H was determined by scintillation counting (as described in Section B.2.3.2). Data points are the mean ± standard deviation, n=3.

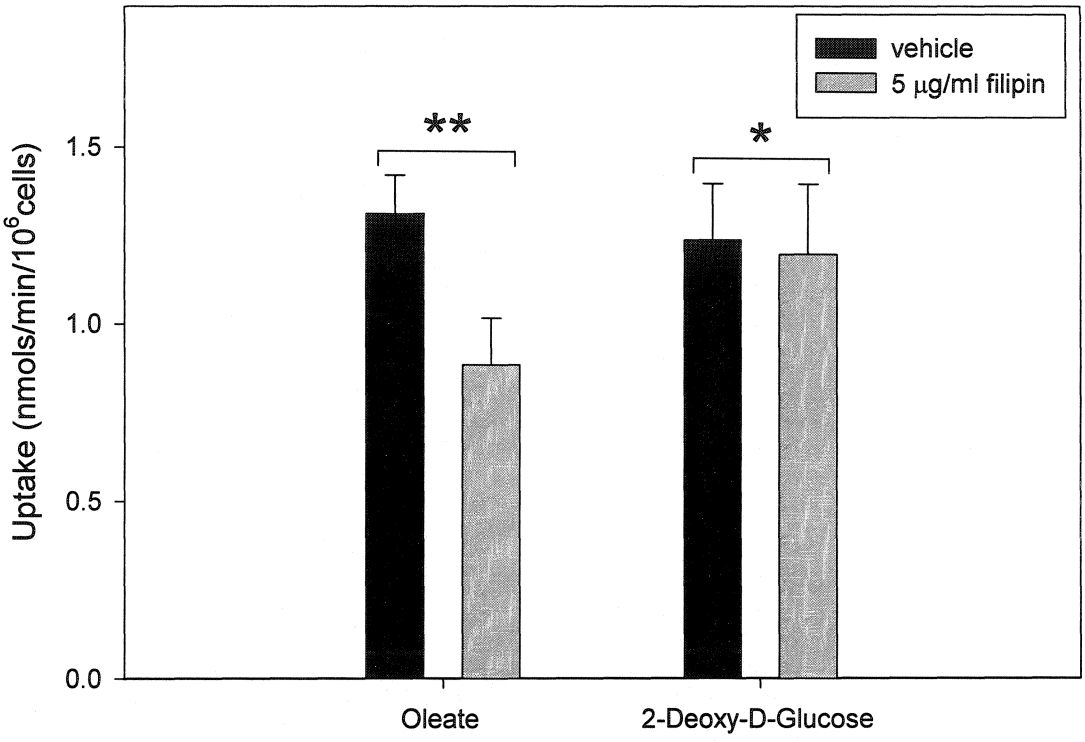

Figure 11. Effect of Filipin Treatment of 3T3-F442A Adipocytes on 2-Deoxy-D-Glucose and Oleate Uptake Activity. $6x10^4$ cells per 10 cm culture plate were stimulated to differentiate as described in Section B.2.2.3. On day 4 of differentiation, adipocytes were either treated with vehicle or 5 µg/ml filipin (as described in the legend to Figure 9). Cells were washed with PBS, harvested and assayed in suspension for oleate and 2-deoxy-D-glucose uptake (as described in Section B.2.3.2). The bars represent the mean rate of uptake ± the standard deviation, n=3. * p=0.399 and ** p=0.006.

resulted in a significant 31% (p=0.006) decrease in oleate uptake, glucose uptake was not significantly affected (1.23 ± 0.16 nmols/min/10^6cells versus 1.19 ± 0.20 nmols/min/10^6cells for vehicle and filipin treated cells respectively, p=0.399). Similarly Ros-Baro et al. also observed no difference in basal glucose uptake when 3T3-L1 adipocytes had been treated with filipin (Ros-Baro et al. 2001). Thus, the inhibition of oleate uptake by filipin was not the result of general inhibition of plasma membrane uptake processes.

C.1.7 Effect of Cholesterol Depletion on Caveolin-1

To determine if treatment with filipin or methyl-β-cyclodextrin altered caveolin-1 levels in 3T3-F442A adipocytes, cells were treated as described in the legends for Figures 8 and 9. Cell lysates were prepared (as described in Section B.2.4.1), proteins separated by SDS-PAGE (as described in Section B.2.5.1) and caveolin-1 was detected by immunoblotting (as described in Section B.2.5.3)(Table 5). There was no difference in the amount of caveolin-1α or β between untreated cells and cells treated with filipin or methyl-β-cyclodextrin (Table 5). In contrast, Hailstones et al. reported that longer (overnight) treatment of MDCK cells with cyclodextrin did decrease caveolin-1 levels (Hailstones et al. 1998). We did not determine if caveolin-1 levels in 3T3-F442A adipocytes were sensitive to a more prolonged treatment. It is clear from our results, however, that the reduced LCFA uptake in cyclodextrin of filipin treated cells was not the result of decreased caveolin-1 levels.

Table 5. Caveolin-1 expression levels in 3T3-F442A adipocytes following cholesterol depletion by filipin and methyl-β-cyclodextrin determined by quantitative immunoblotting.

	10% FBS			10% NCLPDS		
Caveolin-1	Control [c]	Filipin	p [b]	Control [d]	Cyclodextrin	p [b]
α-isoform	0.69±0.04	0.61±0.23	0.305	0.62±0.09	0.55±0.09	0.196
β-isoform	0.31±0.04	0.31±0.15	0.480	0.31±0.09	0.40±0.36	0.351
Total [a]	1.00±0.21	0.92±0.38	0.327	0.93±0.18	0.95±0.46	0.476

-arbitrary luminescence values (detected with a Kodak Image Station 440CF) have been normalized with respect to the caveolin (total) luminescence in control treated cells cultured in 10% FBS
-n=3
-[a] the sum of alpha and beta isoforms
-[b] Student's t-test
-[c] cells were treated with vehicle (methanol 0.5% final concentration)
-[d] cells were treated with vehicle (DMEM supplemented with 50 units/ml penicillin, 50 μg/ml streptomycin and 2 mM L-glutamine)

Cholesterol depletion has also been reported to cause redistribution of caveolin-1 from the plasma membrane to the Golgi apparatus (Smart et al. 1994). We therefore tested if cyclodextrin or filipin treatment of 3T3-F442A differentiating adipocytes affected the subcellular distribution of caveolin-1 in these cells using immunofluorescence microscopy. Cells were cultured and treated with methyl-β-cyclodextrin or filipin as described in figures 8 and 9. Adipocytes were fixed, permeabilized and stained with a polyclonal anti-caveolin-1 antibody and an alexa 488 conjugated anti-rabbit secondary antibody (performed as described in Sections B.2.3.5)(Figure 12). Caveolin-1 was localized at the cell periphery and in what appeared to be perinuclear regions in control untreated cells (panel A). Culturing the cells for 2 days in the absence of lipoproteins (panel E) or treatment with filipin (panel B) or methyl-β-cyclodextrin (panel F) did not affect the distribution of caveolin-1. From these experiments, the decrease in LCFA uptake following treatment with cholesterol binding reagents is not attributable to a major redistribution of caveolin from the plasma membrane.

C.1.8 Conclusions and Implications

We hypothesized that LCFA uptake in 3T3-F442A adipocytes would be sensitive to plasma membrane cholesterol content based on the following observations: 1) caveolin-1, a component of caveolae, is a LCFA binding protein and has been proposed to participate in LCFA uptake and/or trafficking in adipocytes (Trigatti et al. 1999); 2)

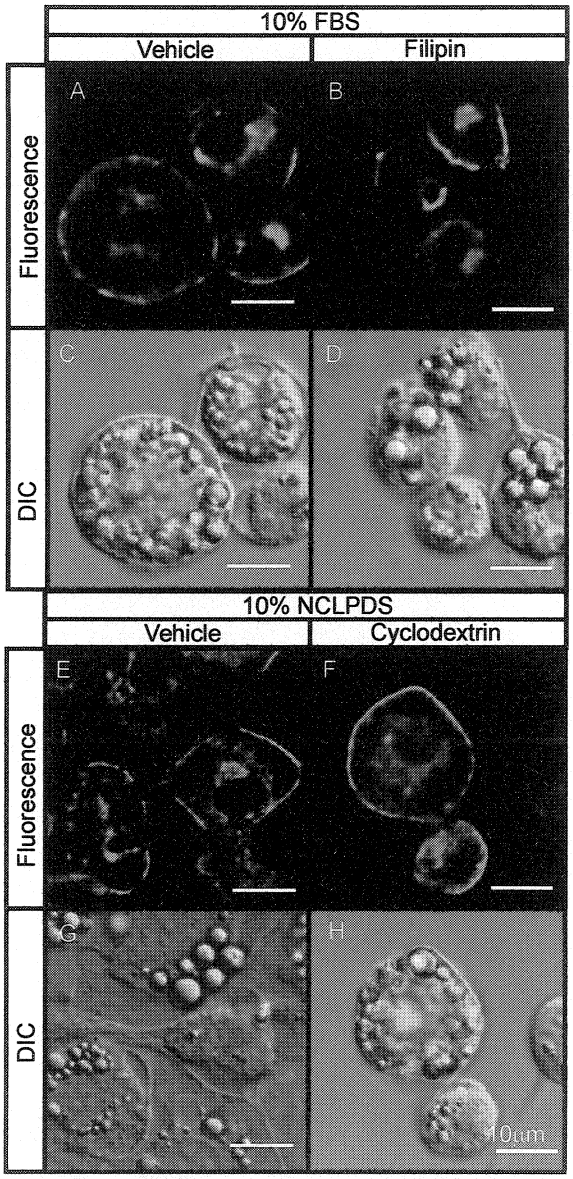

Figure 12. Distribution of Caveolin-1 Following Cholesterol Depletion of 3T3-F442A Adipocytes. $3x10^3$ cells per 35 mm glass bottom culture plate were stimulated to differentiate (as described in Section B.2.2.3) until 2 days post confluence at which point cells were cultured for another 2 days in media supplements with 10% FBS (panels A-D), or in media supplemented with 10% NCLPDS (panels E-H). On day 4 of differentiation, cells were either treated with 5 μg/ml filipin (panels B and D), vehicle (methanol) control (panel A and C), 5 mM methyl-β-cyclodextrin (panels F and H), or vehicle (DMEM) control (panel E and G) as described in the legends to Figures 8 and 9. Cells were processed for immunofluorescence (as described in Section B.2.3.5) using a polyclonal anti-caveolin-1 antibody and an alexa 488 conjugated anti-rabbit secondary antibody. Cells were washed 3 times with cPBS at 37°C and visualized by either DIC or fluorescence microscopy (excitation 450-490 nm emission 515-565). The scale bar corresponds to 10 μm.

CD36/FAT, a known component of the LCFA uptake apparatus, is localized in caveolae (Lisanti et al. 1994); 3) removal of cholesterol from plasma membranes disrupts caveolae structure and function (Rothberg et al. 1992; Schnitzer et al. 1994). To test this hypothesis, we investigated the effect of two well-established cholesterol depleting reagents on LCFA uptake in 3T3-F442A adipocytes. From the experiments presented in this section we found that cholesterol depletion results in inhibition of LCFA uptake, but not glucose uptake, indicating that LCFA uptake is dependent on plasma membrane cholesterol.

Since this work was originally performed, other groups have also reported that LCFA uptake activity is dependent on cellular cholesterol. Pohl et al. have demonstrated that both cyclodextrin and filipin treatment of HepG2 cells (a human hepatocellular carcinoma cell line) resulted in decreased LCFA uptake (Pohl et al. 2002). Furthermore these authors also found the inhibition of uptake by filipin to be reversible, as our results had suggested (Figure 9). Interestingly, another group has reported that increasing cellular cholesterol can stimulate LCFA uptake, in type II pneumocytes. In that study, increasing the cellular content of cholesterol resulted in a 4-fold increase in palmitate uptake (Kolleck et al. 2002).

Depletion of cellular cholesterol could potentially inhibit LCFA uptake via several mechanisms. One possible mechanism is that cholesterol depletion disrupts caveolae.

Disruption of caveolae may directly impair LCFA uptake. Alternatively disruption of caveolae may affect the activity of constituents of caveolae involved in LCFA uptake (i.e. caveolin and CD36/FAT). Our results have shown that cholesterol depletion resulting in inhibition of LCFA uptake did not affect caveolin levels (Table 5) or distribution between internal membranes and the plasma membrane (Figure 12). Alternatively cholesterol depletion may inhibit LCFA in a manner distinct from caveolae, perhaps by affecting the activity of other non-caveolar LCFA transporters (e.g. FATP and FABPpm). In addition cholesterol depletion may affect the activity of proteins downstream of membrane translocation such as FACS (an acyl-CoA synthetase) and ALBP (a cytosolic fatty acid binding protein).

There is further experimental support for a model of LCFA uptake involving caveolae and or caveolin. As stated earlier, caveolin is a LCFA binding protein (Trigatti et al. 1991; Trigatti et al. 1999). Others have shown that a 50% reduction in caveolin-1 levels due to antisense expression in HepG2 cells (a human hepatoma cell line) resulted in a 23% decrease in LCFA uptake (Pohl et al. 2002). In addition recent observations made on caveolin-1 knockout mice suggest that caveolin and or caveolae may be physiologically relevant to adipocyte function and or development. Caveolin-1 knockout mice displayed; 1) Reduced body weights relative to wild-type controls, 2) reduced adiposity (fat to water ratio), reduced adipocyte cell diameter, reduced adipocyte number and smaller lipid droplets and 3) elevated serum triglycerides and free fatty acids (Razani

et al. 2002). These findings indicated that the knockout mice were unable to convert triglycerides in lipoproteins to triglycerides in adipocyte lipid droplets despite the fact that there is no difference in lipoprotein lipase activity between wild type and knockout mice (Razani et al. 2002). As the authors point out, one possible reason for the phenotype of the caveolin-1 knockout mouse is decreased LCFA uptake, which would be consistent with studies on cultured cells (this work and (Pohl et al. 2002)).

C.2 3T3-F442A Cell Surface Albumin Binding Proteins

Unesterified LCFAs in the serum are predominately bound to serum albumin with only a small fraction free or uncomplexed (average resting human serum total fatty acid is 502 ± 150 μM versus free fatty acid is 7.5 ± 2.5 nM (Richieri et al. 1995)). In the traditional view of LCFA uptake, it is this small pool of uncomplexed fatty acid that spontaneously dissociates from albumin that is taken up by cells. In this regard albumin serves as a means to solubilize fatty acids but does not participate directly in cellular uptake. This view was challenged by studies that suggested the kinetics of LCFA uptake in the liver are more compatible with a model of uptake where albumin binds to a cell surface receptor, a observation that came to be know as the albumin receptor effect (Weisiger et al. 1981). Since then the albumin receptor effect has been documented for several other cell types including, T-lymphocytes (Uriel et al. 1994), cardiomyocytes (Hutter et al. 1984), and adipocytes (Trigatti et al. 1995).

Since the original proposal of an albumin receptor, 3 models have been developed to account for the observed kinetics (reviewed in (Sorrentino et al. 1989)). 1) The original theory, that an albumin receptor on the cell surface promotes the dissociation of LCFAs from albumin to the cell has been modified to include any interaction between the cell surface and albumin that promotes LCFA dissociation from albumin (Horie et al. 1988; Reed et al. 1989). 2) The co-diffusion model accounts for albumin receptor kinetics as a consequence of the unstirred layer that surrounds cells. This layer acts as a

barrier, and therefore limits the flux of LCFAs to the cell surface. The amount of albumin present dictates the capacity for diffusion through this layer (Weisiger et al. 1989). However others contend that this theory cannot fully account for the effect of albumin in LCFA uptake (Burczynski et al. 1989). 3) The dissociation limiting uptake model, suggests that albumin receptor kinetics are a result of LCFA uptake being restricted at low albumin concentrations by the limited spontaneous dissociation of LCFAs from albumin (Sorrentino et al. 1989). It has been demonstrated, however, that at low LCFA to albumin ratios the rate of uptake is constant, even though the LCFA taken up exceeded the initial concentration of uncomplexed LCFA, suggesting that at least for adipocytes the dissociation of LCFAs from albumin does not limit uptake (Trigatti et al. 1995).

Consistent with the existence of an albumin receptor, albumin has been reported to bind several cell types including rat hepatocytes (Horie et al. 1988; Reed et al. 1989), rat cardiomyocytes (Popov et al. 1992), human B-lymphoma cells and human blood mononuclear cells (Torres et al. 1992), rat endothelial cells (Schnitzer et al. 1988), mouse 3T3-L1 differentiating adipocytes (Trigatti et al. 1995) and rat primary adipocytes (Brandes et al. 1982). Furthermore several albumin binding proteins have been identified. Numerous groups have identified 31 and 18 kDa glycoproteins as albumin binding proteins (Ghinea et al. 1988; Popov et al. 1992; Torres et al. 1992). However these proteins have subsequently been found to preferentially bind modified albumin and have a role in the catabolism of albumin (Schnitzer et al. 1992) and thus are not likely

involved in LCFA uptake. Along with the 31 and 18 kDa proteins Ghinea et al. identified 56 kDa and 73 kDa proteins with weak albumin binding activity (accounting for less than 30% of the total albumin binding activity) in endothelial cells (Ghinea et al. 1989). Whether the 56 and 73 kDa albumin binding proteins are also involved in albumin catabolism is not known. A 60 kDa protein called albondin is also an albumin binding protein, although this protein is involved in endothelial transcytosis and there has been no evidence supporting a role for this protein in LCFA uptake (Schnitzer et al. 1988; Schnitzer 1992; Tiruppathi et al. 1996).

Since albumin receptor kinetics have been clearly demonstrated in 3T3 adipocytes (Trigatti et al. 1995) and albumin has been shown to bind adipocytes (Brandes et al. 1982; Trigatti et al. 1995) we sought to determine if albumin binding proteins exist on the cell surface of 3T3-F442A adipocytes. This section presents experiments that first addressed the nature of albumin's interaction with adipocytes in a whole cell assay, then the results from 2 different experimental approaches that attempted to detect albumin binding activity in isolated adipocyte plasma membranes.

C.2.1 Association of ^{125}I-BSA with 3T3-F442A Cells

The rate of LCFA uptake is greater in adipocytes than preadipocytes (Figure 5) and (Trigatti et al. 1991). Therefore we postulated that if albumin binding to the cell surface is an important step in LCFA uptake, then albumin binding to adipocytes should

be greater than to preadipocytes. Therefore we investigated if albumin interacts with 3T3-F442A cells in a differentiation dependent manner. ^{125}I labeled bovine serum albumin (^{125}I-BSA) (prepared as described in Section B.2.6.1) was incubated with 3T3-F442A preadipocytes (1 day post confluent) or day 7 3T3-F442A adipocytes in suspension for 45 minutes at 37°C with gentle agitation after which cells were pelleted and washed 3 times with PBS. The amount of ^{125}I-BSA associated with cells was then determined by scintillation counting (Figure 13). Adipocytes bound 2.9 times more ^{125}I-BSA than preadipocytes (10849 ± 1986 DPM versus 31892 ± 1970 DPM were associated with preadipocytes and adipocytes respectively ($p=0.000003$)).

A potential explanation for the increased BSA binding to adipocytes is that the interaction is non-specific, and due to an increase in the surface area. Indeed, Chang et al. have reported that relative to preadipocytes, adipocytes have a 1.8-fold increase in surface area (Chang et al. 1978). This increase cannot account for the 2.9-fold increase in albumin binding. Whether the interaction measured in Figure 13 is a result of albumin binding to a discreet cell surface site is not clear, however this increased interaction is consistent with an albumin receptor being involved in LCFA uptake.

Next we wanted to determine if the albumin binding measured in Figure 13 is mediated by a cell surface protein. To test this, ^{125}I-BSA binding was measured following trypsin-mediated proteolysis of 3T3-F442A adipocyte cell surface proteins.

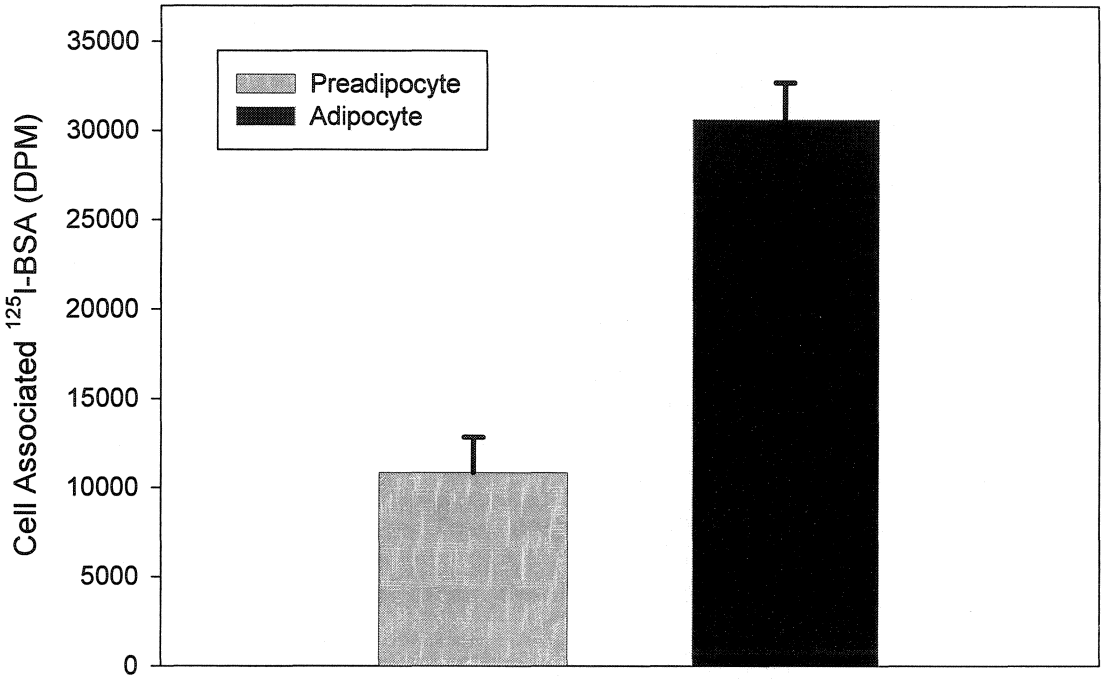

Figure 13. Association of ^{125}I-BSA with 3T3-F442A Preadipocytes and Adipocytes. Cells were seeded at $6x10^4$ cells per 100mm culture dish and were either cultured as preadipocytes (as described in Section B.2.2.1) and used at 1 day post confluence or were stimulated to differentiate (as described in Section B.2.2.3) and used on day 7 of differentiation. Cells were harvested (as described in Section B.2.4.4) in PBS and $2.7x10^6$ cells/ml were incubated with 2.5 μM ^{125}I-BSA (prepared as described in Section B.2.6.1) for 45 minutes at 37°C with gentle agitation and assayed for albumin association as described in Section B.2.3.8. The level of ^{125}I-BSA binding is expressed as the mean ± standard deviation of 3 determinations of the amount of radioactivity (DPM) associated with the cells. The ^{125}I-BSA associated with preadipocytes was 10849 ± 1986 DPM and adipocytes was 31892 ± 1970 DPM (p=0.000003).

3T3-F442A adipocytes (day 7 of differentiation) were harvested and washed 3 times with PBS, then $2.7x10^6$ cells/ml were incubated with 6μM trypsin at 37°C for 1.5, 2.5, 5 and 10 minutes prior to the addition of PMSF to quench the enzymatic activity of trypsin. Binding of ^{125}I-BSA to the cells was then assayed (Figure 14). Following 1.5 minutes of trypsin treatment there was no effect on albumin binding activity (99% of control binding), however with increasing time of trypsin treatment there was a linear decrease in albumin binding to the cells, with only 40% of the original activity remaining after 10 minutes of proteolysis.

A potential complication with this assay was that trypsin treatment might decrease the pelleting efficiency of the cells by rendering the cells less stable. To address if the decrease in albumin binding correlated with a decrease in pelleting efficiency of the cells, the amount of pelleted protein following 0 and 15 minutes of trypsin treatment was determined. 15 minutes of trypsin treatment resulted in a 27% decrease in protein; some of this was certainly attributable to liberated cell surface proteins following cleavage but a certain proportion may have been a result of decreased pelleting following trypsin treatment. However this decrease cannot account for the substantial 60% decrease in albumin binding to adipocytes (Figure 14). Thus albumin's interaction with adipocytes is at least partially protein mediated.

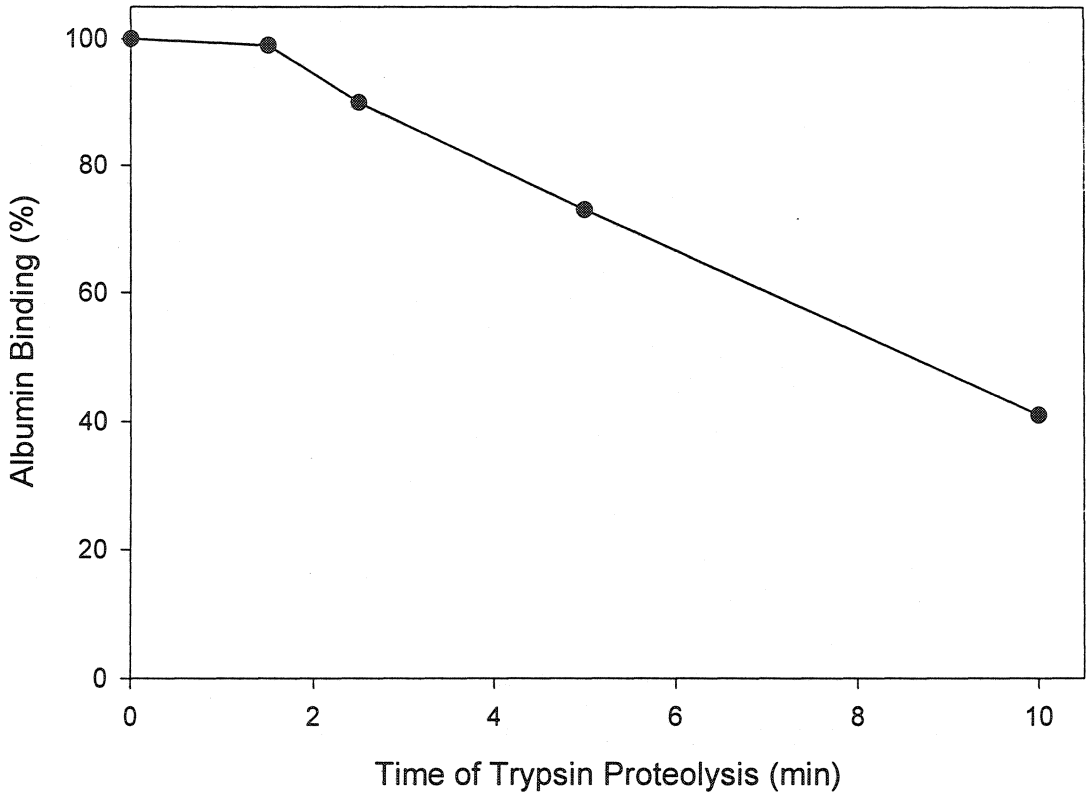

Figure 14. Effect of Trypsin Treatment of 3T3-F442A Adipocytes on ^{125}I-BSA Binding. 3T3-F442A adipocytes were cultured as described in Section B.2.2.3 and on day 7 of differentiation were harvested in PBS (as described in Section B.2.2.4). Cells were washed 3 times in PBS and then $2.7x10^6$ cells/ml were incubated with 6 μM trypsin at 37°C for 1.5, 2.5, 5 and 10 minutes. Proteolysis was terminated by the addition of phenylmethanesulfonyl fluoride to a final concentration of 10 μM. Binding of ^{125}I-BSA to cells was measured as described in the legend to Figure 13 (and in Section B.2.3.8) and is expressed as the percentage of the level of binding to control cells not treated with trypsin (time 0).

C.2.2 Development of a Quantitative Dot Blot Assay for Albumin Binding

Next we sought to develop an assay that would allow for a determination of albumin binding activity in isolated adipocyte plasma membranes. We wanted to develop an assay that would: 1) allow for albumin binding activity to be easily quantified, 2) allow for solubilization of proteins under different conditions, 3) use minimal amounts of membrane samples, and 4) be amenable to downstream use in purification of albumin binding proteins. We decided to design a form of a dot blot assay where membrane proteins would be solubilized and then spotted onto a nitrocellulose membrane that could be probed with ^{125}I-BSA, and the amount of albumin binding activity determined by scintillation counting.

The first step in developing the dot blot assay was determining the appropriate solubilization conditions. We began by testing albumin binding activity in membrane samples following treatment with a variety of detergents, differing in head group, ionic nature and acyl chain length. For this experiment 10 μg of 3T3-F442A adipocyte plasma membranes were solubilized for 30 minutes at 37°C in 1% (w/v) detergent in solubilization buffer (0.1 M phosphate buffer pH 7.4, 0.25 M NaCl, 1 mM EDTA, 1 mM EGTA, 1 mM PMSF, and 10 μg/ml leupeptin). The membranes were then spotted (3.03 μl) onto nitrocellulose, as was an equal volume of solubilization buffer with detergent in the absence of membranes. Once the spots had dried, nonspecific protein binding sites were blocked with 1.5% gelatin. Nitrocellulose membranes were then probed with 50

μg/ml ^{125}I-BSA, washed 3 times with TBS-T dried and then exposed to autoradiography film, (Figure 15). There was a large range in ^{125}I-BSA binding depending on which detergent was used. In several cases (e.g. nonidet P40 and triton X-114, Figure 15 lanes 1 and 2) much of the bound ^{125}I-BSA was due to the detergent itself and not the plasma membrane. Several detergents (e.g. triton X-100, n-octylglucoside, SDS, sarkosyl, sodium cholate and deoxycholate and CHAPS, Figure 15 lanes 3, 8-10 and 12-14) provided good signal when plasma membranes were present and minimal signal in the absence of membranes. The zwitterionic synthetic bile salt, CHAPS, produced a good signal to noise ratio and was chosen as a suitable detergent for solubilizing membranes for the dot blot assay.

For the assay to be quantitative, we needed to ensure that proteins bound to nitrocellulose could be precisely measured. The binding of the ^{125}I-BSA to the nitrocellulose could potentially hinder the precise measurement of the isotope due to point quenching (the absorption of particles before interacting with the solvent). To avoid this complication nitrocellulose filters were dissolved in tetrahydrofuran (THF) for 45 minutes at room temperature. The efficiency of detecting ^{125}I labeled proteins bound to nitrocellulose was evaluated by performing scintillation counting on equal amounts of ^{125}I labeled protein either added directly to scintillation fluid or spotted onto a nitrocellulose membrane, allowed to dry, then treated with THF and added to scintillation fluid. The difference in counts between the sample counted directly and that spotted and treated with

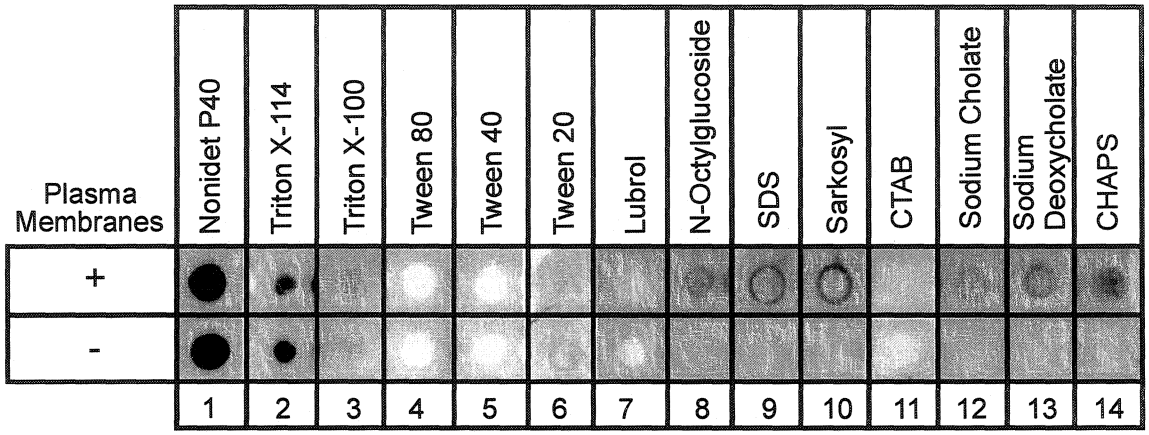

Figure 15. Dot Blot Assay of ^{125}I-BSA Binding to Detergent Treated 3T3-F442A Adipocyte Plasma Membranes. 3T3-F442A adipocytes were cultured (as described in Section B.2.2.3) until day 4 of differentiation at which point plasma membranes were prepared as described in Section B.2.4.3 and 10 μg of protein were solubilized at 37°C for 30 minutes in the presence of the indicated detergent (1% w/v in 0.1 M sodium phosphate pH 7.4, 0.25 M NaCl, 1 mM EDTA, 1 mM EGTA, 1 mM PMSF and 10 μg/ml leupeptin). Solubilized membranes (top row) or buffer with detergent in the absence of membranes (lower row, negative control) were spotted onto nitrocellulose and probed with ^{125}I-BSA (prepared as described in Section B.2.6.1) and visualized by autoradiography (as described in Section B.2.5.4).

THF was only 2% ($4104x10^3 \pm 757x10^3$ and $4023x10^3 \pm 11x10^3$ DPM respectively), indicating that ^{125}I labeled proteins bound to nitrocellulose and processed in this manner could be precisely measured.

The optimal ratio of protein to CHAPS was determined for albumin binding activity. Plasma membranes from 3T3-F442A adipocytes (10 μg at 3 mg/ml) (prepared as described in Section B.2.4.3) were incubated for 30 minutes at 37°C with CHAPS (from 0.1 to 1.5% w/v) then probed with ^{125}I-BSA (as described in Section B.2.5.4) (Figure 16). The albumin binding activity increased with increasing CHAPS concentration up to a maximum at 1% CHAPS (corresponding to a detergent to protein ratio of 3.3:1), after which there was a slight decrease in activity. Thus membranes were solubilized at a CHAPS to protein ratio of 3.3:1 for optimal albumin binding activity.

Next we compared murine serum albumin (MSA) and bovine (BSA) binding to adipocyte plasma membranes. MSA and BSA were iodinated (as described in Sections B.2.6.1) and used to probe albumin binding to 3T3-F442A adipocyte plasma membranes in the dot blot assay (see Section B.2.5.4). The albumin binding activity of BSA was found to be 89% of the activity of MSA (11.2 and 12.6 fmol albumin bound/μg of membrane protein for BSA and MSA respectively) and was therefore deemed an acceptable probe for albumin binding.

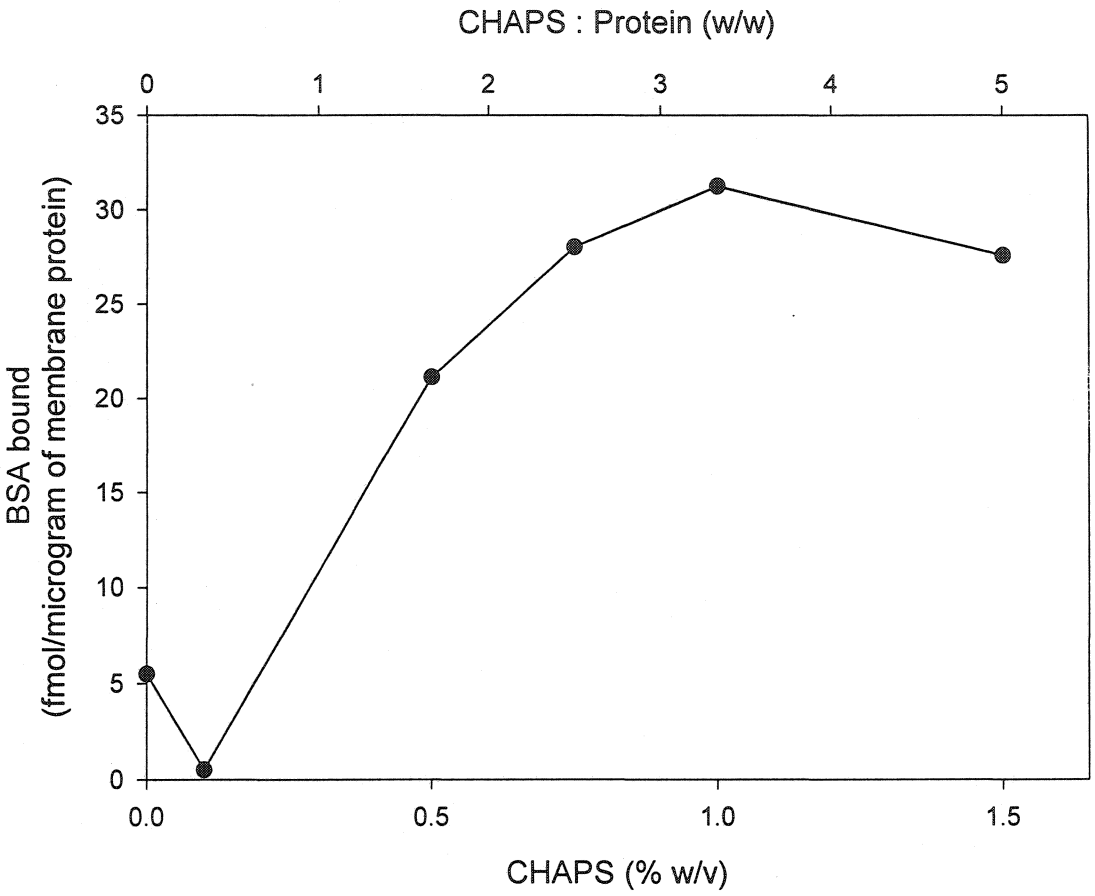

Figure 16. Effect of CHAPS to Plasma Membrane Protein Ratio on ^{125}I-BSA Binding. 3T3-F442A adipocytes were cultured (as described in Section B.2.2.3) until day 4 of differentiation at which point plasma membranes were prepared as described in Section B.2.4.3. 10 μg of plasma membrane were solubilized at 37°C for 30 minutes in the absence and presence of increasing concentrations of the detergent CHAPS. Samples were then spotted onto nitrocellulose and probed for ^{125}I-BSA binding (as described in the legend to Figure 15). ^{125}I-BSA binding was determined by scintillation counting of pieces punched out of the nitrocellulose filter and dissolved in THF (as described in Section B.2.5.4). Values are expressed in fmol of BSA bound/μg membrane protein spotted.

We anticipated that if an albumin binding protein exists, and if it functions in mediating LCFA uptake from albumin, then among the cellular membrane fractions the greatest albumin binding activity should occur in the adipocyte plasma membrane enriched fraction. To test this prediction, albumin binding activity was assayed (as described in Section B.2.5.4) in mitochondria, low density microsomal membrane, and plasma membrane enriched fractions prepared from 3T3-F442A preadipocytes and adipocytes (Figure 17). The albumin binding activity of plasma membranes from adipocytes and preadipocytes were identical, and in fact had an activity similar to that of low density microsomal membranes. The mitochondria enriched fractions had the greatest albumin binding activity. Thus there was not compelling evidence that a specific adipocyte plasma membrane albumin binding protein was being detected by this dot blot assay. Whether that reflected the absence of a high affinity albumin binding protein in the sample or an inability to adequately detect such an activity was not investigated further.

C.2.3 Detection of 3T3-F442A Adipocyte Albumin Binding Proteins by Ligand Blotting

Albumin binding to adipocytes is greater than to preadipocytes (Figure 13) and is sensitive to proteolysis (Figure 14). Therefore we developed a ligand blot assay (see Section (B.2.5.5) to determine if distinct albumin binding proteins were present in 3T3-F442A adipocytes. This methodology has previously been successful in identifying

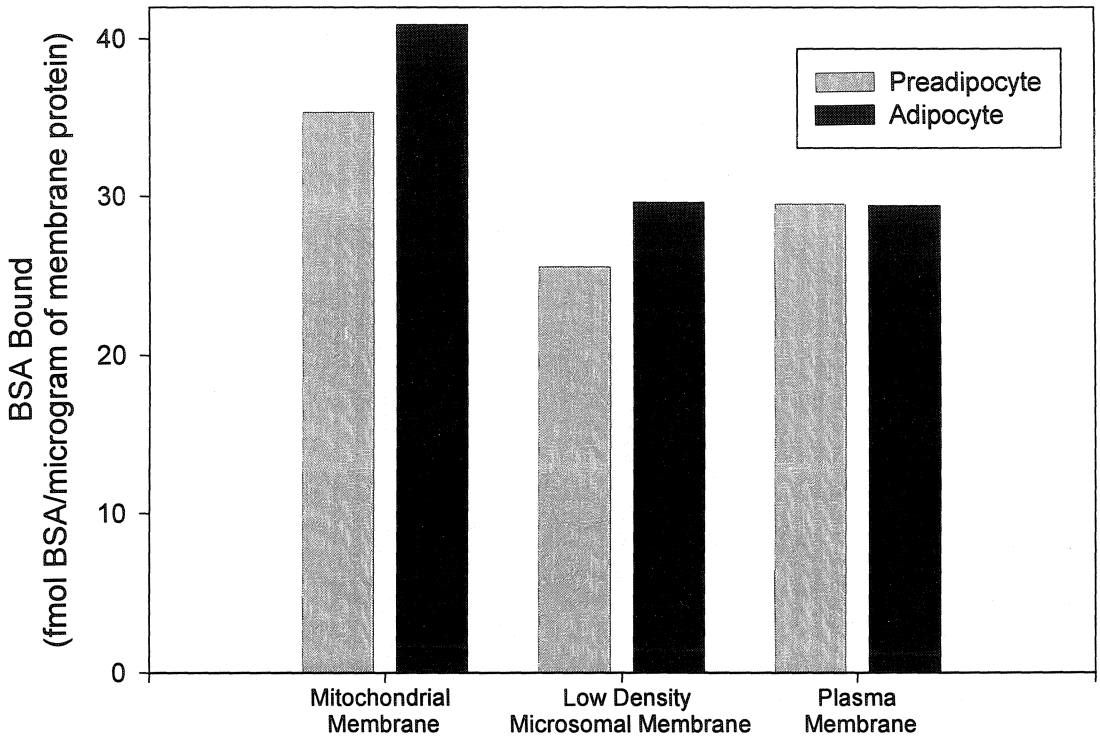

Figure 17. ^{125}I-BSA Binding to Subcellular Membrane Fractions of 3T3-F442A Preadipocytes and Adipocytes. 3T3-F442A cells were either cultured as preadipocytes (1 day post confluence) as described in Section B.2.2.1 or cultured to differentiate (to day 4 of differentiation) as describe in Section B.2.2.3. Membrane fractions were prepared for preadipocytes and adipocytes as described in Section B.2.4.3. 10 μg of protein from each fraction were solubilized with CHAPS (at a final detergent to protein ratio of 3.3:1) at 37°C for 30 minutes, spotted onto nitrocellulose and ^{125}I-BSA binding was measured as described in the legend to Figure 16 and in Section B.2.5.4. The data is expressed as the fmol of ^{125}I-BSA bound per μg of membrane protein spotted.

albumin binding proteins (Schnitzer et al. 1988; Tiruppathi et al. 1996). We separated proteins from different cellular membrane fractions of 3T3-F442A adipocytes by SDS-PAGE (as described in Section B.2.5.1), then transferred them to a PVDF membrane (as described in Section B.2.5.2) and probed the blot with ^{125}I-BSA (prepared as described in Section B.2.6.1), (Figure 18). Albumin binding proteins were detected in all the membrane fractions assayed. In the plasma membrane enriched fraction (Figure 18 lane 3) there were weak bands at 48.3 ± 1.1 and 42.0 ± 1.0 kDa, as well as bands at 36.9 ± 1.1 and 33.4 ± 0.7 kDa with a greater ^{125}I-BSA binding. It was noted that there was significant albumin binding activity in the mitochondria enriched fraction as well (Figure 18 lane 1).

C.2.4 Conclusions and Implications

We postulated that if albumin binding to the cell surface is an important step in LCFA uptake, then adipocytes should bind more albumin than preadipocytes. Indeed we found this to be true (Figure 13). Furthermore the trypsin sensitivity of this binding (Figure 14) was consistent with the existence of a cell surface albumin binding protein. However the specificity of this binding and if it is relevant to LCFA has yet to be determined.

Our ultimate goal was to seek out adipocyte cell surface proteins that bound albumin. Thus we sought to develop an assay that could be used in conjunction with

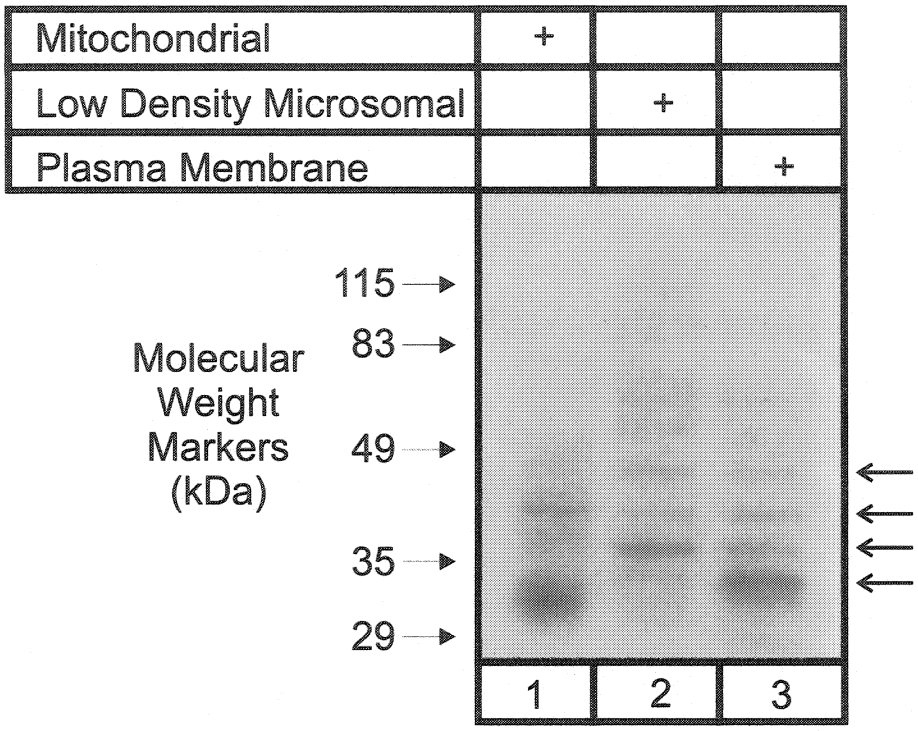

Figure 18. Albumin Binding Proteins in Enriched Membrane Fractions from 3T3-F442A Adipocytes. 3T3-F442A cells were cultured to differentiate (as described in Section B.2.2.3) and on day 4 of differentiation membrane fractions were prepared as described in Section B.2.4.3. 20 μg of protein from plasma, low density microsomal and mitochondrial membranes were separated by 10% SDS-PAGE (see Section B.2.5.1) and transferred (see Section B.2.5.2) to a PVDF membrane. Non-specific protein binding to the membrane was blocked by 1.5% gelatin in TBS-T (Tris buffered saline, 0.1% Tween-20), after which the blot was probed with 50 μg/ml ^{125}I-BSA (prepared as described in Section B.2.6.1) for 60 minutes then washed extensively with TBS-T, dried then exposed to autoradiography film (see Section B.2.5.5). Closed arrowheads mark the migration of prestained molecular weight markers, and open arrowheads indicate the proteins of interest, 48.3 ± 1.1, 42.0 ± 1.0, 36.9 ± 1.1 and 33.4 ± 0.7 kDa, molecular weight estimates are from n=5.

biochemical fractionation techniques to enrich proteins mediating albumin binding activity. The dot blot assay we developed could not detect any difference in albumin binding activity of plasma membrane from preadipocytes and adipocytes (Figure 17), which we expected to see based on our earlier results (Figures 1 and 14). Nor did we detect any substantial difference in activity between the plasma membrane and other membrane fractions. Thus we did not feel that this assay provided a suitable foundation to embark on fractionation of membranes to enrich an albumin binding activity.

We used a ligand blot approach to identify membrane proteins from 3T3-F442A adipocytes that bind albumin (Figure 18). Of the plasma membrane proteins identified in Figure 18, the 33 kDa protein held promise as candidate for mediating albumin binding to the cell surface as relative to other proteins it had a high level albumin binding activity. In addition the 33 kDa protein was detected solely in the plasma membrane, as would be expected for an albumin receptor. We also considered the 48 and 37 kDa proteins that were partially localized in the low density microsomal fraction as candidates, as it is conceivable that a putative albumin receptor could translocate between internal membranes and the plasma membrane. In fact epinephrine, which results in translocation of Glut4 transporters to the plasma membrane (Han et al. 1998) also increases the number of albumin binding sites on rat adipocytes (Brandes et al. 1982).

It is noteworthy that a similar level of albumin binding activity was detected in all the membrane fractions from 3T3-F442A adipocytes in the ligand blot, an observation also made with the dot blot assay. This may be a result of the relatively harsh conditions of the assays (e.g. SDS denaturation and electrophoresis for the ligand blot and immobilization of proteins on membranes in both cases) attenuating the activity of albumin binding proteins. Alternatively all membrane fractions may indeed have similar albumin binding activity, although at least with respect to the plasma membrane fractions we expect to see a difference between preadipocytes and adipocytes (based on Figure 13).

C.3 Expression of SR-BI in Bone Marrow-Derived Cells Protects LDLR KO Mice from Diet Induced Atherosclerosis

The scavenger receptor class B type I (SR-BI) is a HDL receptor that mediates selective lipid uptake, and appears to be a key component of the reverse cholesterol transport (RCT) pathway (reviewed in (Trigatti et al. 2000)). The RCT pathway moves cholesterol from non-hepatic tissue via HDL to the liver for excretion in the bile (reviewed in (Assmann et al. 2003)). RCT can act to promote cholesterol flux from lipid-laden macrophages. Thus this pathway is believed to be antiatherogenic (reviewed in (Assmann et al. 2003)).

Expression of SR-BI in mice is atheroprotective. Complete ablation of SR-BI alone or in the context of either, the apolipoprotein E knockout (ApoE KO) mouse or the fat fed low density lipoprotein receptor knockout (LDLR KO) mouse, results in increased atherosclerosis (Trigatti et al. 1999; Van Eck et al. 2003) (Covey et al. 2003). A 50% attenuation of SR-BI expression in fat fed LDLR KO mice also leads to increased atherosclerosis (Huszar et al. 2000). The mechanism by which ablation or reduction of SR-BI leads to increased atherosclerosis is not fully understood and appears to be multifactorial.

Hepatic expression of SR-BI likely has an important role in SR-BI mediated atheroprotection. Hepatic overexpression of SR-BI in mice can decrease their

susceptibility to atherosclerosis (Arai et al. 1999; Kozarsky et al. 2000). The decreased atherosclerosis appears to be at least partially attributable to increased biliary cholesterol excretion (Kozarsky et al. 1997). Another mechanism by which SR-BI might protect against atherosclerosis is SR-BI mediated cholesterol efflux from lipid laden macrophage foam cells in the arterial wall to HDL thereby promoting RCT (Tall et al. 2001). Consistent with such a model, SR-BI is expressed in macrophages in atherosclerotic plaques (Ji et al. 1997; Hirano et al. 1999; Chinetti et al. 2000). Furthermore the level of SR-BI expression in cell lines correlates with the rate of cholesterol efflux to HDL (Ji et al. 1997). In addition, overexpression of SR-BI in cell lines results in increased cholesterol efflux (Ji et al. 1997; Stangl et al. 1998; Gu et al. 2000; Ohgami et al. 2001; Huang et al. 2002). However the role of SR-BI expression in macrophages in vivo has not been reported.

We hypothesized that a lack of SR-BI expression in macrophage foam cells would enhance the development of atherosclerosis in mice. To test this we used fat fed LDLR KO mice (a well-established mouse model of aortic atherosclerosis (Ishibashi et al. 1994)) with specific ablation of SR-BI in bone marrow-derived cells, which include monocyte-derived macrophages. The generation of the chimeric mice with specific ablation of SR-BI in bone marrow-derived cells was accomplished by radiation induced ablation of endogenous bone marrow followed by bone marrow transplantation.

C.3.1 SR-BI Mediates Cholesterol Efflux from CHO Cells

SR-BI overexpression in transfected cells was first shown by Tall and Rothblat and their coworkers to enhance cholesterol efflux to HDL (Ji et al. 1997). To confirm this, ldlA7 (LDL receptor-deficient mutant Chinese hamster ovary cells (Krieger et al. 1981)) and ldlA[mSR-BI] (ldlA7 cells overexpressing murine SR-BI (Acton et al. 1996)) cells were loaded overnight with [^{3}H]-cholesterol, washed and net cholesterol efflux to fetal bovine serum (which contains cholesterol acceptors, e.g. lipoproteins) was measured in the presence of a blocking anti-SR-BI antiserum or non-immune serum (see Section B.2.3.3)(Figure 19). After eight hours the extent of net [^{3}H]-cholesterol efflux from ldlA[mSR-BI] cells (26.5% of the total cellular cholesterol) was 1.8-fold greater than untransfected cells (14.7% of the total cellular cholesterol), in agreement with results originally reported by Ji et al. (Ji et al. 1997).

Others have reported that SR-BI overexpression enhances net cholesterol efflux to 1-palmitoyl-2-oleoylphoshatidylcholine small unilamellar vesicles (POPC SUV) (de la Llera-Moya et al. 1999). SR-BI, however, has been reported to have a low affinity for these vesicles (Rigotti et al. 1995; de la Llera-Moya et al. 1999), suggesting that it may mediate cholesterol efflux without binding directly to cholesterol acceptors (de la Llera-Moya et al. 1999). To test this we used a previously characterized anti-SR-BI antibody reported to block lipoprotein binding to SR-BI (Gu et al. 2000). Figure 19 demonstrates that the antibody reduced the rate of net efflux in SR-BI transfected cells to that of

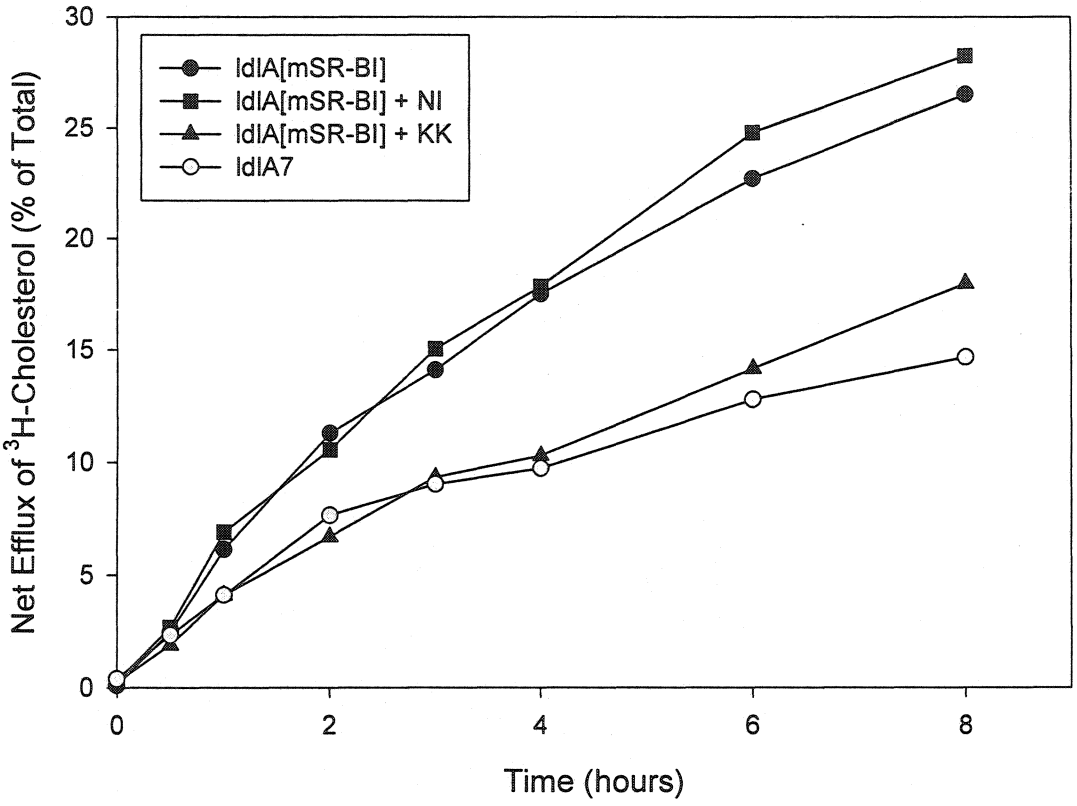

Figure 19. Net Efflux of [^{3}H]-Cholesterol from ldlA7 and ldlA[mSR-BI] Cells. ldlA7 (grey symbols) and ldlA[mSR-BI] cells (black symbols) were loaded for 48 hours with [^{3}H]-cholesterol then incubated overnight in media containing 2% BSA, then net efflux was initiated by the addition of media containing 10% FBS (circles) or pre-incubated for 45 minutes with the anti-SR-BI antibody KK at a 1/1000 dilution (triangle) or a non-immune serum at 1/1000 dilution (square) prior to the addition of media with 10% FBS (as described in Section B.2.3.3). Efflux is expressed as % [^{3}H]-cholesterol in the media relative to the total amount of [^{3}H]-cholesterol.

untransfected cells. In contrast a non-immune serum had no effect. This indicated that the SR-BI enhanced efflux was likely a result of its ability to bind cholesterol acceptors.

C.3.2 Establishing Conditions for Bone Marrow Transplantation

Cholesterol efflux from macrophages to HDL is thought to be an important pathway of atheroprotection. This leads to the prediction that SR-BI expression in macrophages should protect against atherosclerosis. To set up a system in which macrophage SR-BI is ablated in the context of normal hepatic SR-BI expression, bone marrow transplantation was used. This approach allowed for mice to be generated in which SR-BI was inactivated specifically in bone marrow derived cells, including monocyte-derived macrophages. This well-characterized approach has been used to test the role of a variety of monocyte-derived macrophage gene products in atherosclerosis; examples include ABCA1 (Aiello et al. 2002; van Eck et al. 2002), apoE (Fazio et al. 1997; Van Eck et al. 2000), and adipocyte fatty acid binding protein (Layne et al. 2001).

To test the conditions for bone marrow transplantation, a method of detecting donor versus recipient bone marrow derived cells was required. This was achieved through the use of green fluorescent protein transgenic (GFPtg) mice as bone marrow donors, these mice have the enhanced GFP cDNA under control of the chicken beta-actin promoter and cytomegalovirus enhancer and express GFP in all cell types except erythrocytes and hair (Okabe et al. 1997).

First the ability to detect CD11b labeled and GFP expressing cells was determined. Blood from either GFPtg or non-transgenic mice was collected and prepared for flow cytometry by treating the blood with NH_4Cl to lyse erythrocytes, the remaining cells were then incubated with a biotinylated antibody directed against CD11b followed by incubation with a streptavidin-Cy-Chrome conjugate to mark cells of the myeloid lineage (Cheng et al. 1996) including monocytes (Springer et al. 1979). The cells were then analyzed by 2-colour flow cytometry with a BD FACSVantage equipped with an ion gas laser (excitation at 488 nm)(performed by Hong Liang at the McMaster University Flow Cytometry Facility). GFP and cy-chrome fluorescence emission was measured with filters at 550 nm and 695 nm respectively. Representative plots are shown in Figure 20 and the results of 2 experiments are presented in Table 6. The majority of cells from non-transgenic mice had very low GFP fluorescence as expected (Figure 20 left-hand quadrant of panels A and C). While 83 ± 10% (n=4) of the cells from GFPtg mice were positive for GFP (Figure 20 right-hand quadrant of panels B and D). CD11b positive cells (Figure 20 upper quadrant of panels C and D) were not detected when the anti-CD11b antibody was omitted (Figure 20 upper quadrant panels A and B). In the presence of the anti-CD11b antibody 20 ± 5% (n=4) of the cells were CD11b positive. When GFPtg blood cells labeled with anti-CD11b were analyzed, 92% and 93% (n=2) of the $CD11b^+$ cells (upper left and upper right quadrants) were $GFPtg^+$ (upper right quadrant)(Figure 20 panel D).

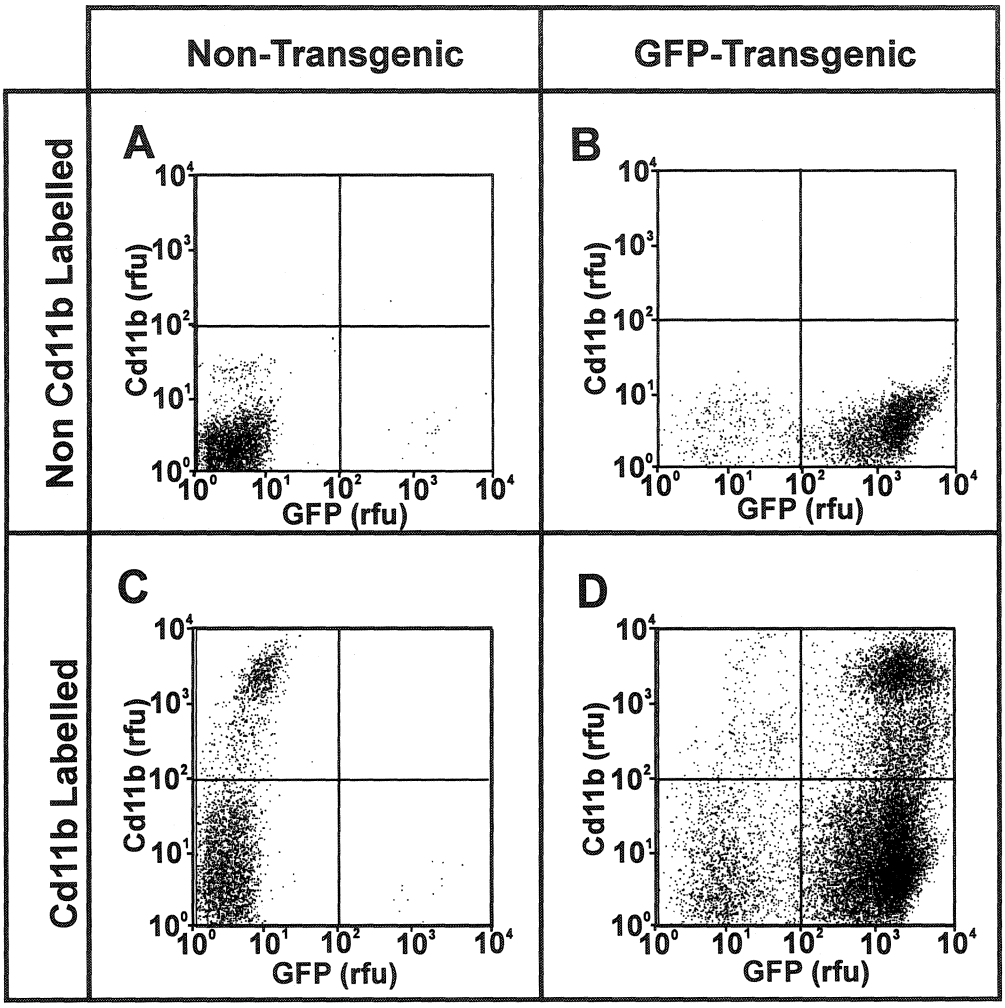

Figure 20. Flow Cytometric Analysis of Cells Prepared from Blood of GFP Transgenic and Non-transgenic Mice. Blood was collected in heparinized tubes from green fluorescent protein expressing transgenic mice (GFPtg) (panels B and D) and non-transgenic mice (A and C), and was then treated with NH_4Cl to lyse erythrocytes, washed and then the cells in panels C and D were treated with a biotinylated anti-CD11b antibody followed by incubation with a streptavidin Cy-Chrome conjugate. Cells were then analyzed with a FACSVantage flow cytometer (Hong Liang, McMaster University Flow Cytometry Facility) using an ion gas laser (excitation at 488 nm), GFP and cy-chrome fluorescence emission was measured with filters at 550nm and 695 nm respectively. Each dot represents an individual cell. GFP expression (relative fluorescent units, rfu) is plotted on the horizontal axis and CD11b expression (rfu) is plotted on the vertical axis. The boundaries to the quadrants were determined empirically from the data in panels A-C.

Table 6. Flow cytometric analysis of blood cells from non-transgenic and GFP-transgenic mice.

Panel [a]	Number of Cells in Quadrant				Total	Upper Right vs. Upper (%) [b]
	Upper Left	Upper Right	Lower Left	Lower Right		
A	0	1	3911	17	3929	na
	2	0	3979	0	3981	na
B	0	0	303	3610	3913	na
	0	5	1128	3193	4326	na
C	950	0	2981	13	3944	na
	6167	2	24857	2	31028	na
D	361	4952	2165	16347	23825	93.2
	40	483	1024	2725	4272	92.4

-[a] panel in Figure 20
-[b] percentage of cells in upper right quadrant versus upper right and upper left
-na not applicable
-each line represents an individual mouse analyzed

Next we determined the radiation dose required to ablate endogenous bone marrow in recipient mice and allow for efficient repopulation of donor derived bone marrow. Recipients (C57BL/6 apoE KO females) were exposed to 600, 800, 1000 and 1200 cGy of irradiation (^{60}Co source, performed by Robert Pasuta McMaster University Nuclear Reactor Hot Cell Facility) delivered in 2 sessions separated by 3 hours. Bone marrow from GFPtg donors was introduced by intravenous injection into the irradiated recipients as described in Section B.2.1.2. Blood was collected 4-weeks post transplantation to test for bone marrow repopulation by flow cytometric analysis as described in Section B.2.1.4. Representative plots are shown in Figure 21, and the compiled results from mice (n=2 or 3) are presented in Table 7. The proportion of $CD11b^+$ cells that were GFP^+ was determined and provided a measure of the percentage of myeloid lineage cells that were donor derived. When irradiated with 1200 cGy, the average repopulation of donor-derived bone marrow was 97 ± 3 % (n=2); mice irradiated with 1000 cGy gave similar results, 98 ± 1 % (n=3). For mice irradiated with 800 and 600 cGy, the average degree of repopulation determined was 93 ± 6 % (n=2). Note that 600 cGy was not a lethal dose as a mouse that was not transplanted survived for greater than 2 months. For subsequent bone marrow transplantation experiments, 1000 cGy of total body irradiation was used.

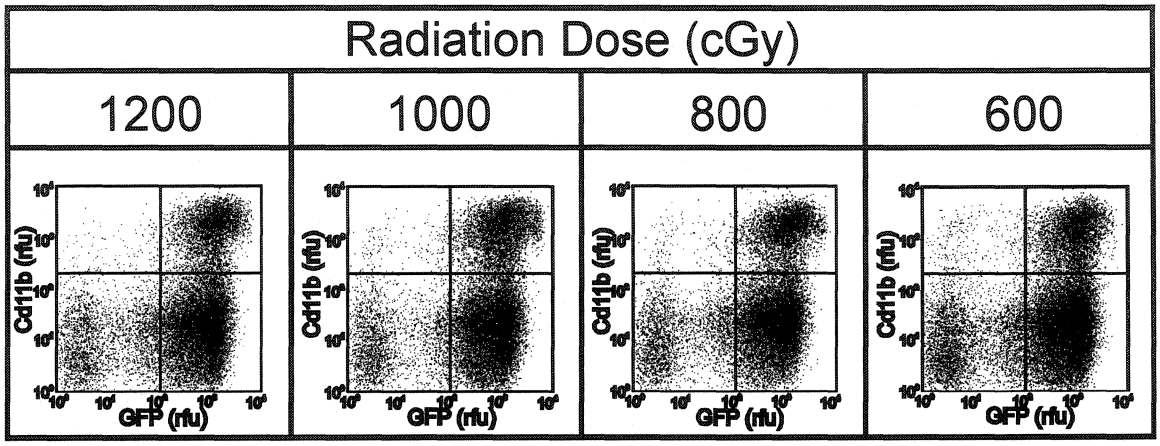

Figure 21. Flow Cytometric Analysis of Blood Cell Preparations from Irradiated Mice Transplanted with Bone Marrow from GFPtg Mice. C57BL/6 apolipoprotein E knockout ($ApoE^{-/-}$) mice were irradiated with 600 cGy then 3 hours later mice were either used for bone marrow transplants or were irradiated with a further 200, 400 or 600 cGy from a ^{60}Co source (performed by Robert Pasuta, McMaster University Nuclear Reactor Hot Cell). Irradiated mice were transplanted with bone marrow form GFPtg mice (as described in Section B.2.1.2). Four weeks post transplant, blood was collected via the tail vein, into heparinized tubes. Red blood cells were lysed and the remainder of the blood cell preparation was labelled with a biotinylated anti-CD11b antibody and a Cy-Chrome /streptavidin conjugate as described in the legend to Figure 20 and in Section B.2.1.4. GFP and CD11b expression (relative fluorescence units horizontal and vertical axes respectively) were determined by flow cytometry as described in the legend to Figure 20 and in Section B.2.1.4 and each dot represents an individual cell. Experiment was performed in conjunction with Ali Rizvi.

Table 7. Analysis of bone marrow repopulation by flow cytometry in irradiated mice transplanted with GFPtg$^+$ bone marrow.

Mouse #	Radiation Dose (cGy)	Bone Marrow Transplanted	Survival 1-Month Post Transplant	% of Donor Derived CD11b$^+$ Cells [a]	Average (%)
1	600	no	yes		
2		yes	yes	96	93 ± 6 [b]
3		yes	yes	90	
4	800	no	no		
5		yes	yes	96	93 ± 6 [b]
6		yes	yes	89	
7	1000	no	no		
8		yes	yes	98	98 ± 1 [c]
9		yes	yes	98	
10		yes	yes	97	
11	1200	no	no		
12		yes	yes	99	97 ± 3 [b]
13		yes	yes	96	

[a] the number of cells in the upper right quadrant versus both upper quadrants
[b] the difference between the repopulation of the two mice
[c] the standard deviation of the repopulation of the three mice

C.3.3 The Effect of GFP Expression in Bone Marrow Derived Cells on Atherosclerosis in LDLR KO Mice.

GFP serves as a convenient marker of donor derived cells in circulation (Figure 21 and Table 7) and may also facilitate the identification of donor-derived cells contributing to atherosclerotic plaques. However, to be useful, GFP expression should not effect the development of atherosclerosis. To test this LDLR KO mice (on a mixed genetic background) were transplanted with bone marrow from either LDLR KO mice or LDLR KO GFPtg mice. LDLR KO mice were used as recipients as when these mice are fed a high fat, high cholesterol, "Western-type" diet, they develop aortic atherosclerosis and are a well-characterized mouse model of this disease (Ishibashi et al. 1994). One month post transplantation mice were fed a high fat diet for 2 months, sacrificed and the vasculature perfused and the aorta and heart harvested (bone marrow transplantation, repopulation analysis and tissue harvesting all performed at MIT by Dr. B. Trigatti). The amount of atherosclerosis was analyzed as; 1) the surface area covered by lipid rich plaques in the aorta (aortic arch and descending aorta)(as described in Section B.2.1.6), and 2) the cross sectional area of lesions in the aortic sinus (as described in Section B.2.1.7).

To measure the cross sectional area of lesions, hearts that had been embedded in cryomatrix were sectioned on a cryostat and 10 μm thick sections of the aortic sinus collected and stained with oil red O (see Section B.2.1.7) (sections were collected and stained by D. Wang). The lesion area was measured in sections corresponding to the end

of the aortic sinus (defined by an irregular vessel perimeter as well as the presence of 3 valves and their attachment sites (Paigen et al. 1987))(Figure 22). The area of the lipid lesions were similar regardless of the bone marrow donor, with mean lesion areas ± standard error of the mean of 87419 ± 29044 μm^2 and 72964 ± 32686 μm^2 for mice receiving LDLR KO (Figure 23 panel A black bars, n=9) and LDLR KO GFPtg (Figure 23 panel A grey bars, n=4) bone marrow respectively (p=0.368).

To measure the percentage of the inner surface area of the aorta covered by lipid rich lesions, aortas (from the aortic arch to the iliac bifurcation) that had been fixed in 3.8% neutral buffered formaldehyde (formalin) were dissected free of all adventitial fat tissue, stained with Sudan IV, dissected longitudinally and mounted onto glass slides (see Section B.2.1.6)(Figure 23 panel B). For lethally irradiated LDLR KO mice the mean percentage surface area of the aorta lumen covered by lipid rich lesions ± the standard error of the mean was 1.37% ± 0.24% for mice receiving LDLR KO bone marrow (Figure 23 panel B black bars) and 1.53% ± 0.87% for mice receiving LDLR KO GFPtg bone marrow (Figure 23 panel B grey bars) (p=0.407).

Thus GFP expression in bone marrow derived cells did not affect either the lesion size or the amount of aorta surface area covered by lesions. Thus we concluded that GFP expression in bone marrow derived cells does not appear to influence the progression of

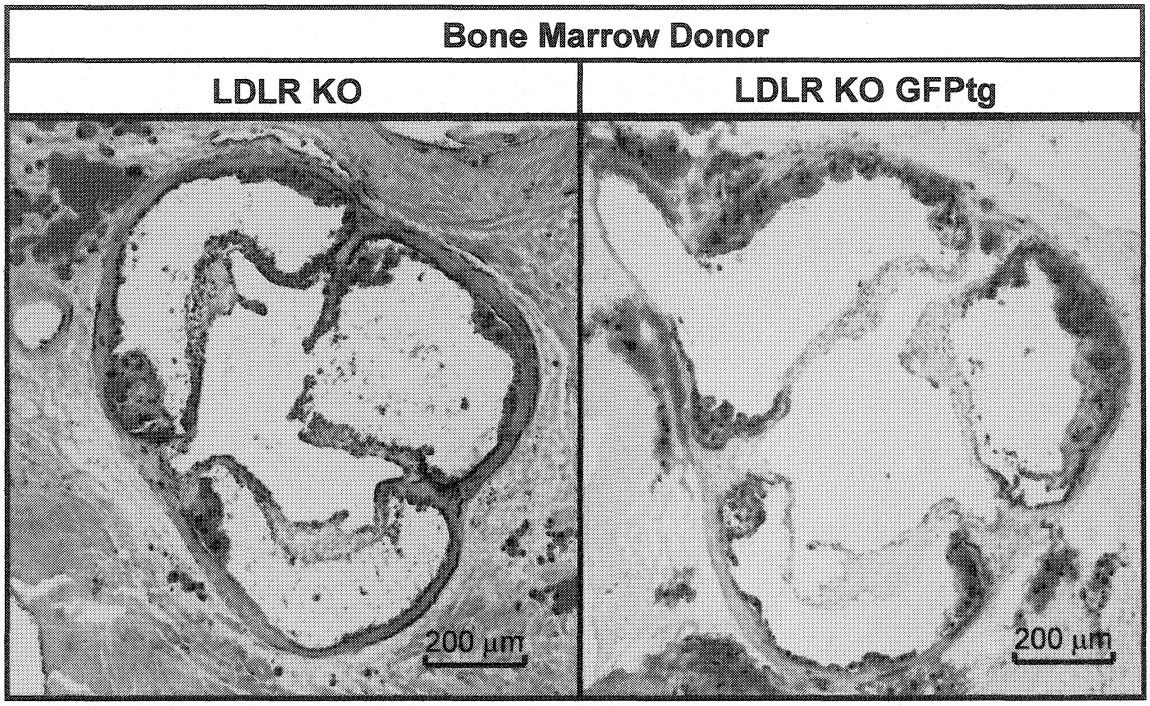

Figure 22. Oil Red O Stained Cross Sections Through the Aortic Sinus of Fat Fed LDLR KO Mice Transplanted with LDLR KO or LDLR KO GFPtg Bone Marrow. Perfused hearts were collected from LDLR KO mice that had been transplanted with bone marrow from LDLR KO (left panel) or LDLR KO GFPtg (right panel) mice and then fed a high fat diet for 2 months (initiated 1 month post transplantation). Hearts were embedded in cryomatrix and 10 µm thick sections were prepared then stained with oil red O (as described in Section B.2.1.7).

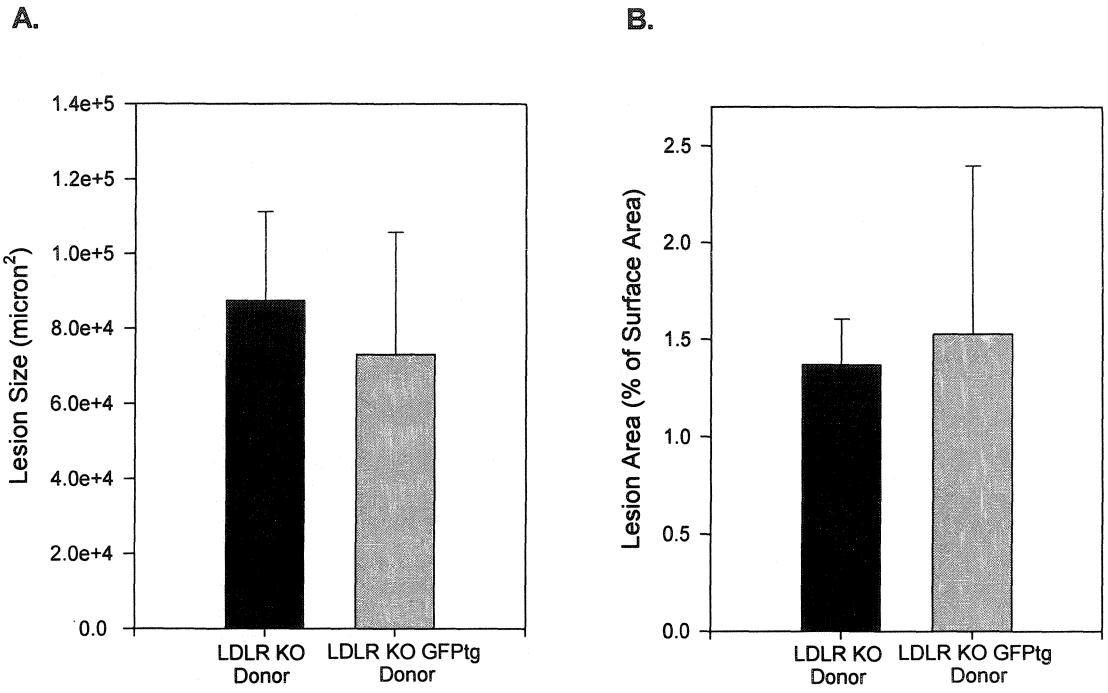

Figure 23. Aortic Atherosclerosis in Fat Fed LDLR KO Mice Transplanted with LDLR KO or LDLR KO GFPtg Bone Marrow. One month post transplantation LDLR KO mice reconstituted with either LDLR KO (black) or LDLR KO GFPtg (grey) were fed a high fat diet for 2 months. The cross sectional size of lesions in the aortic sinus (as described in Section B.2.1.7, panel A) and the percentage of the aorta surface area covered by lipid rich lesions (as described in Section B.2.1.6, panel B) were measured. Bars represent the mean value ± the standard error of the mean, for LDLR KO donors n=9 and for LDLR KO GFPtg donors n=4. Both panel A and B $p>0.368$.

atherosclerosis in these mice and therefore should serve as a useful means in marking and tracking donor derived bone marrow and bone marrow-derived cells.

C.3.4 Generating Chimeric Mice with Bone Marrow Specific Ablation of SR-BI

To test our hypothesis that a lack of SR-BI expression in macrophages would be proatherogenic, we set out to generate LDLR knockout mice that had a selective disruption of SR-BI in bone marrow-derived cells. Despite the validation that GFPtg mice could be used as bone marrow donors, they were not used in these studies due to the unavailability of SR-BI KO/GFPtg mice on a pure C57BL/6 genetic background at the time the experiments were performed. We chose to use donor and recipient mice that were on the C57BL/6 background, a strain that is predisposed to atherosclerosis (Paigen et al. 1990). This will avoid variations in the development of atherosclerosis due to differences in the genetic backgrounds of the mice and should thereby facilitate the detection of subtle differences between experimental groups. LDLR KO mice were used as the bone marrow recipients, as discussed in Section C.3.3 fat-fed LDLR KO mice are a well-characterized mouse model of aortic atherosclerosis (Ishibashi et al. 1994). $LDLR^{+/+}SR\text{-}BI^{-/-}$ or wild type ($LDLR^{+/+}SR\text{-}BI^{+/+}$) mice were used as bone marrow donors. Others have demonstrated that reconstitution of LDLR KO mice with $LDLR^{+/+}$ bone marrow has no effect on diet-induced atherosclerosis (Boisvert et al. 1997; Herijgers et al. 1997; Linton et al. 1999).

One-month post transplantation, we used PCR to analyze the genotype of blood cells collected from the recipient mice as a qualitative measure of bone marrow engraftment (see Section B.2.1.3). We tested for the presence of either the mutant or wild-type alleles of the LDLR and SR-BI genes. Blood cells derived from bone marrow donor mice should posses only the wild-type LDLR allele and either the wild-type or mutant SR-BI allele (depending on whether donors were SR-BI$^{+/+}$ or SR-BI$^{-/-}$ respectively). Cells derived from the recipient mice should contain only the mutant LDLR and wild-type SR-BI alleles. Figure 24 shows representative results of PCR for the LDLR and SR-BI alleles of lethally irradiated LDLR KO mice transplanted with bone marrow from wild-type or SR-BI KO mice (see Table 3 for the PCR amplicon sizes). Consistent with successful repopulation of donor-derived bone marrow, the DNA from blood cells of all transplanted mice carried the wild-type LDLR allele, but not the mutant LDLR allele (at least within the detection limits of the PCR assay). Likewise, the prominent product of the SR-BI PCR reaction in mice transplanted with SR-BI KO bone marrow was that of the mutant SR-BI allele. As expected, in mice transplanted with wild-type bone marrow, only the product of the wild-type SR-BI allele could be detected. Similar genotyping analysis was performed on all mice 1-month post transplantation.

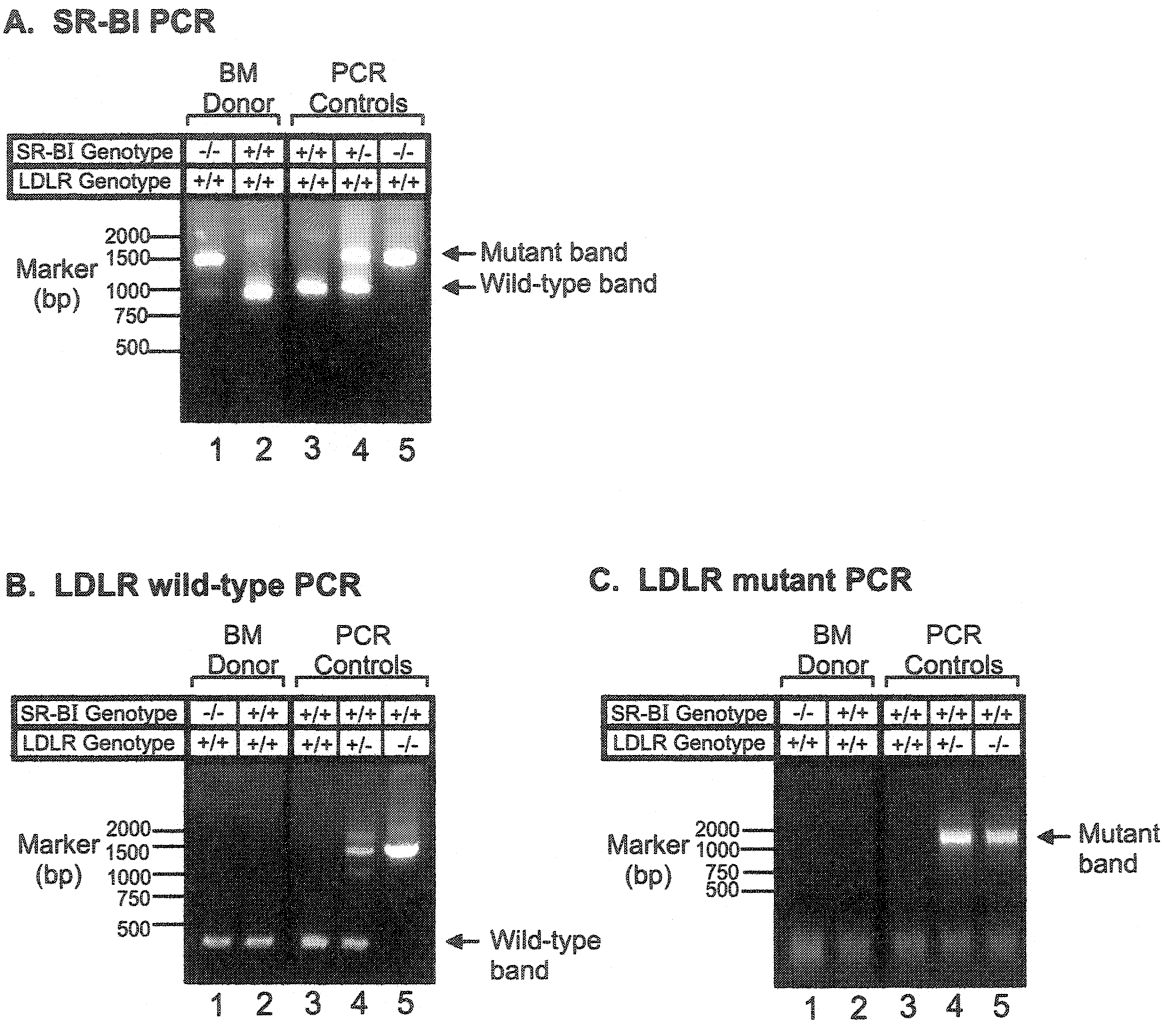

Figure 24. PCR Analysis of SR-BI and LDLR Alleles in Blood Cells of Recipient Mice One-Month Post Transplantation. One month following bone marrow transplants of SR-BI wild-type or SR-BI knockout (SR-BI KO) bone marrow into LDLR knockout mice, blood was collected and DNA was prepared from the blood using BD Quickblood kits, DNA for controls was obtained from tail biopsies (see Section B.2.1.3). Template DNA was then used to perform PCR analysis of the SR-BI (panel A) and LDLR (wild-type and mutant, panels B and C respectively) alleles, see table 3 for primers and amplicon sizes. Note the DNA template for PCR reactions in panel A lanes 1 and 2 is from different mice than panel B and C (lanes 1 and 2), but results are representative.

C.3.5 Bone Marrow Specific Ablation of SR-BI in LDLR KO Mice Does Not Alter Plasma Cholesterol Levels or Lipoprotein Profiles.

SR-BI expression can influence plasma cholesterol levels. In SR-BI KO mice, plasma cholesterol was increased 2.2-fold relative to wild-type controls (216 ± 37 mg/dl for SR-BI KO versus 96 ± 17 mg/dl for wild-type controls) (Rigotti et al. 1997). This change in plasma cholesterol was associated with an increase in the size and cholesterol content of HDL (Rigotti et al. 1997). In a similar manner, SR-BI/apoE dKO mice had increased plasma cholesterol relative to mice with either individual mutant allele. However, in this case there is an increase in VLDL sized particles (Trigatti et al. 1999). On the LDLR KO background, on a low fat diet there was a 1.7-fold increase in plasma cholesterol in the SR-BI/LDLR dKO mice (430 ± 80 mg/dl) compared to the LDLR KO mice (253 ± 7 mg/dl) (Covey et al. 2003). This correlated with an increase in the size and cholesterol content of HDL sized particles. However, in contrast, on a high fat diet the SR-BI/LDLR dKO mice had 1.2-fold less plasma cholesterol relative to the LDLR dKO mice, 617 ± 52 mg/dl versus 768 ± 43 (Covey et al. 2003). This occurred despite an increase in cholesterol in HDL sized particles. The decreased plasma cholesterol was attributable to a decrease in the cholesterol content of IDL/LDL sized particles in the SR-BI/LDLR dKO mice relative to the LDLR KO mice (Covey et al. 2003). Presumably the alterations in plasma cholesterol and lipoproteins occurring in SR-BI KO mice are mainly attributable to a loss of hepatic SR-BI. Based on the work of others (Kozarsky et al. 1997; Wang et al. 1998; Ueda et al. 1999) it is expected that alterations in plasma

lipoprotein concentrations in SR-BI KO mice are a consequence of eliminating hepatic SR-BI. The contribution of SR-BI in non-hepatic tissue has not been addressed.

To determine if SR-BI in bone marrow-derived cells normally plays a role in control of overall plasma cholesterol levels we measured plasma total, free, and esterified cholesterol levels (as described in Section B.2.1.10) in LDLR KO mice transplanted with wild-type or SR-BI KO bone marrow at 4 weeks post transplant (fed a standard low fat rodent diet) and at 5 months post transplant (fed a high fat diet for 4 months)(Figure 25). On a low fat diet, the plasma total cholesterol was 313 ± 38 mg/dl and 306 ± 26 mg/dl, the free cholesterol was 101 ± 16 mg/dl and 96 ± 16 mg/dl, and the esterified cholesterol was 212 ± 23 mg/dl and 210 ± 23 mg/dl, for mice receiving wild-type and SR-BI KO bone marrow respectively. On a high fat diet, the plasma cholesterol was 971 ± 355 mg/dl and 838 ± 332 mg/dl, the free cholesterol was 258 ± 83 mg/dl and 211 ± 47 mg/dl, and the esterified cholesterol was 603 ± 196 mg/dl and 507 ± 121 mg/dl, for mice receiving wild-type and SR-BI KO bone marrow respectively. There were no statistically significant differences in plasma cholesterol levels between mice receiving wild-type and SR-BI KO bone marrow.

To test if the distribution of cholesterol amongst lipoproteins was altered by ablation of SR-BI in bone marrow-derived cells, we fractionated plasma by size exclusion FPLC (as described in Section B.2.1.9) and assayed for cholesterol content. Figure 26 shows representative profiles of total, free and esterified cholesterol for

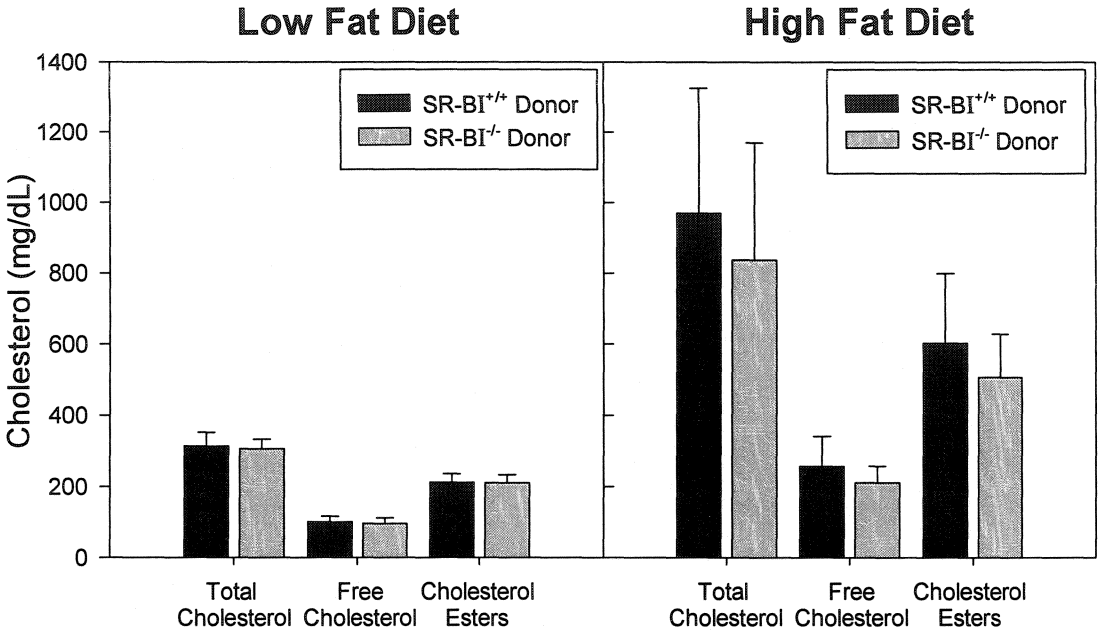

Figure 25. Plasma Cholesterol Levels in LDLR KO Mice Transplanted with Wild-type or SR-BI KO Bone Marrow on a Low Fat and High Fat Diet. Plasma samples were taken (as described in Section B.2.1.8) from LDLR KO mice transplanted with wild-type bone marrow (black) or SR-BI KO bone marrow (grey), at 4 weeks post transplant (fed a low fat diet) and at 5 months post transplant, (4 months on a high fat diet). Cholesterol levels were measured with kits from Wako Diagnostic as described in Section B.2.1.10). None of the differences between mice receiving wild-type or SR-BI KO bone marrow were statistically significant. On a low fat diet the total cholesterol was 313 ± 38 mg/dl and 306 ± 26 mg/dl, free cholesterol was 101 ± 16 mg/dl and 96 ± 16 mg/dl, and esterified cholesterol was 212 ± 23 mg/dl and 210 ± 23 mg/dl for mice receiving wild-type (n=4) and SR-BI KO (n=4) bone marrow respectively. On a high fat diet the total cholesterol was 971 ± 355 mg/dl (n=8) and 838 ± 332 mg/dl (n=12), free cholesterol was 258 ± 83 mg/dl (n=3) and 211 ± 47 mg/dl (n=6), and esterified cholesterol was 603 ± 196 mg/dl (n=3) and 507 ± 121 mg/dl (n=6) for mice receiving wild-type and SR-BI KO bone marrow respectively.

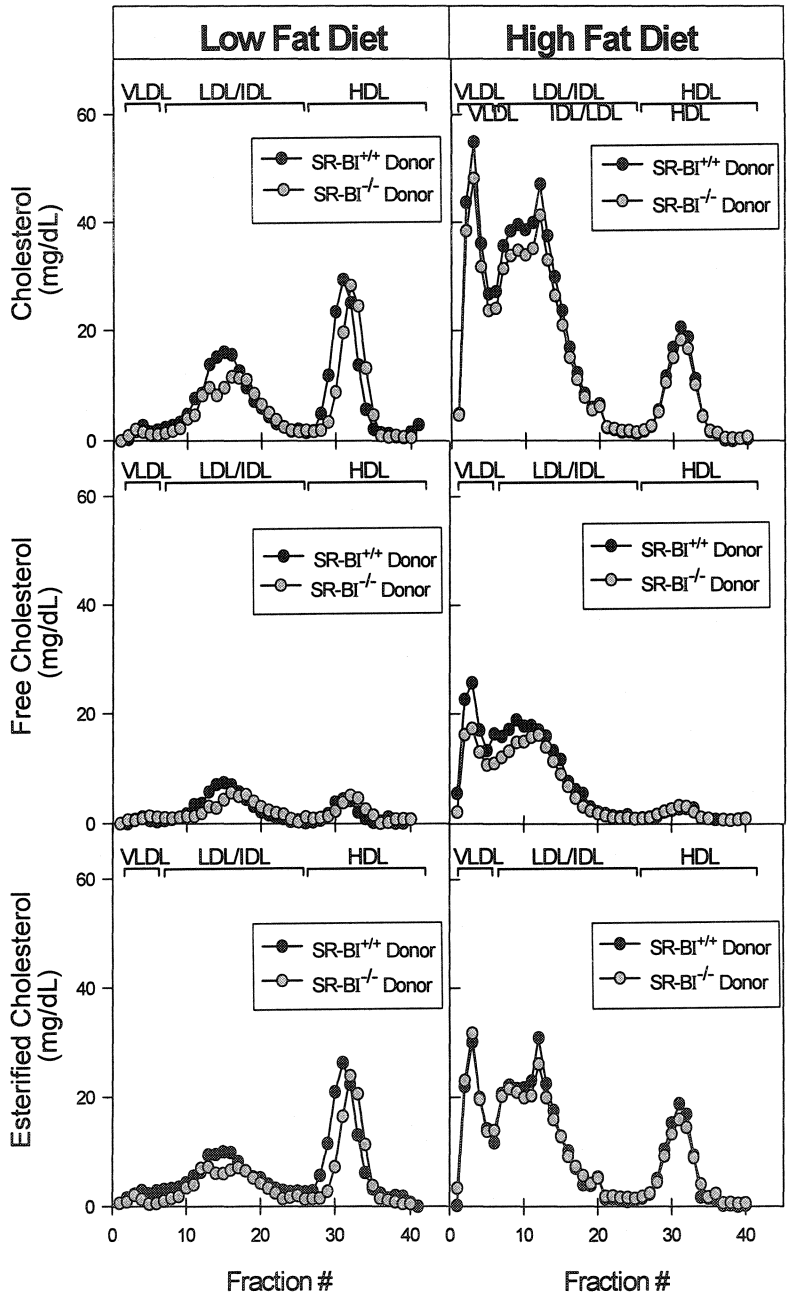

Figure 26. Lipoprotein Profiles from LDLR KO Mice Transplanted with Wild-type or SR-BI KO Bone Marrow. Blood samples were taken from LDLR KO mice transplanted with wild-type (black) or SR-BI KO (grey) bone marrow at 4 weeks post transplant (4 weeks on a low fat diet) or after 5 months (4 months on a high fat diet) and plasma (prepared as described in Section B.2.1.8) was fractionated by size exclusion FPLC (as described in Sections B.2.1.9). Fractions were assayed for total cholesterol and free cholesterol using kits from Wako Diagnostic, and cholesterol esters were calculated as the difference between total and free cholesterol (as described in Section B.2.1.10). Profiles are from plasma pooled from 3 to 4 mice and are representative profiles.

Table 8. Cholesterol analysis of LDLR KO mice reconstituted with either wild-type or SR-BI KO bone marrow.

	Low Fat Diet			High Fat Diet		
	Bone Marrow Donor		p [d]	Bone Marrow Donor		p [d]
	SR-BI$^{+/+}$	SR-BI$^{-/-}$		SR-BI$^{+/+}$	SR-BI$^{-/-}$	
Plasma						
Total	314±38 (4)	306±26 (4)	0.374	970±354 (8)	837±332 (12)	0.201
Free	100±16 (4)	96±16 (4)	0.325	258±83 (3)	211±47 (6)	0.153
Ester	212±23 (4)	210±23 (4)	0.442	602±196 (3)	507±121 (6)	0.193
VLDL [a]						
Total	pd	pd	nd	195±90 (3)	251±194 (3)	0.337
Free	pd	pd	nd	92±38 (3)	113±94 (3)	0.370
Ester	pd	pd	nd	104±52 (3)	140±99 (3)	0.306
IDL/LDL [b]						
Total	pd	pd	nd	633±245 (3)	626±343 (3)	0.489
Free	pd	pd	nd	270±129 (3)	314±200 (3)	0.384
Ester	pd	pd	nd	463±290 (3)	325±133 (3)	0.248
HDL [c]						
Total	pd	pd	nd	84±10 (3)	79±12 (3)	0.290
Free	pd	pd	nd	33±12 (3)	35±14 (3)	0.431
Ester	pd	pd	nd	32±12 (3)	42±22 (3)	0.261

-values correspond to the average ± standard deviation and the number in () the number of mice
-[a] the VLDL fraction is defined as fractions 1 through 5
-[b] the IDL/LDL fraction is defined as fractions 6 through 25
-[c] the HDL fraction is defined as fractions 26 through 41
-[d] value of Student's t-test
-pd preliminary data see text
-nd not determined

transplanted mice on a high fat diet (data compiled in Table 8). Preliminary data for the transplanted mice fed a low fat diet is as follows; for the total, free and esterified cholesterol associated with VLDL (4, 2, and 2 mg/dl compared to 6, 2 and 4 mg/dl for mice receiving SR-BIKO and wild-type bone marrow respectively) IDL/LDL (114, 49, and 65 mg/dl compared to 141, 59 and 83 mg/dl for mice receiving SR-BIKO and wild-type bone marrow respectively) and HDL (110, 24, and 85 mg/dl compared to 121, 18 and 103 mg/dl for mice receiving SR-BIKO and wild-type bone marrow respectively) were similar between the two groups. Following the high fat diet there were no statistically significant differences in cholesterol associated with VLDL, LDL/IDL or HDL in mice receiving wild-type or SR-BI KO bone marrow (Table 8). Thus expression of SR-BI in bone marrow-derived cells of LDLR KO mice fed a high-fat diet does not influence plasma cholesterol levels or the distribution of cholesterol among lipoproteins.

C.3.6 LDLR KO Mice with a Bone Marrow Specific Ablation of SR-BI Have Increased Diet Induced Aortic Atherosclerosis.

Next, the effect of the bone marrow specific ablation of SR-BI on aortic atherosclerosis was investigated. Following 4 months on the high fat diet mice were sacrificed and the aorta's were removed and assayed for the percentage of the surface area covered by lipid rich atherosclerotic lesions (as described in Section B.2.1.6)(Figure 27 and 28). LDLR KO mice transplanted with SR-BI KO bone marrow had 1.4-fold higher atherosclerosis over the entire aorta than those transplanted with wild-

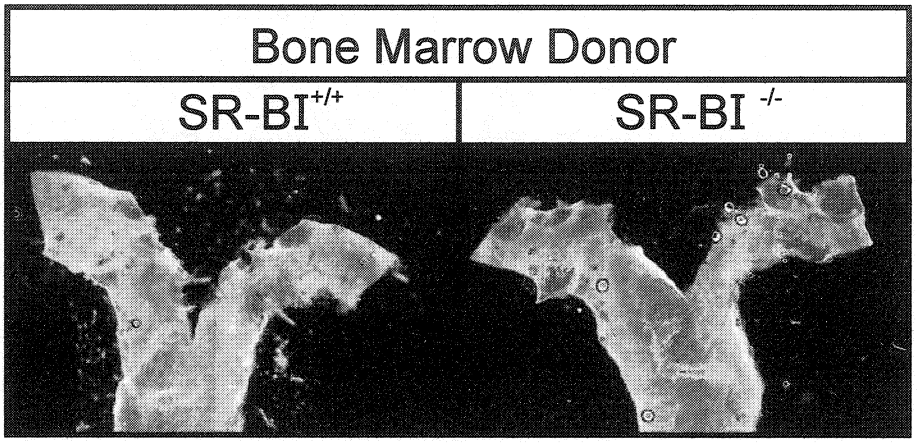

Figure 27. Sudan IV Stained Aortic Arches of LDLR KO Mice Transplanted with SR-BI Wild-type or KO Bone Marrow. Aorta's from female LDLR KO mice transplanted with either SR-BI wild-type (left panel) or KO (right panel) bone marrow fed a high fat diet for 4 months were harvested from mice, fixed in neutral buffered formaldehyde and then stained with Sudan IV (as described in Section B.2.1.6). Stained aorta's were bisected open from the aortic arch to the iliac bifurcation and mounted lumen side up onto glass slides with glycerol gelatin and then imaged in bright field with a 5X objective (the images shown are the aortic arch).

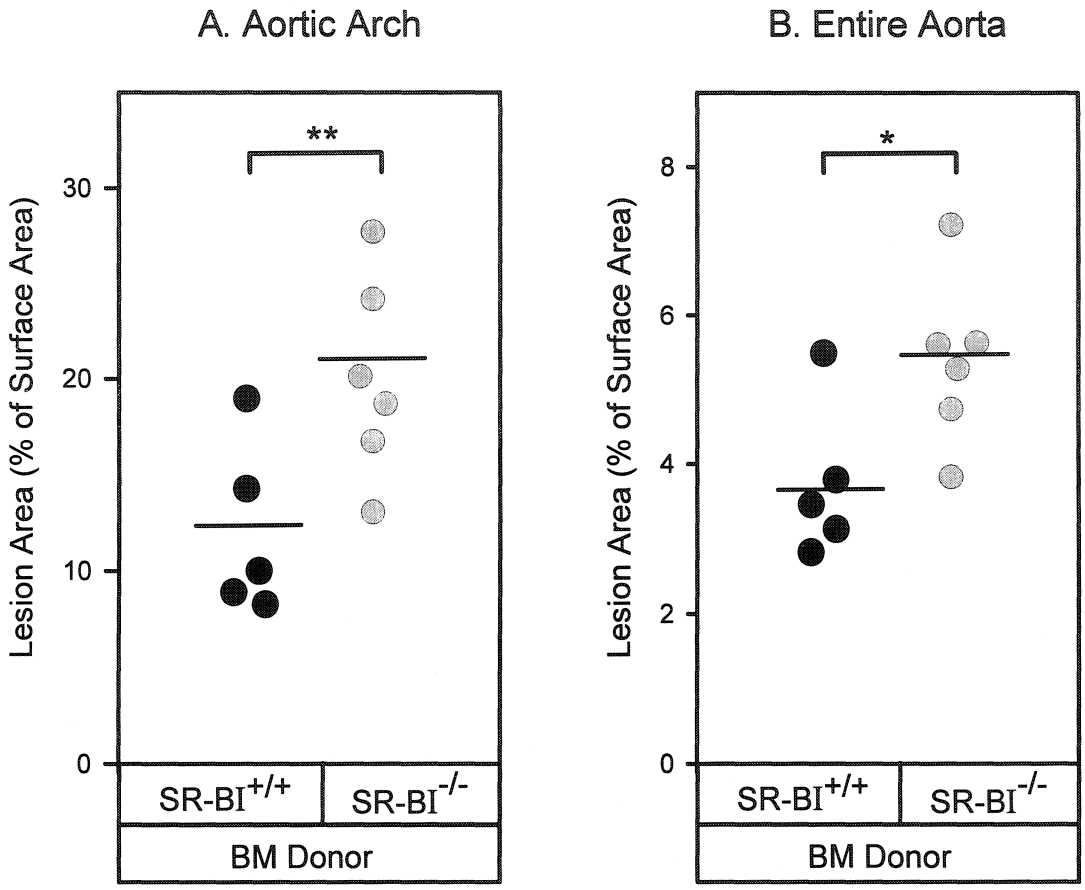

Figure 28. Aortic Atherosclerosis in Fat Fed LDLR KO Mice Transplanted with Wild-type or SR-BI KO Bone Marrow. One month post transplantation female LDLR KO mice reconstituted with either wild-type (black circles) or SR-BI KO (grey circles) bone marrow were fed a high fat diet for 4 months and then the aorta's were removed and stained for lipid with Sudan IV and the percentage of the surface area covered by lipid rich lesions was determined (as described in Section B.2.1.6). The percentage of the inner aortic surface covered by lipid rich plaques was 20.1 ± 5.2 % and 12.1 ± 4.5 % in the arch and 5.4 ± 1.1 % and 3.7 ± 1.0 % in the entire aorta for mice receiving SR-BI KO (n=6) and wild-type (n=5) bone marrow respectively. * p=0.012 and ** p=0.017.

type bone marrow (5.4 ± 1.1% and 3.7 ± 1.0 % coverage respectively, Figure 28 panel B, p=0.017). However the majority of aortic atherosclerotic plaque was found in the aortic arch of chimeric mice regardless of the bone marrow donor, so we also compared atherosclerosis in this region. Mice receiving SR-BI KO bone marrow had 1.7-fold as much atherosclerotic plaque in the aortic arch as those receiving wild-type bone marrow (20.1 ± 5.2 % and 12.1 ± 4.5 % coverage respectively, Figure 28 panel A, p=0.012). In the descending aorta there was 3.1 ± 0.8% plaque coverage in mice receiving SR-BI KO bone marrow and 2.5 ± 1.4% coverage in mice transplanted with wild-type bone marrow, however this difference was not statistically significant (p=0.23). Therefore a lack of SR-BI in bone marrow-derived cells increases atherosclerosis in LDLR KO mice on a high fat diet.

C.3.7 Bone Marrow Specific Ablation of SR-BI in LDLR KO Mice Does Not Inhibit Red Blood Cell Maturation.

Bone marrow specific ablation of SR-BI increased atherosclerosis without affecting plasma lipoprotein cholesterol levels. A potential mechanism for the increased atherosclerosis in mice with an ablation of SR-BI in bone marrow derived cells is a defect in erythrocyte maturation. Erythrocytes may be important cells with respect to the development of atherosclerosis as; 1) the erythrocyte plasma membrane protein glycophorin has been found to be a component of atherosclerotic plaques, suggesting that erythrocytes or at least erythrocyte plasma membranes accumulate and contribute to

atherosclerotic plaque development (Arbustini et al. 2002; Pasterkamp et al. 2002), and 2) defects in erythrocyte function can lead to anemia and arterial wall hypoxia, conditions proposed to contribute to atherosclerotic development (Boxen 1985; Gainer 1987). Potential mechanisms for this include, hypoxia induced release of growth factors leading to intimal cellular proliferation (Simanonok 1996), hypoxia induced increased activity of acyl CoA:cholesterol acyltransferase in the arterial walls (Martin et al. 1991), or hypoxia generated oxyradicals enhancing the atherogenic potential of lipoproteins (Crawford et al. 1991). However in studies with apoE KO mice treated with phenylhydrazine (to induce anemia) there was a positive correlation between circulating red blood cell levels and atherosclerotic lesion size, suggesting that anemia may be antiatherogenic (Paul et al. 1999).

Proper maturation and development of erythrocytes is hampered in SR-BI KO mice and conditions resulting in a hypercholesterolemic state can exacerbate this defect (Holm et al. 2002). These included 1) feeding mice a high cholesterol diet and 2) inactivation of the apoE gene (Holm et al. 2002). In SR-BI KO mice, erythrocyte phagolysosome expulsion appears to be inhibited, resulting in altered cell morphology and intracellular inclusions not typically seen in normal red blood cells (Holm et al. 2002). To investigate if similar defects in erythrocyte maturation occurred in LDLR KO mice transplanted with SR-BI KO bone marrow the red blood cell morphology was

investigated by transmission electron microscopy (Figure 29)(performed by Ernie Spitzer at the McMaster University Medical Centre Electron Microscopy Facility). The cells from wild-type mice fed a high fat diet for 14 weeks (Figure 29 panel A) or 29 weeks (not shown) have typical erythrocyte morphology. Likewise the cells from the 14-week fat fed LDLR KO mice also appeared to have a normal morphology (Figure 29 panel B). Erythrocytes from SR-BI KO mice on a high fat diet had an altered morphology and intracellular inclusions (Figure 29 panel C). These changes were even more pronounced in cells from SR-BI/apoE dKO mice (Figure 29 panel E). Similarly the fat fed SR-BI/LDLR dKO mice also had altered morphology and prominent intracellular inclusions (Figure 29 panel D).

Since fat-fed LDLR KO mice only show defects in erythrocyte development in the absence of SR-BI (Figure 29 compare panels B and D), we sought to determine if the defect in red blood cell morphology was also present in the LDLR KO mice transplanted with SR-BI KO bone marrow relative to mice receiving wild-type bone marrow. Blood samples were taken from LDLR KO mice transplanted with wild-type (Figure 29 panels F and H) or SR-BI KO bone marrow (Figure 29 panels G and I) at 4 weeks post transplantation (fed a low fat diet, panels F and G) and at 5 months post transplant (16 weeks on a high fat diet, panels H and I). At either the 4 week point or at the 5 month point there was no evidence of intracellular inclusions in mice transplanted with wild-type or SR-BI KO bone marrow. Note that at the 4-week point there were a small number of

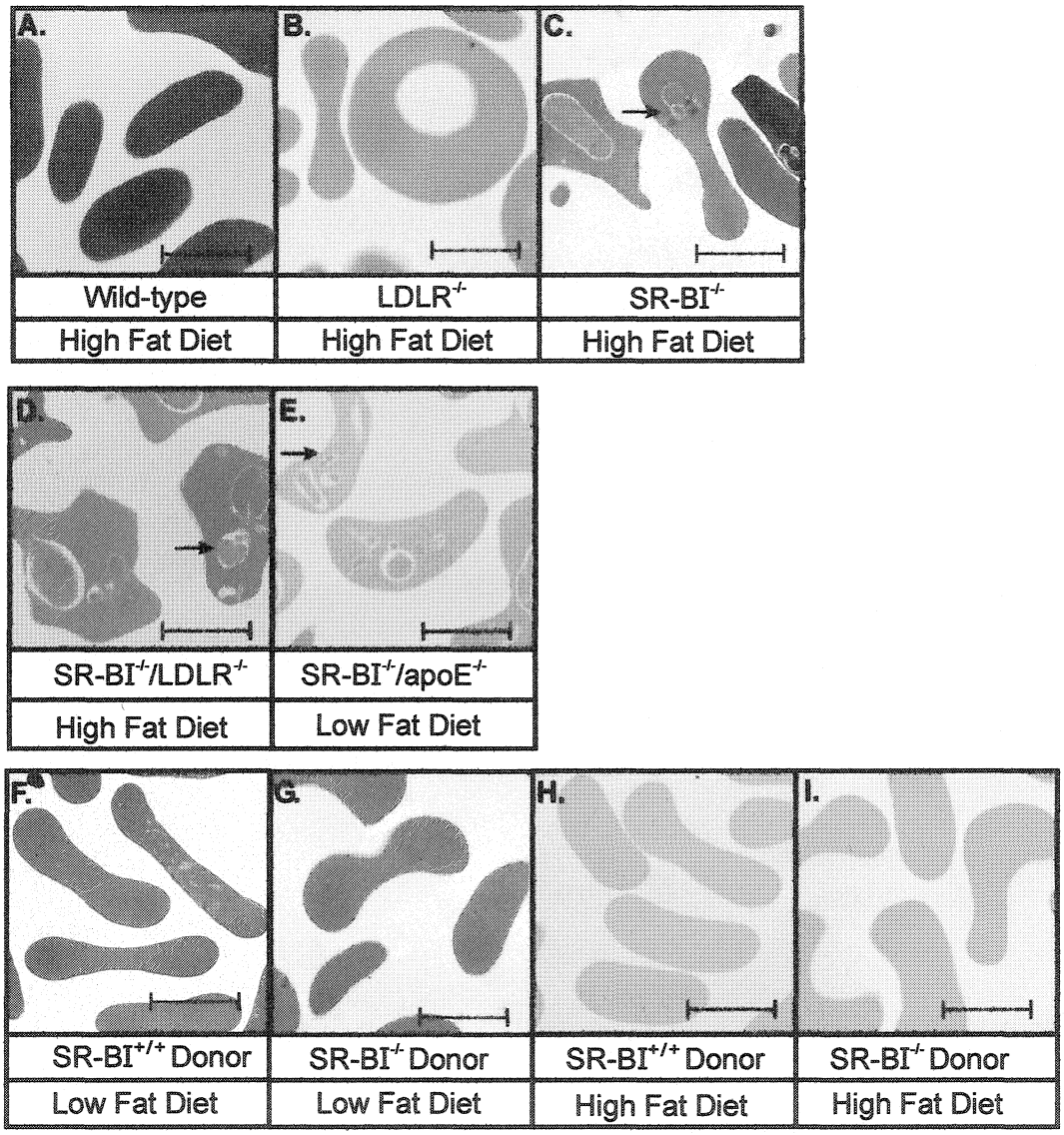

Figure 29. Transmission Electron Microscopic Images of Blood Samples from SR-BI KO and Chimeric Mice. Blood samples were collected, treated with heparin and fixed overnight at 4 C in 2% glutaraldehyde and were then processed for transmission electron microscopy (as described in Section B.2.3.6, performed by Ernie Spitzer at the McMaster University Medical Center Electron Microscopy Facility). Samples in panels A-D were from mice fed a high fat diet for 14 weeks, while panel E was maintained on a low fat diet. The samples in panels F-I were LDLR KO mice transplanted with bone marrow from either wild-type mice (panels F and H) or SR-BI KO mice (panels G and I), panels F and G were 4 weeks post transplant (on a low fat diet) and H and I were 5 months post transplant (16 weeks on a high fat diet). Representative images are shown, A n=3 mice x 4 fields, B n=2 mice x 4 fields, C n=2 mice x 4 fields, D n=6 mice x 4 fields, E n=2 mice x 4 fields, F n=pooled plasma from 4 mice x 4 fields, G n=pooled plasma from 4 mice x 4 fields, H n=3 mice x 4 fields, and I n=6 mice x 4 fields. The scale bar corresponds to 2.5 μm. Arrows in panels C-E mark examples of intracellular inclusions.

irregularly shaped cells (approximately 1:33 cells, 4 fields of view from the pooled plasma of 4 mice) in the mice transplanted with SR-BI KO bone marrow. Whether these cells were derived from one mouse, or if these are erythrocytes from the donor mouse (note the normal life span for murine erythrocytes is over 40 days (Horky et al. 1978)) is unclear. Nevertheless these cells did not contain intracellular inclusions and there was no evidence of them at the 5-month time point. Holm et al. also demonstrated that transplantation of SR-BI/apoE dKO bone marrow into apoE KO mice resulted in normal red blood cells (Holm et al. 2002). Together these studies demonstrate that the defects are not a result of a lack of SR-BI in bone marrow derived cells.

In the study by Holm et al., the altered morphology in SR-BI/apoE dKO mice correlated with decreased hematocrit values, an indicator of anemia (Holm et al. 2002). To investigate if anemia may be occurring in the absence of changes in red blood cell morphology, hematocrit values were determined for LDLR KO mice transplanted with wild-type or SR-BI KO bone marrow. In preliminary data there was no statistically significant differences in hematocrit values between mice transplanted with SR-BI KO or wild-type bone marrow. Thus improper red blood cell maturation and/or anemia, does not appear to be the underlying mechanism for increased atherosclerosis in mice with SR-BI ablated from bone marrow-derived cells.

C.3.8 Cholesterol Efflux From Peritoneal Macrophages From Wild-type and SR-BI KO Mice

To test if cholesterol efflux from macrophages to HDL was affected by a lack of SR-BI we examined net cholesterol efflux from wild-type and SR-BI KO macrophages. Peritoneal macrophages provide a convenient source of mouse-derived macrophages (Fortier 1994); furthermore several studies have used these cells to measure macrophage cholesterol efflux (Cao et al. 2002; Feng et al. 2002; Lee et al. 2002; Wang et al. 2002). Peritoneal macrophages from wild-type and SR-BI KO mice were loaded with [^{3}H]-cholesterol, harvested and cultured as described in Section B.2.3.3. Net cholesterol efflux was assayed as in Figure 19 with the exception that HDL was used as the cholesterol acceptor (Figure 30). The amount of [^{3}H]-cholesterol in the media increased over time reaching 36% of the total label in the media by 26 hours. There was no detectable difference in net cholesterol efflux from the peritoneal macrophages from wild-type or SR-BI KO mice.

One possible explanation for the absence of a difference in net cholesterol efflux from wild-type and SR-BI KO mice was that SR-BI may not be expressed at appreciable levels in peritoneal macrophages. Expression of SR-BI in peritoneal macrophages was examined by western blot analysis (as described in Section B.2.5.3) for SR-BI in total membrane preparations (prepared as described in Section B.2.4.2) from wild-type and SR-BI KO peritoneal macrophages, ldlA7 cells and ldlA[mSR-BI] cells (Figure 31). Equal amounts of protein were loaded (except for lane 4, macrophages from

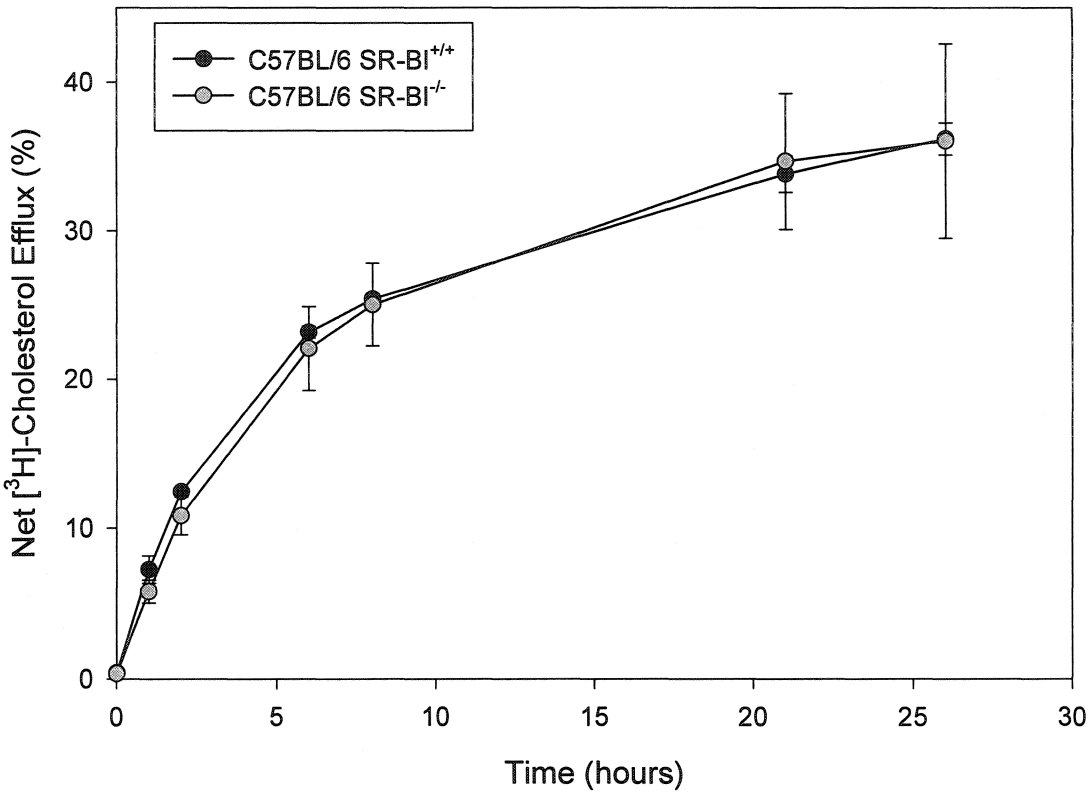

Figure 30. Net Efflux of [^{3}H]-Cholesterol from Wild-type and SR-BI KO Elicited Peritoneal Macrophages. Wild-type (black circles) and SR-BI KO (grey circles) mice were injected intraperitoneally with 10% thioglycollate and then 5 days later mice were injected with [^{3}H]-cholesterol in FBS into the peritoneal cavity. Following a 3-hour incubation, 10 ml of 5mM EDTA in PBS was injected into the peritoneal cavity followed by vigorous agitation. Isolated cells from the lavage were plated for 1-hour and then the monolayer was washed vigorously and then the culture media was then replaced with media containing 50 μg/ml HDL (as described in Section B.2.3.3). Media was then sampled at the indicated time the amount of [^{3}H] label was determined by scintillation counting and plotted as the percent of total [^{3}H]-cholesterol at time zero.

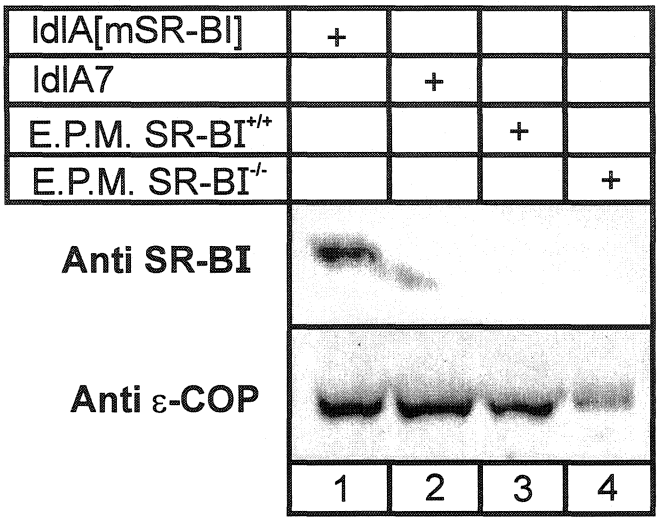

Figure 31. Western Blot Analysis of SR-BI in Elicited Peritoneal Macrophages from Wild-type and SR-BI KO Mice. Samples of total membranes were prepared (as described in Section B.2.4.2) from ldlA[mSR-BI] lane 1, ldlA7 lane 2, elicited peritoneal macrophages (E.P.M.) from SR-BI$^{+/+}$ (lane 3) and SR-BI$^{-/-}$ (lane 4). 10 μg of protein from each sample was separated by SDS-PAGE (as described in Section B.2.5.1) and transferred to a PVDF membrane (as described in Section B.2.5.2) and immunoblotting was performed (as described in Section B.2.5.3) with either an anti-SR-BI antibody (495 antibody diluted 1:50 000) or an anti- ε–COP antibody (diluted 1:5000).

SR-BI KO mice) as verified by using ε-COP as a loading control. SR-BI was detected in ldlA[mSR-BI] cells (Figure 31 upper panel, lane 1) but not in untransfected ldlA7 cells (Figure 31 upper panel, lane 2) or peritoneal macrophages from SR-BI$^{+/+}$ or SR-BI$^{-/-}$ mice (Figure 31 upper panel, lanes 3 and 4 respectively). The lack of detectable SR-BI in peritoneal macrophages may account for the similar level of net cholesterol efflux in these cells between wild-type and SR-BI KO mice.

SR-BI is not expressed at detectable levels in mouse elicited peritoneal macrophages, but is expressed in macrophages in atherosclerotic plaques (Ji et al. 1997; Hirano et al. 1999; Chinetti et al. 2000). Thus at least with respect to SR-BI, elicited peritoneal macrophages may not be a good model of macrophage foam cells in the arterial wall. Numerous studies have reported differences between resident and elicited macrophages within the peritoneal cavity (Kiss et al. 2002) (Papadimitriou et al. 1981; Grigoriadis et al. 1996), by extension there may be significant differences between elicited peritoneal macrophages and macrophage foam cells. Therefore we need to test cholesterol efflux in different macrophages from mice.

C.3.9 Conclusions and Implications

In this chapter experiments were aimed at testing the hypothesis that a lack of SR-BI expression in macrophage foam cells would enhance the development of atherosclerosis in mice. The rationale for this hypothesis was that SR-BI might contribute

to reverse cholesterol transport by mediating efflux from lipid-laden macrophage foam cells in the arterial wall to HDL, as over expression of SR-BI has been shown to promote cholesterol efflux in cultured cells ((Ji et al. 1997) and Figure 19). To test the hypothesis, we sought to use bone marrow transplantation to generate chimeric LDLR KO mice that have specific ablation or expression of SR-BI in bone marrow derived cells. The results presented in this chapter demonstrate that the bone marrow transplantation procedure was successful in generating chimeric mice (Figures 21, 24 and Table 7). The bone marrow specific ablation of SR-BI did not affect either the total plasma cholesterol levels or the plasma lipoprotein distribution in the chimeric mice (Figures 25, 26 and Table 8). However the bone marrow specific ablation of SR-BI did result in a substantial increase in aortic atherosclerosis in the mice (Figure 28) that is consistent with the hypothesis.

Ablation of SR-BI in bone marrow derived cells does not account for all of SR-BI's atheroprotective effect as global ablation of SR-BI in LDLR KO mice led to a 6-fold increase in atherosclerosis relative to LDLR KO mice (24% versus 3.9% coverage) (Covey et al. 2003), while selective ablation of SR-BI in LDLR KO mice led to a 1.4-fold increase in atherosclerosis (5.4% versus 3.7% coverage, Figure 28). Clearly SR-BI expression in other tissues, especially the liver, which has a profound influence on lipoprotein metabolism (Kozarsky et al. 2000), also plays an important atheroprotective role. Nevertheless, the near 2-fold effect of bone marrow specific SR-BI deficiency on atherosclerosis is striking. For example, bone marrow specific elimination of ABCA1, a

bona fide component of the in vivo cholesterol efflux pathway (Brooks-Wilson et al. 1999; Lawn et al. 1999), gives a 1.6 to 3-fold increase in diet-induced atherosclerosis in apoE or LDLR KO mice (Aiello et al. 2002; van Eck et al. 2002).

The mechanism of increased atherosclerosis by bone marrow specific ablation of SR-BI is not clear. However we have been able to establish that the effect is not a result of changes in plasma cholesterol content or distribution among lipoproteins (Figure 25,26 and Table 8). Furthermore our results indicate that defects in erythrocyte maturation are not the cause of the increased atherosclerosis (Figure 29). Experiments to determine if ablation of macrophage SR-BI inhibits net cholesterol efflux from macrophages and thus leads to increased atherosclerosis via diminished RCT will require a suitable model system (Figure 30 and 23).

D Concluding Remarks

D.1 Mechanisms of LCFA Membrane Translocation

Our results and those of others (Pohl et al. 2002) that cholesterol depletion inhibits LCFA uptake generates many questions. First and foremost, does cholesterol depletion affect passive diffusion of LCFA or does it alter the function of proteins involved in LCFA uptake such as an albumin receptor or a transporter? Alternatively cholesterol depletion may affect membrane structures required for LCFA uptake (e.g. lipid rafts or caveolae). There is compelling circumstantial evidence that LCFA uptake involves caveolin and or caveolae (see Section C.1.8). If so then a critical issue to resolve is if caveolin's role in LCFA uptake is an intrinsic function of caveolin (e.g. as a scaffolding protein, or fatty acid transporter) or a result of its structural role in caveolae which in turn may be required for the proper plasma membrane localization of proteins involved in LCFA uptake (e.g. CD36/FAT).

Despite a large body of work by numerous investigators a thorough understanding of the molecular mechanisms of LCFA uptake remain elusive. It is clear that numerous proteins are at least partially involved in LCFA uptake. Studies that seek to determine if and how these may function with respect to each other could provide significant insight into the mechanisms of LCFA uptake.

D.2 Adipocyte Albumin Binding Proteins

From our studies on albumin interaction with 3T3-F442A adipocytes several candidate albumin binding proteins were found. However it is not clear whether these proteins are real albumin receptors. Identification of these proteins, and their expression in cells would be key steps towards gaining insight into their potential as functional albumin receptors. Alternatively an approach such as expression cloning may be a more fruitful in identifying albumin receptors, especially in identifying albumin receptors that may participate in LCFA uptake.

The existence of albumin receptors in LCFA uptake is heavily disputed and therefore further searches for albumin receptors may be risky endeavors. However, just as there is a debate regarding the role of an albumin receptor in LCFA uptake, there was significant controversy over the existence and function of HDL receptors, until the discovery of SR-BI (Krieger 1999).

From a theoretical perspective we can draw on the cholesterol metabolism pathways for possible insight into albumin mediated LCFA transport and uptake. Cholesterol uptake from lipoproteins is receptor mediated. Furthermore selective lipid uptake serves as an example of receptor mediated lipid uptake without the concomitant uptake of the carrier molecule. Thus the proposed action of an albumin receptor in LCFA uptake is not without precedent.

D.3 Atheroprotection Mediated by Bone Marrow-Derived Cells

Our results have shown that normal expression of SR-BI in bone marrow-derived cells is atheroprotective in fat fed LDLR KO mice. Defining the mechanism of this atheroprotection is the next challenge. A major step towards achieving that goal would be the identification of a suitable macrophage cell preparation from mice to study cholesterol efflux from wild-type and SR-BI KO mice.

In addition variations of the experiments performed in this thesis could contribute substantially to the understanding of the role of SR-BI in bone marrow derived cells. For instance does expression of SR-BI in bone marrow derived cells in SR-BI KO mice protect against atherosclerosis? Can overexpression of SR-BI in macrophages confer increased atheroprotection over endogenous levels? In addition studies that investigate the effect of a dual ablation of SR-BI and ABCA1 in macrophages on atherosclerosis would be interesting. Studies such as these could indicate if macrophage SR-BI is a worthy potential therapeutic target for atherosclerosis prevention.

E Bibliography

Abumrad, N., Harmon, C. and Ibrahimi, A. (1998) Membrane transport of long-chain fatty acids: evidence for a facilitated process. *J Lipid Res.* **39,** 2309-2318.

Abumrad, N. A., el-Maghrabi, M. R., Amri, E. Z., Lopez, E. and Grimaldi, P. A. (1993) Cloning of a rat adipocyte membrane protein implicated in binding or transport of long-chain fatty acids that is induced during preadipocyte differentiation. Homology with human CD36. *J Biol Chem.* **268,** 17665-17668.

Abumrad, N. A., Park, J. H. and Park, C. R. (1984) Permeation of long-chain fatty acid into adipocytes. Kinetics, specificity, and evidence for involvement of a membrane protein. *J Biol Chem.* **259,** 8945-8953.

Abumrad, N. A., Perkins, R. C., Park, J. H. and Park, C. R. (1981) Mechanism of long chain fatty acid permeation in the isolated adipocyte. *J Biol Chem.* **256,** 9183-9191.

Acton, S., Osgood, D., et al. (1999) Association of polymorphisms at the SR-BI gene locus with plasma lipid levels and body mass index in a white population. *Arterioscler Thromb Vasc Biol.* **19,** 1734-1743.

Acton, S., Rigotti, A., Landschulz, K. T., Xu, S., Hobbs, H. H. and Krieger, M. (1996) Identification of scavenger receptor SR-BI as a high density lipoprotein receptor. *Science.* **271,** 518-520.

Acton, S. L., Scherer, P. E., Lodish, H. F. and Krieger, M. (1994) Expression cloning of SR-BI, a CD36-related class B scavenger receptor. *J Biol Chem.* **269,** 21003-21009.

Aiello, R. J., Brees, D., Bourassa, P. A., Royer, L., Lindsey, S., Coskran, T., Haghpassand, M. and Francone, O. L. (2002) Increased atherosclerosis in hyperlipidemic mice with inactivation of ABCA1 in macrophages. *Arterioscler Thromb Vasc Biol.* **22,** 630-637.

Aitman, T. J., Glazier, A. M., et al. (1999) Identification of Cd36 (Fat) as an insulin-resistance gene causing defective fatty acid and glucose metabolism in hypertensive rats. *Nat Genet.* **21,** 76-83.

Alaupovic, P. (1996) Significance of apolipoproteins for structure, function, and classification of plasma lipoproteins. *Methods Enzymol.* **263,** 32-60.

Altmann, S. W., Davis, H. R., Jr., et al. (2002) The identification of intestinal scavenger receptor class B, type I (SR-BI) by expression cloning and its role in cholesterol absorption. *Biochim Biophys Acta.* **1580,** 77-93.

Anderson, R. G. (1998) The caveolae membrane system. *Annu Rev Biochem.* **67,** 199-225.

Anderson, R. G., Brown, M. S. and Goldstein, J. L. (1977) Role of the coated endocytic vesicle in the uptake of receptor-bound low density lipoprotein in human fibroblasts. *Cell.* **10,** 351-364.

Angelin, B., Parini, P. and Eriksson, M. (2002) Reverse cholesterol transport in man: promotion of fecal steroid excretion by infusion of reconstituted HDL. *Atheroscler Suppl.* **3,** 23-30.

Arai, T., Wang, N., Bezouevski, M., Welch, C. and Tall, A. R. (1999) Decreased atherosclerosis in heterozygous low density lipoprotein receptor-deficient mice expressing the scavenger receptor BI transgene. *J Biol Chem.* **274,** 2366-2371.

Arbustini, E., Morbini, P., D'Armini, A. M., Repetto, A., Minzioni, G., Piovella, F., Vigano, M. and Tavazzi, L. (2002) Plaque composition in plexogenic and thromboembolic pulmonary hypertension: the critical role of thrombotic material in pultaceous core formation. *Heart.* **88,** 177-182.

Assmann, G. and Nofer, J. R. (2003) Atheroprotective effects of high-density lipoproteins. *Annu Rev Med.* **54,** 321-341.

Babitt, J., Trigatti, B., Rigotti, A., Smart, E. J., Anderson, R. G., Xu, S. and Krieger, M. (1997) Murine SR-BI, a high density lipoprotein receptor that mediates selective lipid uptake, is N-glycosylated and fatty acylated and colocalizes with plasma membrane caveolae. *J Biol Chem.* **272,** 13242-13249.

Barter, P. J., Brewer, H. B., Jr., Chapman, M. J., Hennekens, C. H., Rader, D. J. and Tall, A. R. (2003) Cholesteryl ester transfer protein: a novel target for raising HDL and inhibiting atherosclerosis. *Arterioscler Thromb Vasc Biol.* **23,** 160-167.

Bays, H. E., Moore, P. B., et al. (2001) Effectiveness and tolerability of ezetimibe in patients with primary hypercholesterolemia: pooled analysis of two phase II studies. *Clin Ther.* **23,** 1209-1230.

Behrens, W. A., Thompson, J. N. and Madere, R. (1982) Distribution of alpha-tocopherol in human plasma lipoproteins. *Am J Clin Nutr.* **35,** 691-696.

Bell, R. M. and Coleman, R. A. (1980) Enzymes of glycerolipid synthesis in eukaryotes. *Annu Rev Biochem.* **49,** 459-487.

Berge, K. E., Tian, H., et al. (2000) Accumulation of dietary cholesterol in sitosterolemia caused by mutations in adjacent ABC transporters. *Science.* **290,** 1771-1775.

Berk, P. D. and Stump, D. D. (1999) Mechanisms of cellular uptake of long chain free fatty acids. *Mol Cell Biochem.* **192,** 17-31.

Bloch, K. (1965) The biological synthesis of cholesterol. *Science.* **150,** 19-28.

Bodzioch, M., Orso, E., et al. (1999) The gene encoding ATP-binding cassette transporter 1 is mutated in Tangier disease. *Nat Genet.* **22,** 347-351.

Boisvert, W. A., Spangenberg, J. and Curtiss, L. K. (1997) Role of leukocyte-specific LDL receptors on plasma lipoprotein cholesterol and atherosclerosis in mice. *Arterioscler Thromb Vasc Biol.* **17,** 340-347.

Bolard, J. (1986) How do the polyene macrolide antibiotics affect the cellular membrane properties? *Biochim Biophys Acta.* **864,** 257-304.

Boxen, I. (1985) Mechanisms of atherogenesis: endothelial hypoxia proposed as the major initiator. *Med Hypotheses.* **18,** 297-311.

Brandes, R., Ockner, R. K., Weisiger, R. A. and Lysenko, N. (1982) Specific and saturable binding of albumin to rat adipocytes: modulation by epinephrine and possible role in free fatty acid transfer. *Biochem Biophys Res Commun.* **105,** 821-827.

Brasaemle, D. L., Barber, T., Wolins, N. E., Serrero, G., Blanchette-Mackie, E. J. and Londos, C. (1997) Adipose differentiation-related protein is an ubiquitously expressed lipid storage droplet-associated protein. *J Lipid Res.* **38,** 2249-2263.

Braun, A., Trigatti, B. L., Post, M. J., Sato, K., Simons, M., Edelberg, J. M., Rosenberg, R. D., Schrenzel, M. and Krieger, M. (2002) Loss of SR-BI expression leads to the early onset of occlusive atherosclerotic coronary artery disease, spontaneous myocardial infarctions, severe cardiac dysfunction, and premature death in apolipoprotein E-deficient mice. *Circ Res.* **90,** 270-276.

Brigelius-Flohe, R. and Traber, M. G. (1999) Vitamin E: function and metabolism. *Faseb J.* **13,** 1145-1155.

Brooks-Wilson, A., Marcil, M., et al. (1999) Mutations in ABC1 in Tangier disease and familial high-density lipoprotein deficiency. *Nat Genet.* **22,** 336-345.

Brown, D. A. and London, E. (2000) Structure and function of sphingolipid- and cholesterol-rich membrane rafts. *J Biol Chem.* **275,** 17221-17224.

Brown, D. A. and Rose, J. K. (1992) Sorting of GPI-anchored proteins to glycolipid-enriched membrane subdomains during transport to the apical cell surface. *Cell.* **68,** 533-544.

Brown, M. S. and Goldstein, J. L. (1986) A receptor-mediated pathway for cholesterol homeostasis. *Science.* **232,** 34-47.

Brown, M. S. and Goldstein, J. L. (1999) A proteolytic pathway that controls the cholesterol content of membranes, cells, and blood. *Proc Natl Acad Sci U S A.* **96,** 11041-11048.

Bultel-Brienne, S., Lestavel, S., Pilon, A., Laffont, I., Tailleux, A., Fruchart, J. C., Siest, G. and Clavey, V. (2002) Lipid free apolipoprotein E binds to the class B Type I scavenger receptor I (SR-BI) and enhances cholesteryl ester uptake from lipoproteins. *J Biol Chem.* **277,** 36092-36099.

Burczynski, F. J. and Cai, Z. S. (1994) Palmitate uptake by hepatocyte suspensions: effect of albumin. *Am J Physiol.* **267,** G371-379.

Burczynski, F. J., Cai, Z. S., Moran, J. B. and Forker, E. L. (1989) Palmitate uptake by cultured hepatocytes: albumin binding and stagnant layer phenomena. *Am J Physiol.* **257,** G584-593.

Burczynski, F. J., Wang, G. Q. and Hnatowich, M. (1997) Effect of binding protein surface charge on palmitate uptake by hepatocyte suspensions. *Br J Pharmacol.* **120,** 1215-1220.

Calder, P. C. (2002) Dietary modification of inflammation with lipids. *Proc Nutr Soc.* **61,** 345-358.

Calvo, D., Gomez-Coronado, D., Lasuncion, M. A. and Vega, M. A. (1997) CLA-1 is an 85-kD plasma membrane glycoprotein that acts as a high-affinity receptor for both native (HDL, LDL, and VLDL) and modified (OxLDL and AcLDL) lipoproteins. *Arterioscler Thromb Vasc Biol.* **17,** 2341-2349.

Campbell, I. (2003) The obesity epidemic: can we turn the tide? *Heart.* **89 Suppl 2,** ii22-24; discussion ii35-27.

Cao, G., Beyer, T. P., et al. (2002) Phospholipid transfer protein is regulated by liver X receptors in vivo. *J Biol Chem.* **277,** 39561-39565.

Carey, M. C., Small, D. M. and Bliss, C. M. (1983) Lipid digestion and absorption. *Annu Rev Physiol.* **45,** 651-677.

Carnicero, H. H. (1984) Changes in the metabolism of long chain fatty acids during adipose differentiation of 3T3 L1 cells. *J Biol Chem.* **259,** 3844-3850.

Cechetto, J. D., Sadacharan, S. K., Berk, P. D. and Gupta, R. S. (2002) Immunogold localization of mitochondrial aspartate aminotransferase in mitochondria and on the cell surface in normal rat tissues. *Histol Histopathol.* **17,** 353-364.

Chang, T. H. and Polakis, S. E. (1978) Differentiation of 3T3-L1 fibroblasts to adipocytes. Effect of insulin and indomethacin on the levels of insulin receptors. *J Biol Chem.* **253,** 4693-4696.

Chappell, D. A. and Medh, J. D. (1998) Receptor-mediated mechanisms of lipoprotein remnant catabolism. *Prog Lipid Res.* **37,** 393-422.

Cheng, T., Shen, H., Giokas, D., Gere, J., Tenen, D. G. and Scadden, D. T. (1996) Temporal mapping of gene expression levels during the differentiation of individual primary hematopoietic cells. *Proc Natl Acad Sci U S A.* **93,** 13158-13163.

Chinetti, G., Gbaguidi, F. G., et al. (2000) CLA-1/SR-BI is expressed in atherosclerotic lesion macrophages and regulated by activators of peroxisome proliferator-activated receptors. *Circulation.* **101,** 2411-2417.

Coe, N. R., Smith, A. J., Frohnert, B. I., Watkins, P. A. and Bernlohr, D. A. (1999) The fatty acid transport protein (FATP1) is a very long chain acyl-CoA synthetase. *J Biol Chem.* **274,** 36300-36304.

Connelly, M. A., de la Llera-Moya, M., et al. (2001) Analysis of chimeric receptors shows that multiple distinct functional activities of scavenger receptor, class B, type I (SR-BI), are localized to the extracellular receptor domain. *Biochemistry.* **40,** 5249-5259.

Connelly, M. A., De La Llera-Moya, M., Peng, Y., Drazul-Schrader, D., Rothblat, G. H. and Williams, D. L. (2003) Separation of lipid transport functions by mutations in the

extracellular domain of scavenger receptor class B, type I. *J Biol Chem.* **278,** 25773-25782.

Cooke, J. P. and Dzau, V. J. (1997) Nitric oxide synthase: role in the genesis of vascular disease. *Annu Rev Med.* **48,** 489-509.

Covey, S. D., Krieger, M., Wang, W., Penman, M. and Trigatti, B. L. (2003) Scavenger Receptor Class B Type I-Mediated Protection Against Atherosclerosis in LDL Receptor-Negative Mice Involves Its Expression in Bone Marrow-Derived Cells. *Arterioscler Thromb Vasc Biol.* **23,** 1589-1594.

Crawford, D. W. and Blankenhorn, D. H. (1991) Arterial wall oxygenation, oxyradicals, and atherosclerosis. *Atherosclerosis.* **89,** 97-108.

Cushman, S. W. and Wardzala, L. J. (1980) Potential mechanism of insulin action on glucose transport in the isolated rat adipose cell. Apparent translocation of intracellular transport systems to the plasma membrane. *J Biol Chem.* **255,** 4758-4762.

de la Llera-Moya, M., Rothblat, G. H., Connelly, M. A., Kellner-Weibel, G., Sakr, S. W., Phillips, M. C. and Williams, D. L. (1999) Scavenger receptor BI (SR-BI) mediates free cholesterol flux independently of HDL tethering to the cell surface. *J Lipid Res.* **40,** 575-580.

Engelman, J. A., Zhang, X., et al. (1998) Molecular genetics of the caveolin gene family: implications for human cancers, diabetes, Alzheimer disease, and muscular dystrophy. *Am J Hum Genet.* **63,** 1578-1587.

Fazio, S., Babaev, V. R., Murray, A. B., Hasty, A. H., Carter, K. J., Gleaves, L. A., Atkinson, J. B. and Linton, M. F. (1997) Increased atherosclerosis in mice reconstituted with apolipoprotein E null macrophages. *Proc Natl Acad Sci U S A.* **94,** 4647-4652.

Febbraio, M., Abumrad, N. A., Hajjar, D. P., Sharma, K., Cheng, W., Pearce, S. F. and Silverstein, R. L. (1999) A null mutation in murine CD36 reveals an important role in fatty acid and lipoprotein metabolism. *J Biol Chem.* **274,** 19055-19062.

Feng, B. and Tabas, I. (2002) ABCA1-mediated cholesterol efflux is defective in free cholesterol- loaded macrophages. Mechanism involves enhanced ABCA1 degradation in a process requiring full NPC1 activity. *J Biol Chem.* **277,** 43271-43280.

Fielding, C. J. and Fielding, P. E. (1995) Molecular physiology of reverse cholesterol transport. *J Lipid Res.* **36,** 211-228.

Flier, J. S. (1995) The adipocyte: storage depot or node on the energy information superhighway? *Cell.* **80,** 15-18.

Fortier, A. H. (1994). Isolation of Murine Macrophages. *Current Protocols in Immunology.* J. E. Coligan. New York, John Wiley and Sons, Inc. **1:** 14.11.11-14.11.19.

Francis, G. A., Knopp, R. H. and Oram, J. F. (1995) Defective removal of cellular cholesterol and phospholipids by apolipoprotein A-I in Tangier Disease. *J Clin Invest.* **96,** 78-87.

Furuhashi, M., Ura, N., Nakata, T. and Shimamoto, K. (2003) Insulin sensitivity and lipid metabolism in human CD36 deficiency. *Diabetes Care.* **26,** 471-474.

Gainer, J. L. (1987) Hypoxia and atherosclerosis: re-evaluation of an old hypothesis. *Atherosclerosis.* **68,** 263-266.

Gao, J. and Serrero, G. (1999) Adipose differentiation related protein (ADRP) expressed in transfected COS-7 cells selectively stimulates long chain fatty acid uptake. *J Biol Chem.* **274,** 16825-16830.

Ghinea, N., Eskenasy, M., Simionescu, M. and Simionescu, N. (1989) Endothelial albumin binding proteins are membrane-associated components exposed on the cell surface. *J Biol Chem.* **264,** 4755-4758.

Ghinea, N., Fixman, A., Alexandru, D., Popov, D., Hasu, M., Ghitescu, L., Eskenasy, M., Simionescu, M. and Simionescu, N. (1988) Identification of albumin-binding proteins in capillary endothelial cells. *J Cell Biol.* **107,** 231-239.

Gillotte-Taylor, K., Boullier, A., Witztum, J. L., Steinberg, D. and Quehenberger, O. (2001) Scavenger receptor class B type I as a receptor for oxidized low density lipoprotein. *J Lipid Res.* **42,** 1474-1482.

Gimbrone, M. A., Jr. (1999) Vascular endothelium, hemodynamic forces, and atherogenesis. *Am J Pathol.* **155,** 1-5.

Gimeno, R. E., Ortegon, A. M., Patel, S., Punreddy, S., Ge, P., Sun, Y., Lodish, H. F. and Stahl, A. (2003) Characterization of a heart-specific fatty acid transport protein. *J Biol Chem.* **278,** 16039-16044.

Glass, C., Pittman, R. C., Civen, M. and Steinberg, D. (1985) Uptake of high-density lipoprotein-associated apoprotein A-I and cholesterol esters by 16 tissues of the rat in vivo and by adrenal cells and hepatocytes in vitro. *J Biol Chem.* **260,** 744-750.

Glass, C., Pittman, R. C., Weinstein, D. B. and Steinberg, D. (1983) Dissociation of tissue uptake of cholesterol ester from that of apoprotein A-I of rat plasma high density lipoprotein: selective delivery of cholesterol ester to liver, adrenal, and gonad. *Proc Natl Acad Sci U S A.* **80,** 5435-5439.

Glomset, J. A. (1968) The plasma lecithins:cholesterol acyltransferase reaction. *J Lipid Res.* **9,** 155-167.

Goldstein, J. L., Brunschede, G. Y. and Brown, M. S. (1975) Inhibition of proteolytic degradation of low density lipoprotein in human fibroblasts by chloroquine, concanavalin A, and Triton WR 1339. *J Biol Chem.* **250,** 7854-7862.

Green, H. and Kehinde, O. (1976) Spontaneous heritable changes leading to increased adipose conversion in 3T3 cells. *Cell.* **7,** 105-113.

Greenberger, N. J., Rodgers, J. B. and Isselbacher, K. J. (1966) Absorption of medium and long chain triglycerides: factors influencing their hydrolysis and transport. *J Clin Invest.* **45,** 217-227.

Grigoriadis, G., Zhan, Y., Grumont, R. J., Metcalf, D., Handman, E., Cheers, C. and Gerondakis, S. (1996) The Rel subunit of NF-kappaB-like transcription factors is a positive and negative regulator of macrophage gene expression: distinct roles for Rel in different macrophage populations. *Embo J.* **15,** 7099-7107.

Gu, X., Kozarsky, K. and Krieger, M. (2000) Scavenger receptor class B, type I-mediated [3H]cholesterol efflux to high and low density lipoproteins is dependent on lipoprotein binding to the receptor. *J Biol Chem.* **275,** 29993-30001.

Gu, X., Trigatti, B., Xu, S., Acton, S., Babitt, J. and Krieger, M. (1998) The efficient cellular uptake of high density lipoprotein lipids via scavenger receptor class B type I requires not only receptor-mediated surface binding but also receptor-specific lipid transfer mediated by its extracellular domain. *J Biol Chem.* **273,** 26338-26348.

Ha, Y. C. and Barter, P. J. (1982) Differences in plasma cholesteryl ester transfer activity in sixteen vertebrate species. *Comp Biochem Physiol B.* **71,** 265-269.

Hackam, D. G. and Anand, S. S. (2003) Emerging risk factors for atherosclerotic vascular disease: a critical review of the evidence. *Jama.* **290,** 932-940.

Hailstones, D., Sleer, L. S., Parton, R. G. and Stanley, K. K. (1998) Regulation of caveolin and caveolae by cholesterol in MDCK cells. *J Lipid Res.* **39,** 369-379.

Hamilton, J. A. (1998) Fatty acid transport: difficult or easy? *J Lipid Res.* **39,** 467-481.

Hamilton, J. A. and Cistola, D. P. (1986) Transfer of oleic acid between albumin and phospholipid vesicles. *Proc Natl Acad Sci U S A.* **83,** 82-86.

Han, X. X. and Bonen, A. (1998) Epinephrine translocates GLUT-4 but inhibits insulin-stimulated glucose transport in rat muscle. *Am J Physiol.* **274,** E700-707.

Harmon, C. M., Luce, P., Beth, A. H. and Abumrad, N. A. (1991) Labeling of adipocyte membranes by sulfo-N-succinimidyl derivatives of long-chain fatty acids: inhibition of fatty acid transport. *J Membr Biol.* **121,** 261-268.

Herijgers, N., Van Eck, M., Groot, P. H., Hoogerbrugge, P. M. and Van Berkel, T. J. (1997) Effect of bone marrow transplantation on lipoprotein metabolism and atherosclerosis in LDL receptor-knockout mice. *Arterioscler Thromb Vasc Biol.* **17,** 1995-2003.

Herrmann, T., Buchkremer, F., Gosch, I., Hall, A. M., Bernlohr, D. A. and Stremmel, W. (2001) Mouse fatty acid transport protein 4 (FATP4): characterization of the gene and functional assessment as a very long chain acyl-CoA synthetase. *Gene.* **270,** 31-40.

Herrmann, T., Van Der Hoeven, F., et al. (2003) Mice with targeted disruption of the fatty acid transport protein 4 (Fatp 4, Slc27a4) gene show features of lethal restrictive dermopathy. *J Cell Biol.* **161,** 1105-1115.

Hirano, K., Yamashita, S., et al. (1999) Expression of human scavenger receptor class B type I in cultured human monocyte-derived macrophages and atherosclerotic lesions. *Circ Res.* **85,** 108-116.

Hirsch, D., Stahl, A. and Lodish, H. F. (1998) A family of fatty acid transporters conserved from mycobacterium to man. *Proc Natl Acad Sci U S A.* **95,** 8625-8629.

Ho, S. Y. and Storch, J. (2001) Common mechanisms of monoacylglycerol and fatty acid uptake by human intestinal Caco-2 cells. *Am J Physiol Cell Physiol.* **281,** C1106-1117.

Hogarth, C. A., Roy, A. and Ebert, D. L. (2003) Genomic evidence for the absence of a functional cholesteryl ester transfer protein gene in mice and rats. *Comp Biochem Physiol B Biochem Mol Biol.* **135,** 219-229.

Holm, T. M., Braun, A., Trigatti, B. L., Brugnara, C., Sakamoto, M., Krieger, M. and Andrews, N. C. (2002) Failure of red blood cell maturation in mice with defects in the high- density lipoprotein receptor SR-BI. *Blood.* **99,** 1817-1824.

Horie, T., Mizuma, T., Kasai, S. and Awazu, S. (1988) Conformational change in plasma albumin due to interaction with isolated rat hepatocyte. *Am J Physiol.* **254,** G465-470.

Horky, J., Vacha, J. and Znojil, V. (1978) Comparison of life span of erythrocytes in some inbred strains of mouse using 14C-labelled glycine. *Physiol Bohemoslov.* **27,** 209-217.

Howell, J. L. and Truant, R. (2002) Live-cell nucleocytoplasmic protein shuttle assay utilizing laser confocal microscopy and FRAP. *Biotechniques.* **32,** 80-82, 84, 86-87.

Hsu, L. A., Ko, Y. L., Wu, S., Teng, M. S., Peng, T. Y., Chen, C. F. and Lee, Y. S. (2003) Association Between a Novel 11-Base Pair Deletion Mutation in the Promoter Region of the Scavenger Receptor Class B Type I Gene and Plasma HDL Cholesterol Levels in Taiwanese Chinese. *Arterioscler Thromb Vasc Biol.* **19,** 19.

Huang, Z. H. and Mazzone, T. (2002) ApoE-dependent sterol efflux from macrophages is modulated by scavenger receptor class B type I expression. *J Lipid Res.* **43,** 375-382.

Hui, T. Y. and Bernlohr, D. A. (1997) Fatty acid transporters in animal cells. *Front Biosci.* **2,** d222-231.

Huo, H., Guo, X., Hong, S., Jiang, M., Liu, X. and Liao, K. (2003) Lipid rafts/caveolae are essential for insulin-like growth factor-1 receptor signaling during 3T3-L1 preadipocyte differentiation induction. *J Biol Chem.* **278,** 11561-11569.

Husemann, J., Loike, J. D., Kodama, T. and Silverstein, S. C. (2001) Scavenger receptor class B type I (SR-BI) mediates adhesion of neonatal murine microglia to fibrillar beta-amyloid. *J Neuroimmunol.* **114,** 142-150.

Husemann, J. and Silverstein, S. C. (2001) Expression of scavenger receptor class B, type I, by astrocytes and vascular smooth muscle cells in normal adult mouse and human brain and in Alzheimer's disease brain. *Am J Pathol.* **158,** 825-832.

Huszar, D., Varban, M. L., Rinninger, F., Feeley, R., Arai, T., Fairchild-Huntress, V., Donovan, M. J. and Tall, A. R. (2000) Increased LDL cholesterol and atherosclerosis in LDL receptor-deficient mice with attenuated expression of scavenger receptor B1. *Arterioscler Thromb Vasc Biol.* **20,** 1068-1073.

Hutter, J. F., Piper, H. M. and Spieckermann, P. G. (1984) Kinetic analysis of myocardial fatty acid oxidation suggesting an albumin receptor mediated uptake process. *J Mol Cell Cardiol.* **16,** 219-226.

Ibrahimi, A., Sfeir, Z., Magharaie, H., Amri, E. Z., Grimaldi, P. and Abumrad, N. A. (1996) Expression of the CD36 homolog (FAT) in fibroblast cells: effects on fatty acid transport. *Proc Natl Acad Sci U S A.* **93,** 2646-2651.

Ishibashi, S., Brown, M. S., Goldstein, J. L., Gerard, R. D., Hammer, R. E. and Herz, J. (1993) Hypercholesterolemia in low density lipoprotein receptor knockout mice and its reversal by adenovirus-mediated gene delivery. *J Clin Invest.* **92,** 883-893.

Ishibashi, S., Goldstein, J. L., Brown, M. S., Herz, J. and Burns, D. K. (1994) Massive xanthomatosis and atherosclerosis in cholesterol-fed low density lipoprotein receptor-negative mice. *J Clin Invest.* **93,** 1885-1893.

Isola, L. M., Zhou, S. L., Kiang, C. L., Stump, D. D., Bradbury, M. W. and Berk, P. D. (1995) 3T3 fibroblasts transfected with a cDNA for mitochondrial aspartate aminotransferase express plasma membrane fatty acid-binding protein and saturable fatty acid uptake. *Proc Natl Acad Sci U S A.* **92,** 9866-9870.

Itabe, H. (2003) Oxidized low-density lipoproteins: what is understood and what remains to be clarified. *Biol Pharm Bull.* **26,** 1-9.

Ji, Y., Jian, B., Wang, N., Sun, Y., Moya, M. L., Phillips, M. C., Rothblat, G. H., Swaney, J. B. and Tall, A. R. (1997) Scavenger receptor BI promotes high density lipoprotein-mediated cellular cholesterol efflux. *J Biol Chem.* **272,** 20982-20985.

Jian, B., de la Llera-Moya, M., Ji, Y., Wang, N., Phillips, M. C., Swaney, J. B., Tall, A. R. and Rothblat, G. H. (1998) Scavenger receptor class B type I as a mediator of cellular cholesterol efflux to lipoproteins and phospholipid acceptors. *J Biol Chem.* **273,** 5599-5606.

Jiang, H. P., Harris, S. E. and Serrero, G. (1992) Molecular cloning of a differentiation-related mRNA in the adipogenic cell line 1246. *Cell Growth Differ.* **3,** 21-30.

Jiang, H. P. and Serrero, G. (1992) Isolation and characterization of a full-length cDNA coding for an adipose differentiation-related protein. *Proc Natl Acad Sci U S A.* **89,** 7856-7860.

John, T. A., Vogel, S. M., Minshall, R. D., Ridge, K., Tiruppathi, C. and Malik, A. B. (2001) Evidence for the role of alveolar epithelial gp60 in active transalveolar albumin transport in the rat lung. *J Physiol.* **533,** 547-559.

Kamp, F., Guo, W., Souto, R., Pilch, P. F., Corkey, B. E. and Hamilton, J. A. (2003) Rapid flip-flop of oleic acid across the plasma membrane of adipocytes. *J Biol Chem.* **278,** 7988-7995.

Kent, C. (1995) Eukaryotic phospholipid biosynthesis. *Annu Rev Biochem.* **64,** 315-343.

Kersten, S. (2002) Peroxisome proliferator activated receptors and obesity. *Eur J Pharmacol.* **440,** 223-234.

Kintaka, T., Tanaka, T., Imai, M., Adachi, I., Narabayashi, I. and Kitaura, Y. (2002) CD36 genotype and long-chain fatty acid uptake in the heart. *Circ J.* **66,** 819-825.

Kiss, A. L., Turi, A., Muller, N., Kantor, O. and Botos, E. (2002) Caveolae and caveolin isoforms in rat peritoneal macrophages. *Micron.* **33,** 75-93.

Kleinfeld, A. M., Chu, P. and Romero, C. (1997) Transport of long-chain native fatty acids across lipid bilayer membranes indicates that transbilayer flip-flop is rate limiting. *Biochemistry.* **36,** 14146-14158.

Kolleck, I., Guthmann, F., Ladhoff, A. M., Tandon, N. N., Schlame, M. and Rustow, B. (2002) Cellular cholesterol stimulates acute uptake of palmitate by redistribution of fatty acid translocase in type II pneumocytes. *Biochemistry.* **41,** 6369-6375.

Kozarsky, K. F., Donahee, M. H., Glick, J. M., Krieger, M. and Rader, D. J. (2000) Gene transfer and hepatic overexpression of the HDL receptor SR-BI reduces atherosclerosis in the cholesterol-fed LDL receptor-deficient mouse. *Arterioscler Thromb Vasc Biol.* **20,** 721-727.

Kozarsky, K. F., Donahee, M. H., Rigotti, A., Iqbal, S. N., Edelman, E. R. and Krieger, M. (1997) Overexpression of the HDL receptor SR-BI alters plasma HDL and bile cholesterol levels. *Nature.* **387,** 414-417.

Krieger, M. (1999) Charting the fate of the "good cholesterol": identification and characterization of the high-density lipoprotein receptor SR-BI. *Annu Rev Biochem.* **68,** 523-558.

Krieger, M. (1999) Charting the fate of the "good cholesterol": identification and characterization of the high-density lipoprotein receptor SR-BI. *Annu Rev Biochem.* **68,** 523-558.

Krieger, M. (2001) Scavenger receptor class B type I is a multiligand HDL receptor that influences diverse physiologic systems. *J Clin Invest.* **108,** 793-797.

Krieger, M., Brown, M. S. and Goldstein, J. L. (1981) Isolation of Chinese hamster cell mutants defective in the receptor- mediated endocytosis of low density lipoprotein. *J Mol Biol.* **150,** 167-184.

Kunjathoor, V. V., Febbraio, M., et al. (2002) Scavenger receptors class A-I/II and CD36 are the principal receptors responsible for the uptake of modified low density lipoprotein leading to lipid loading in macrophages. *J Biol Chem.* **277,** 49982-49988.

Kurzchalia, T. V., Dupree, P., Parton, R. G., Kellner, R., Virta, H., Lehnert, M. and Simons, K. (1992) VIP21, a 21-kD membrane protein is an integral component of trans-Golgi-network-derived transport vesicles. *J Cell Biol.* **118,** 1003-1014.

Kwiterovich, P. O., Jr. (2000) The metabolic pathways of high-density lipoprotein, low-density lipoprotein, and triglycerides: a current review. *Am J Cardiol.* **86,** 5L-10L.

Laemmli, U. K. (1970) Cleavage of structural proteins during the assembly of the head of bacteriophage T4. *Nature.* **227,** 680-685.

Lai, E. C. (2003) Lipid rafts make for slippery platforms. *J Cell Biol.* **162,** 365-370.

Laird, P. W., Zijderveld, A., Linders, K., Rudnicki, M. A., Jaenisch, R. and Berns, A. (1991) Simplified mammalian DNA isolation procedure. *Nucleic Acids Res.* **19,** 4293.

Lawn, R. M., Wade, D. P., Garvin, M. R., Wang, X., Schwartz, K., Porter, J. G., Seilhamer, J. J., Vaughan, A. M. and Oram, J. F. (1999) The Tangier disease gene product ABC1 controls the cellular apolipoprotein-mediated lipid removal pathway. *J Clin Invest.* **104,** R25-31.

Layne, M. D., Patel, A., et al. (2001) Role of macrophage-expressed adipocyte fatty acid binding protein in the development of accelerated atherosclerosis in hypercholesterolemic mice. *Faseb J.* **15,** 2733-2735.

Lee, M., Calabresi, L., Chiesa, G., Franceschini, G. and Kovanen, P. T. (2002) Mast cell chymase degrades apoE and apoA-II in apoA-I-knockout mouse plasma and reduces its

ability to promote cellular cholesterol efflux. *Arterioscler Thromb Vasc Biol.* **22,** 1475-1481.

Leitersdorf, E., Stein, O., Eisenberg, S. and Stein, Y. (1984) Uptake of rat plasma HDL subfractions labeled with [3H]cholesteryl linoleyl ether or with 125I by cultured rat hepatocytes and adrenal cells. *Biochim Biophys Acta.* **796,** 72-82.

Li, A. C. and Glass, C. K. (2002) The macrophage foam cell as a target for therapeutic intervention. *Nat Med.* **8,** 1235-1242.

Li, W. P., Liu, P., Pilcher, B. K. and Anderson, R. G. (2001) Cell-specific targeting of caveolin-1 to caveolae, secretory vesicles, cytoplasm or mitochondria. *J Cell Sci.* **114,** 1397-1408.

Liadaki, K. N., Liu, T., Xu, S., Ishida, B. Y., Duchateaux, P. N., Krieger, J. P., Kane, J., Krieger, M. and Zannis, V. I. (2000) Binding of high density lipoprotein (HDL) and discoidal reconstituted HDL to the HDL receptor scavenger receptor class B type I. Effect of lipid association and APOA-I mutations on receptor binding. *J Biol Chem.* **275,** 21262-21271.

Linton, M. F., Babaev, V. R., Gleaves, L. A. and Fazio, S. (1999) A direct role for the macrophage low density lipoprotein receptor in atherosclerotic lesion formation. *J Biol Chem.* **274,** 19204-19210.

Lisanti, M. P., Scherer, P. E., Vidugiriene, J., Tang, Z., Hermanowski-Vosatka, A., Tu, Y. H., Cook, R. F. and Sargiacomo, M. (1994) Characterization of caveolin-rich membrane domains isolated from an endothelial-rich source: implications for human disease. *J Cell Biol.* **126,** 111-126.

Liu, B. and Krieger, M. (2002) Highly purified scavenger receptor class B, type I reconstituted into phosphatidylcholine/cholesterol liposomes mediates high affinity high density lipoprotein binding and selective lipid uptake. *J Biol Chem.* **277,** 34125-34135.

Liu, P., Rudick, M. and Anderson, R. G. (2002) Multiple functions of caveolin-1. *J Biol Chem.* **277,** 41295-41298.

Luiken, J. J., Schaap, F. G., van Nieuwenhoven, F. A., van der Vusse, G. J., Bonen, A. and Glatz, J. F. (1999) Cellular fatty acid transport in heart and skeletal muscle as facilitated by proteins. *Lipids.* **34,** S169-175.

Lusis, A. J. (2000) Atherosclerosis. *Nature.* **407,** 233-241.

Mackness, M. I., Mackness, B. and Durrington, P. N. (2002) Paraoxonase and coronary heart disease. *Atheroscler Suppl.* **3,** 49-55.

Marsche, G., Hammer, A., Oskolkova, O., Kozarsky, K. F., Sattler, W. and Malle, E. (2002) Hypochlorite-modified high density lipoprotein, a high affinity ligand to scavenger receptor class B, type I, impairs high density lipoprotein-dependent selective lipid uptake and reverse cholesterol transport. *J Biol Chem.* **277,** 32172-32179.

Martin, J. F., Booth, R. F. and Moncada, S. (1991) Arterial wall hypoxia following thrombosis of the vasa vasorum is an initial lesion in atherosclerosis. *Eur J Clin Invest.* **21,** 355-359.

Mathews, C. K., van Holde, K. E. and Ahern, K. G. (2000). Biochemistry. *Biochemistry.* B. Roberts. San Fransico, Benjamin/Cummings: 627-640.

Maxfield, F. R. (2002) Plasma membrane microdomains. *Curr Opin Cell Biol.* **14,** 483-487.

Mead, J. R., Irvine, S. A. and Ramji, D. P. (2002) Lipoprotein lipase: structure, function, regulation, and role in disease. *J Mol Med.* **80,** 753-769.

Miettinen, H. E., Rayburn, H. and Krieger, M. (2001) Abnormal lipoprotein metabolism and reversible female infertility in HDL receptor (SR-BI)-deficient mice. *J Clin Invest.* **108,** 1717-1722.

Murao, K., Terpstra, V., Green, S. R., Kondratenko, N., Steinberg, D. and Quehenberger, O. (1997) Characterization of CLA-1, a human homologue of rodent scavenger receptor BI, as a receptor for high density lipoprotein and apoptotic thymocytes. *J Biol Chem.* **272,** 17551-17557.

Nieland, T. J., Penman, M., Dori, L., Krieger, M. and Kirchhausen, T. (2002) Discovery of chemical inhibitors of the selective transfer of lipids mediated by the HDL receptor SR-BI. *Proc Natl Acad Sci U S A.* **99,** 15422-15427.

Nohturfft, A., DeBose-Boyd, R. A., Scheek, S., Goldstein, J. L. and Brown, M. S. (1999) Sterols regulate cycling of SREBP cleavage-activating protein (SCAP) between endoplasmic reticulum and Golgi. *Proc Natl Acad Sci U S A.* **96,** 11235-11240.

Ockner, R. K., Weisiger, R. A. and Gollan, J. L. (1983) Hepatic uptake of albumin-bound substances: albumin receptor concept. *Am J Physiol.* **245,** G13-18.

Ohgami, N., Nagai, R., Miyazaki, A., Ikemoto, M., Arai, H., Horiuchi, S. and Nakayama, H. (2001) Scavenger receptor class B type I-mediated reverse cholesterol transport is inhibited by advanced glycation end products. *J Biol Chem.* **276,** 13348-13355.

Okabe, M., Ikawa, M., Kominami, K., Nakanishi, T. and Nishimune, Y. (1997) 'Green mice' as a source of ubiquitous green cells. *FEBS Lett.* **407,** 313-319.

Orlandi, P. A. and Fishman, P. H. (1998) Filipin-dependent inhibition of cholera toxin: evidence for toxin internalization and activation through caveolae-like domains. *J Cell Biol.* **141,** 905-915.

Osgood, D., Corella, D., Demissie, S., Cupples, L. A., Wilson, P. W., Meigs, J. B., Schaefer, E. J., Coltell, O. and Ordovas, J. M. (2003) Genetic variation at the scavenger receptor class B type I gene locus determines plasma lipoprotein concentrations and particle size and interacts with type 2 diabetes: the framingham study. *J Clin Endocrinol Metab.* **88,** 2869-2879.

Paigen, B., Ishida, B. Y., Verstuyft, J., Winters, R. B. and Albee, D. (1990) Atherosclerosis susceptibility differences among progenitors of recombinant inbred strains of mice. *Arteriosclerosis.* **10,** 316-323.

Paigen, B., Morrow, A., Holmes, P. A., Mitchell, D. and Williams, R. A. (1987) Quantitative assessment of atherosclerotic lesions in mice. *Atherosclerosis.* **68,** 231-240.

Palade, G. E. (1953) The fine structure of blood capillaries. *J. Appl. Phys.* **24,** 1424.

Papadimitriou, J. M. and van Bruggen, I. (1981) A quantitative cytochemical analysis of resident and exudate macrophages. *J Pathol.* **134,** 27-38.

Park, H., Go, Y. M., St John, P. L., Maland, M. C., Lisanti, M. P., Abrahamson, D. R. and Jo, H. (1998) Plasma membrane cholesterol is a key molecule in shear stress-dependent activation of extracellular signal-regulated kinase. *J Biol Chem.* **273,** 32304-32311.

Parpal, S., Karlsson, M., Thorn, H. and Stralfors, P. (2001) Cholesterol depletion disrupts caveolae and insulin receptor signaling for metabolic control via insulin receptor substrate-1, but not for mitogen-activated protein kinase control. *J Biol Chem.* **276,** 9670-9678.

Pasterkamp, G. and Virmani, R. (2002) The erythrocyte: a new player in atheromatous core formation. *Heart.* **88,** 115-116.

Paul, A., Calleja, L., Vilella, E., Martinez, R., Osada, J. and Joven, J. (1999) Reduced progression of atherosclerosis in apolipoprotein E-deficient mice with phenylhydrazine-induced anemia. *Atherosclerosis.* **147,** 61-68.

Pedersen, M. E., Cohen, M. and Schotz, M. C. (1983) Immunocytochemical localization of the functional fraction of lipoprotein lipase in the perfused heart. *J Lipid Res.* **24,** 512-521.

Pentikainen, M. O., Oorni, K., Ala-Korpela, M. and Kovanen, P. T. (2000) Modified LDL - trigger of atherosclerosis and inflammation in the arterial intima. *J Intern Med.* **247,** 359-370.

Pohl, J., Ring, A. and Stremmel, W. (2002) Uptake of long-chain fatty acids in HepG2 cells involves caveolae: analysis of a novel pathway. *J Lipid Res.* **43,** 1390-1399.

Pol, A., Martin, S., Fernandez, M. A., Ferguson, C., Carozzi, A., Luetterforst, R., Enrich, C. and Parton, R. G. (2003) Dynamic and Regulated Association of Caveolin With Lipid Bodies; Modulation of Lipid Body Motility and Function By a Dominant Negative Mutant. *Mol Biol Cell.* **3,** 3.

Popov, D., Hasu, M., Ghinea, N., Simionescu, N. and Simionescu, M. (1992) Cardiomyocytes express albumin binding proteins. *J Mol Cell Cardiol.* **24,** 989-1002.

Potter, B. J., Stump, D., Schwieterman, W., Sorrentino, D., Jacobs, L. N., Kiang, C. L., Rand, J. H. and Berk, P. D. (1987) Isolation and partial characterization of plasma membrane fatty acid binding proteins from myocardium and adipose tissue and their relationship to analogous proteins in liver and gut. *Biochem Biophys Res Commun.* **148,** 1370-1376.

Preiss-Landl, K., Zimmermann, R., Hammerle, G. and Zechner, R. (2002) Lipoprotein lipase: the regulation of tissue specific expression and its role in lipid and energy metabolism. *Curr Opin Lipidol.* **13,** 471-481.

Purcell-Huynh, D. A., Farese, R. V., Jr., Johnson, D. F., Flynn, L. M., Pierotti, V., Newland, D. L., Linton, M. F., Sanan, D. A. and Young, S. G. (1995) Transgenic mice expressing high levels of human apolipoprotein B develop severe atherosclerotic lesions in response to a high-fat diet. *J Clin Invest.* **95,** 2246-2257.

Rawson, R. B., Zelenski, N. G., Nijhawan, D., Ye, J., Sakai, J., Hasan, M. T., Chang, T. Y., Brown, M. S. and Goldstein, J. L. (1997) Complementation cloning of S2P, a gene encoding a putative metalloprotease required for intramembrane cleavage of SREBPs. *Mol Cell.* **1,** 47-57.

Razani, B., Combs, T. P., et al. (2002) Caveolin-1-deficient mice are lean, resistant to diet-induced obesity, and show hypertriglyceridemia with adipocyte abnormalities. *J Biol Chem.* **277,** 8635-8647.

Reed, R. G. and Burrington, C. M. (1989) The albumin receptor effect may be due to a surface-induced conformational change in albumin. *J Biol Chem.* **264,** 9867-9872.

Rhainds, D., Brodeur, M., Lapointe, J., Charpentier, D., Falstrault, L. and Brissette, L. (2003) The role of human and mouse hepatic scavenger receptor class B type I (SR-BI) in the selective uptake of low-density lipoprotein-cholesteryl esters. *Biochemistry.* **42,** 7527-7538.

Richieri, G. V. and Kleinfeld, A. M. (1995) Unbound free fatty acid levels in human serum. *J Lipid Res.* **36,** 229-240.

Rigotti, A., Acton, S. L. and Krieger, M. (1995) The class B scavenger receptors SR-BI and CD36 are receptors for anionic phospholipids. *J Biol Chem.* **270,** 16221-16224.

Rigotti, A., Trigatti, B. L., Penman, M., Rayburn, H., Herz, J. and Krieger, M. (1997) A targeted mutation in the murine gene encoding the high density lipoprotein (HDL) receptor scavenger receptor class B type I reveals its key role in HDL metabolism. *Proc Natl Acad Sci U S A.* **94,** 12610-12615.

Ros-Baro, A., Lopez-Iglesias, C., Peiro, S., Bellido, D., Palacin, M., Zorzano, A. and Camps, M. (2001) Lipid rafts are required for GLUT4 internalization in adipose cells. *Proc Natl Acad Sci U S A.* **98,** 12050-12055.

Ross, R. (1993) The pathogenesis of atherosclerosis: a perspective for the 1990s. *Nature.* **362,** 801-809.

Rothberg, K. G., Heuser, J. E., Donzell, W. C., Ying, Y. S., Glenney, J. R. and Anderson, R. G. (1992) Caveolin, a protein component of caveolae membrane coats. *Cell.* **68,** 673-682.

Rust, S., Rosier, M., et al. (1999) Tangier disease is caused by mutations in the gene encoding ATP-binding cassette transporter 1. *Nat Genet.* **22,** 352-355.

Sakai, J., Duncan, E. A., Rawson, R. B., Hua, X., Brown, M. S. and Goldstein, J. L. (1996) Sterol-regulated release of SREBP-2 from cell membranes requires two sequential cleavages, one within a transmembrane segment. *Cell.* **85,** 1037-1046.

Sakai, J., Nohturfft, A., Cheng, D., Ho, Y. K., Brown, M. S. and Goldstein, J. L. (1997) Identification of complexes between the COOH-terminal domains of sterol regulatory element-binding proteins (SREBPs) and SREBP cleavage-activating protein. *J Biol Chem.* **272,** 20213-20221.

Sakai, J., Rawson, R. B., Espenshade, P. J., Cheng, D., Seegmiller, A. C., Goldstein, J. L. and Brown, M. S. (1998) Molecular identification of the sterol-regulated luminal protease that cleaves SREBPs and controls lipid composition of animal cells. *Mol Cell.* **2,** 505-514.

Sambrook, J. and Russell, D. W. (2001). *Molecular Cloning A Laboratory Manual.* Cold Spring Harbor, Cold Spring Harbor Laboratory Press.

Samuel, D., Paris, S. and Ailhaud, G. (1976) Uptake and metabolism of fatty acids and analogues by cultured cardiac cells from chick embryo. *Eur J Biochem.* **64,** 583-595.

Schaffer, J. E. and Lodish, H. F. (1994) Expression cloning and characterization of a novel adipocyte long chain fatty acid transport protein. *Cell.* **79,** 427-436.

Scherer, P. E., Lewis, R. Y., et al. (1997) Cell-type and tissue-specific expression of caveolin-2. Caveolins 1 and 2 co-localize and form a stable hetero-oligomeric complex in vivo. *J Biol Chem.* **272,** 29337-29346.

Scherer, P. E., Tang, Z., Chun, M., Sargiacomo, M., Lodish, H. F. and Lisanti, M. P. (1995) Caveolin isoforms differ in their N-terminal protein sequence and subcellular distribution. Identification and epitope mapping of an isoform-specific monoclonal antibody probe. *J Biol Chem.* **270,** 16395-16401.

Schnitzer, J. E. (1992) gp60 is an albumin-binding glycoprotein expressed by continuous endothelium involved in albumin transcytosis. *Am J Physiol.* **262,** H246-254.

Schnitzer, J. E. and Bravo, J. (1993) High affinity binding, endocytosis, and degradation of conformationally modified albumins. Potential role of gp30 and gp18 as novel scavenger receptors. *J Biol Chem.* **268,** 7562-7570.

Schnitzer, J. E., Carley, W. W. and Palade, G. E. (1988) Albumin interacts specifically with a 60-kDa microvascular endothelial glycoprotein. *Proc Natl Acad Sci U S A.* **85,** 6773-6777.

Schnitzer, J. E., Carley, W. W. and Palade, G. E. (1988) Specific albumin binding to microvascular endothelium in culture. *Am J Physiol.* **254,** H425-437.

Schnitzer, J. E. and Oh, P. (1994) Albondin-mediated capillary permeability to albumin. Differential role of receptors in endothelial transcytosis and endocytosis of native and modified albumins. *J Biol Chem.* **269,** 6072-6082.

Schnitzer, J. E., Oh, P., Pinney, E. and Allard, J. (1994) Filipin-sensitive caveolae-mediated transport in endothelium: reduced transcytosis, scavenger endocytosis, and capillary permeability of select macromolecules. *J Cell Biol.* **127,** 1217-1232.

Schnitzer, J. E., Sung, A., Horvat, R. and Bravo, J. (1992) Preferential interaction of albumin-binding proteins, gp30 and gp18, with conformationally modified albumins. Presence in many cells and tissues with a possible role in catabolism. *J Biol Chem.* **267,** 24544-24553.

Schwieterman, W., Sorrentino, D., Potter, B. J., Rand, J., Kiang, C. L., Stump, D. and Berk, P. D. (1988) Uptake of oleate by isolated rat adipocytes is mediated by a 40-kDa plasma membrane fatty acid binding protein closely related to that in liver and gut. *Proc Natl Acad Sci U S A.* **85,** 359-363.

Sehayek, E., Ono, J. G., et al. (1998) Biliary cholesterol excretion: a novel mechanism that regulates dietary cholesterol absorption. *Proc Natl Acad Sci U S A.* **95,** 10194-10199.

Sfeir, Z., Ibrahimi, A., Amri, E., Grimaldi, P. and Abumrad, N. (1999) CD36 antisense expression in 3T3-F442A preadipocytes. *Mol Cell Biochem.* **192,** 3-8.

Shelness, G. S. and Sellers, J. A. (2001) Very-low-density lipoprotein assembly and secretion. *Curr Opin Lipidol.* **12,** 151-157.

Shih, D. M., Gu, L., et al. (1998) Mice lacking serum paraoxonase are susceptible to organophosphate toxicity and atherosclerosis. *Nature.* **394,** 284-287.

Silver, D. L. and Tall, A. R. (2001) The cellular biology of scavenger receptor class B type I. *Curr Opin Lipidol.* **12,** 497-504.

Silver, D. L., Wang, N., Xiao, X. and Tall, A. R. (2001) High density lipoprotein (HDL) particle uptake mediated by scavenger receptor class B type 1 results in selective sorting of HDL cholesterol from protein and polarized cholesterol secretion. *J Biol Chem.* **276,** 25287-25293.

Simanonok, J. P. (1996) Non-ischemic hypoxia of the arterial wall is a primary cause of atherosclerosis. *Med Hypotheses.* **46,** 155-161.

Simpson, E. R. and Boyd, G. S. (1967) The cholesterol side-chain cleavage system of bovine adrenal cortex. *Eur J Biochem.* **2,** 275-285.

Smart, E. J., Ying, Y. S., Conrad, P. A. and Anderson, R. G. (1994) Caveolin moves from caveolae to the Golgi apparatus in response to cholesterol oxidation. *J Cell Biol.* **127,** 1185-1197.

Smith, L. C., Pownall, H. J. and Gotto, A. M., Jr. (1978) The plasma lipoproteins: structure and metabolism. *Annu Rev Biochem.* **47,** 751-757.

Sorrentino, D., Robinson, R. B., Kiang, C. L. and Berk, P. D. (1989) At physiologic albumin/oleate concentrations oleate uptake by isolated hepatocytes, cardiac myocytes, and adipocytes is a saturable function of the unbound oleate concentration. Uptake kinetics are consistent with the conventional theory. *J Clin Invest.* **84,** 1325-1333.

Sorrentino, D., Stump, D., Potter, B. J., Robinson, R. B., White, R., Kiang, C. L. and Berk, P. D. (1988) Oleate uptake by cardiac myocytes is carrier mediated and involves a 40-kD plasma membrane fatty acid binding protein similar to that in liver, adipose tissue, and gut. *J Clin Invest.* **82,** 928-935.

Souto, R. P., Vallega, G., Wharton, J., Vinten, J., Tranum-Jensen, J. and Pilch, P. F. (2003) Immunopurification and characterization of rat adipocyte caveolae suggest their dissociation from insulin signaling. *J Biol Chem.* **278,** 18321-18329.

Spector, A. A., John, K. and Fletcher, J. E. (1969) Binding of long-chain fatty acids to bovine serum albumin. *J Lipid Res.* **10,** 56-67.

Springer, T., Galfre, G., Secher, D. S. and Milstein, C. (1979) Mac-1: a macrophage differentiation antigen identified by monoclonal antibody. *Eur J Immunol.* **9,** 301-306.

Stahl, A. (2003) A current review of fatty acid transport proteins (SLC27). *Pflugers Arch.* **11,** 11.

Stangl, H., Cao, G., Wyne, K. L. and Hobbs, H. H. (1998) Scavenger receptor, class B, type I-dependent stimulation of cholesterol esterification by high density lipoproteins, low density lipoproteins, and nonlipoprotein cholesterol. *J Biol Chem.* **273,** 31002-31008.

Stangl, H., Hyatt, M. and Hobbs, H. H. (1999) Transport of lipids from high and low density lipoproteins via scavenger receptor-BI. *J Biol Chem.* **274,** 32692-32698.

Stremmel, W. (1988) Uptake of fatty acids by jejunal mucosal cells is mediated by a fatty acid binding membrane protein. *J Clin Invest.* **82,** 2001-2010.

Stremmel, W., Strohmeyer, G. and Berk, P. D. (1986) Hepatocellular uptake of oleate is energy dependent, sodium linked, and inhibited by an antibody to a hepatocyte plasma membrane fatty acid binding protein. *Proc Natl Acad Sci U S A.* **83,** 3584-3588.

Stremmel, W., Strohmeyer, G., Borchard, F., Kochwa, S. and Berk, P. D. (1985) Isolation and partial characterization of a fatty acid binding protein in rat liver plasma membranes. *Proc Natl Acad Sci U S A.* **82,** 4-8.

Stump, D. D., Zhou, S. L. and Berk, P. D. (1993) Comparison of plasma membrane FABP and mitochondrial isoform of aspartate aminotransferase from rat liver. *Am J Physiol.* **265,** G894-902.

Sviridov, D. and Nestel, P. (2002) Dynamics of reverse cholesterol transport: protection against atherosclerosis. *Atherosclerosis.* **161,** 245-254.

Swarnakar, S., Temel, R. E., Connelly, M. A., Azhar, S. and Williams, D. L. (1999) Scavenger receptor class B, type I, mediates selective uptake of low density lipoprotein cholesteryl ester. *J Biol Chem.* **274,** 29733-29739.

Tall, A. R., Wang, N. and Mucksavage, P. (2001) Is it time to modify the reverse cholesterol transport model? *J Clin Invest.* **108,** 1273-1275.

Tang, Z., Scherer, P. E., Okamoto, T., Song, K., Chu, C., Kohtz, D. S., Nishimoto, I., Lodish, H. F. and Lisanti, M. P. (1996) Molecular cloning of caveolin-3, a novel member of the caveolin gene family expressed predominantly in muscle. *J Biol Chem.* **271,** 2255-2261.

Tangirala, R. K., Rubin, E. M. and Palinski, W. (1995) Quantitation of atherosclerosis in murine models: correlation between lesions in the aortic origin and in the entire aorta, and differences in the extent of lesions between sexes in LDL receptor-deficient and apolipoprotein E-deficient mice. *J Lipid Res.* **36,** 2320-2328.

Thomas, R. M., Baici, A., Werder, M., Schulthess, G. and Hauser, H. (2002) Kinetics and mechanism of long-chain fatty acid transport into phosphatidylcholine vesicles from various donor systems. *Biochemistry.* **41,** 1591-1601.

Tiruppathi, C., Finnegan, A. and Malik, A. B. (1996) Isolation and characterization of a cell surface albumin-binding protein from vascular endothelial cells. *Proc Natl Acad Sci U S A.* **93,** 250-254.

Torres, J. M., Darracq, N. and Uriel, J. (1992) Membrane proteins from lymphoblastoid cells showing cross-affinity for alpha-fetoprotein and albumin. Isolation and characterization. *Biochim Biophys Acta.* **1159,** 60-66.

Towbin, H., Staehelin, T. and Gordon, J. (1979) Electrophoretic transfer of proteins from polyacrylamide gels to nitrocellulose sheets: procedure and some applications. *Proc Natl Acad Sci U S A.* **76,** 4350-4354.

Trigatti, B., Rayburn, H., et al. (1999) Influence of the high density lipoprotein receptor SR-BI on reproductive and cardiovascular pathophysiology. *Proc Natl Acad Sci U S A.* **96,** 9322-9327.

Trigatti, B., Rigotti, A. and Krieger, M. (2000) The role of the high-density lipoprotein receptor SR-BI in cholesterol metabolism. *Curr Opin Lipidol.* **11,** 123-131.

Trigatti, B. L., Anderson, R. G. and Gerber, G. E. (1999) Identification of caveolin-1 as a fatty acid binding protein. *Biochem Biophys Res Commun.* **255,** 34-39.

Trigatti, B. L. and Gerber, G. E. (1995) A direct role for serum albumin in the cellular uptake of long-chain fatty acids. *Biochem J.* **308,** 155-159.

Trigatti, B. L. and Gerber, G. E. (1996) The effect of intracellular pH on long-chain fatty acid uptake in 3T3- L1 adipocytes: evidence that uptake involves the passive diffusion of protonated long-chain fatty acids across the plasma membrane. *Biochem J.* **313,** 487-494.

Trigatti, B. L., Mangroo, D. and Gerber, G. E. (1991) Photoaffinity labeling and fatty acid permeation in 3T3-L1 adipocytes. *J Biol Chem.* **266,** 22621-22625.

Turley, S. D. and Dietschy, J. M. (2003) Sterol absorption by the small intestine. *Curr Opin Lipidol.* **14,** 233-240.

Ueda, Y., Gong, E., Royer, L., Cooper, P. N., Francone, O. L. and Rubin, E. M. (2000) Relationship between expression levels and atherogenesis in scavenger receptor class B, type I transgenics. *J Biol Chem.* **275,** 20368-20373.

Ueda, Y., Royer, L., Gong, E., Zhang, J., Cooper, P. N., Francone, O. and Rubin, E. M. (1999) Lower plasma levels and accelerated clearance of high density lipoprotein (HDL) and non-HDL cholesterol in scavenger receptor class B type I transgenic mice. *J Biol Chem.* **274,** 7165-7171.

Uittenbogaard, A., Everson, W. V., Matveev, S. V. and Smart, E. J. (2002) Cholesteryl ester is transported from caveolae to internal membranes as part of a caveolin-annexin II lipid-protein complex. *J Biol Chem.* **277,** 4925-4931.

Uittenbogaard, A., Shaul, P. W., Yuhanna, I. S., Blair, A. and Smart, E. J. (2000) High density lipoprotein prevents oxidized low density lipoprotein-induced inhibition of endothelial nitric-oxide synthase localization and activation in caveolae. *J Biol Chem.* **275,** 11278-11283.

Uittenbogaard, A., Ying, Y. and Smart, E. J. (1998) Characterization of a cytosolic heat-shock protein-caveolin chaperone complex. Involvement in cholesterol trafficking. *J Biol Chem.* **273,** 6525-6532.

Uriel, J., Torres, J. M. and Anel, A. (1994) Carrier-protein-mediated enhancement of fatty-acid binding and internalization in human T-lymphocytes. *Biochim Biophys Acta.* **1220,** 231-240.

van Eck, M., Bos, I. S., et al. (2002) Leukocyte ABCA1 controls susceptibility to atherosclerosis and macrophage recruitment into tissues. *Proc Natl Acad Sci U S A.* **99,** 6298-6303.

Van Eck, M., Herijgers, N., Vidgeon-Hart, M., Pearce, N. J., Hoogerbrugge, P. M., Groot, P. H. and Van Berkel, T. J. (2000) Accelerated atherosclerosis in C57Bl/6 mice transplanted with ApoE- deficient bone marrow. *Atherosclerosis.* **150,** 71-80.

Van Eck, M., Twisk, J., Hoekstra, M., Van Rij, B. T., Van der Lans, C. A., Bos, I. S., Kruijt, J. K., Kuipers, F. and Van Berkel, T. J. (2003) Differential effects of scavenger receptor BI deficiency on lipid metabolism in cells of the arterial wall and in the liver. *J Biol Chem.* **278,** 23699-23705.

Varban, M. L., Rinninger, F., et al. (1998) Targeted mutation reveals a central role for SR-BI in hepatic selective uptake of high density lipoprotein cholesterol. *Proc Natl Acad Sci U S A.* **95,** 4619-4624.

von Eckardstein, A., Nofer, J. R. and Assmann, G. (2001) High density lipoproteins and arteriosclerosis. Role of cholesterol efflux and reverse cholesterol transport. *Arterioscler Thromb Vasc Biol.* **21,** 13-27.

Wang, N., Arai, T., Ji, Y., Rinninger, F. and Tall, A. R. (1998) Liver-specific overexpression of scavenger receptor BI decreases levels of very low density lipoprotein ApoB, low density lipoprotein ApoB, and high density lipoprotein in transgenic mice. *J Biol Chem.* **273,** 32920-32926.

Wang, N., Silver, D. L., Costet, P. and Tall, A. R. (2000) Specific binding of ApoA-I, enhanced cholesterol efflux, and altered plasma membrane morphology in cells expressing ABC1. *J Biol Chem.* **275,** 33053-33058.

Wang, X. Q., Panousis, C. G., Alfaro, M. L., Evans, G. F. and Zuckerman, S. H. (2002) Interferon-gamma-mediated downregulation of cholesterol efflux and ABC1 expression is by the Stat1 pathway. *Arterioscler Thromb Vasc Biol.* **22,** e5-9.

Webb, N. R., Connell, P. M., Graf, G. A., Smart, E. J., de Villiers, W. J., de Beer, F. C. and van der Westhuyzen, D. R. (1998) SR-BII, an isoform of the scavenger receptor BI containing an alternate cytoplasmic tail, mediates lipid transfer between high density lipoprotein and cells. *J Biol Chem.* **273,** 15241-15248.

Weisiger, R., Gollan, J. and Ockner, R. (1981) Receptor for albumin on the liver cell surface may mediate uptake of fatty acids and other albumin-bound substances. *Science.* **211,** 1048-1051.

Weisiger, R. A. (1985) Dissociation from albumin: a potentially rate-limiting step in the clearance of substances by the liver. *Proc Natl Acad Sci U S A.* **82,** 1563-1567.

Weisiger, R. A., Pond, S. M. and Bass, L. (1989) Albumin enhances unidirectional fluxes of fatty acid across a lipid-water interface: theory and experiments. *Am J Physiol.* **257,** G904-916.

Wilson, M. D. and Rudel, L. L. (1994) Review of cholesterol absorption with emphasis on dietary and biliary cholesterol. *J Lipid Res.* **35,** 943-955.

Xu, S., Laccotripe, M., Huang, X., Rigotti, A., Zannis, V. I. and Krieger, M. (1997) Apolipoproteins of HDL can directly mediate binding to the scavenger receptor SR-BI, an HDL receptor that mediates selective lipid uptake. *J Lipid Res.* **38,** 1289-1298.

Yabe, D., Brown, M. S. and Goldstein, J. L. (2002) Insig-2, a second endoplasmic reticulum protein that binds SCAP and blocks export of sterol regulatory element-binding proteins. *Proc Natl Acad Sci U S A.* **99,** 12753-12758.

Yang, T., Espenshade, P. J., Wright, M. E., Yabe, D., Gong, Y., Aebersold, R., Goldstein, J. L. and Brown, M. S. (2002) Crucial step in cholesterol homeostasis: sterols promote binding of SCAP to INSIG-1, a membrane protein that facilitates retention of SREBPs in ER. *Cell.* **110,** 489-500.

Yeagle, P. L. (1985) Cholesterol and the cell membrane. *Biochim Biophys Acta.* **822,** 267-287.

Yoshizumi, T., Nozaki, S., et al. (2000) Pharmacokinetics and metabolism of 123I-BMIPP fatty acid analog in healthy and CD36-deficient subjects. *J Nucl Med.* **41,** 1134-1138.

Yuhanna, I. S., Zhu, Y., et al. (2001) High-density lipoprotein binding to scavenger receptor-BI activates endothelial nitric oxide synthase. *Nat Med.* **7,** 853-857.

Zambon, A., Bertocco, S., Vitturi, N., Polentarutti, V., Vianello, D. and Crepaldi, G. (2003) Relevance of hepatic lipase to the metabolism of triacylglycerol-rich lipoproteins. *Biochem Soc Trans.* **31,** 1070-1074.

Zhang, F., Kamp, F. and Hamilton, J. A. (1996) Dissociation of long and very long chain fatty acids from phospholipid bilayers. *Biochemistry.* **35,** 16055-16060.

Zhang, S. H., Reddick, R. L., Piedrahita, J. A. and Maeda, N. (1992) Spontaneous hypercholesterolemia and arterial lesions in mice lacking apolipoprotein E. *Science.* **258,** 468-471.

Zierler, K. L. (1976) Fatty acids as substrates for heart and skeletal muscle. *Circ Res.* **38,** 459-463.